Studies in Fungi

ARTICLE

Open Access

https://doi.org/10.48130/sif-0025-0016
Studies in Fungi **2025**, 10: e017

Unexplored microfungal diversity from dead woody litter in the dry-hot valleys of Honghe (Yunnan, China)

Dhanushka N. Wanasinghe[1,2], Rungtiwa Phookamsak[1,3*], Lakmali S. Dissanayake[1,3] and Jianchu Xu[1,3*]

[1] *Center for Mountain Futures, Kunming Institute of Botany, Chinese Academy of Sciences, Honghe County 654400, China*
[2] *Department of Soil Science, College of Food and Agriculture Sciences, King Saud University, P.O. Box 145111, Riyadh 11362, Saudi Arabia*
[3] *Department of Economic Plants and Biotechnology, Yunnan Key Laboratory for Wild Plant Resources, Kunming Institute of Botany, Chinese Academy of Sciences, Kunming, Yunnan 650201, China*
* Corresponding authors, E-mail: phookamsak@mail.kib.ac.cn; jxu@mail.kib.ac.cn

Abstract

Despite the critical ecological role fungi play across various ecosystems, the mycoflora of dry-hot valleys remains largely underexplored. This study aims to fill this gap by documenting the diversity and taxonomy of microfungal species in this unique environment. Employing a combination of field sampling, morphological analysis, and molecular techniques, the study conducted a comprehensive survey of microfungi in selected dry-hot valleys of the Honghe region in Yunnan (China). The findings reveal a rich and previously undocumented diversity of *Dothideomycetes* (*Ascomycota*). Among the collected samples, 34.9% of the *Dothideomycetes* isolates were identified as new species described in this study. The identified microfungi belong to six orders encompassing 18 families and 26 genera. A total of 34 microfungal taxa are documented, including two new families, two new genera, 15 new species, and 15 existing records. During this study, *Mangifericomitaceae* (*Pleosporales*) and *Mucomycosphaerellaceae* (*Mycosphaerellales*) are introduced as new families. *Gruyteromyces* and *Longiascospora* are introduced as new genera in *Didymellaceae* (*Pleosporales*) and *Pleurotremataceae* (*Dyfrolomycetales*), respectively. The study also introduces new species: *Anteaglonium hongheense*, *Anthosulcatispora hongheensis*, *Chromolaenicola hongheensis*, *Gruyteromyces hongheensis*, *Helminthosporium hongheense*, *Longiascospora hongheensis*, *Magnibotryascoma hongheense*, *Mangifericomes yunnanensis*, *Mucomycosphaerella hongheensis*, *Neomultiseptospora hongheensis*, *Paulkirkia hongheensis*, *Pseudocapulatispora hongheensis*, *Pseudochaetosphaeronema hongheense*, *P. punithalingamii,* and *Pseudostaurosphaeria hongheensis*. *Aplosporella artocarpi*, *A. hesperidica*, *Chromolaenicola clematidis*, *Dendryphion hydei*, *Leptospora phraeana*, *Murichromolaenicola thailandensis*, *Neomultiseptospora yunnanensis*, *Neoroussoella bambusae*, *Neovaginatispora fuckelii*, *Paraphaeosphaeria jaguarinae*, *Patellaria microspora*, *Pseudocapulatispora longiappendiculata*, *Rhytidhysteron neorufulum*, *Tremateia guiyangensis*, and *Xenoroussoella triseptata*, reported as new records. These results highlight the significance of dry-hot valleys as reservoirs of fungal biodiversity and highlight the importance of including these ecosystems in conservation strategies. This study contributes to the expanding knowledge on fungal diversity in extreme environments and calls attention to the need for further research into the ecological roles and potential applications of these neglected mycoflora.

Citation: Wanasinghe DN, Phookamsak R, Dissanayake LS, Xu J. 2025. Unexplored microfungal diversity from dead woody litter in the dry-hot valleys of Honghe (Yunnan, China). *Studies in Fungi* 10: e017 https://doi.org/10.48130/sif-0025-0016

Introduction

Fungi are crucial for maintaining the health and sustainability of terrestrial ecosystems, primarily through their roles in nutrient cycling, organic matter decomposition, and symbiotic interactions with nearly all plant species[1–3]. Beyond these fundamental ecological contributions, fungi significantly impact agricultural productivity and forest ecosystem stability[4–6]. Despite their vital ecological importance, fungal biodiversity remains unevenly studied across ecosystems, with particularly limited research focusing on extreme environments such as dry-hot valleys[7–10]. These unique habitats, characterized by arid conditions, severe temperature fluctuations, and limited vegetation[11–13], represent largely unexplored areas where studying fungi could reveal novel insights into biodiversity, ecological roles, and adaptive strategies under conditions typically considered challenging for life[14–16]. Studying fungal diversity in extreme environments is critical, as it deepens our understanding of fungal resilience and adaptability[9,17], revealing how these organisms survive and flourish under severe stress conditions. Such insights are particularly valuable in the context of climate change, providing important lessons on biological adaptation strategies and ecosystem resilience under increasingly challenging conditions. Documenting fungal diversity in dry-hot valleys enhances our global understanding of biodiversity, emphasizing the ecological significance of fungi in environments historically underrepresented in scientific research[14,15].

The majority of mycological research has concentrated on hospitable environments where fungal populations are abundant and diverse[18]. Consequently, dry-hot valleys remain underexplored, despite their potential to harbor fungal species uniquely adapted to extreme aridity and temperature fluctuations[10]. Logistical challenges associated with fieldwork in these remote regions have further contributed to their neglect in biodiversity studies. Addressing this knowledge gap is not only a matter of scientific curiosity but also essential for developing biodiversity conservation strategies encompassing all ecosystem types. Motivated by this necessity, the present study aims to uncover the hidden diversity of microfungi in dry-hot valleys. In southwestern (SW) China, savanna-like vegetation predominantly occurs in deep, hot, and dry valleys formed by several major rivers. Specifically, native seed plants comprising 3,217 species and varieties belonging to 1,038 genera and 163 families have been documented from the savanna-like vegetation in valleys of the three major rivers (Jinshajiang, Yuanjiang, and Nujiang) in SW China[19]. By applying estimation of approximately six fungal species per vascular plant species[20], the fungal diversity in these valleys could potentially exceed 20,000 species. Despite this substantial

predicted diversity, studies on microfungi utilizing both morphological and phylogenetic analyses were virtually non-existent in the Yuanjiang (Honghe) valley prior to 2019[21]. However, interest in microfungal research in this region has significantly increased over the last five years, leading to several recent contributions[21–34].

Therefore, this study specifically conducted comprehensive surveys in the dry-hot valleys of the Honghe region, Yunnan Province, to identify fungal taxa using morphological and phylogenetic methods and document their diversity. By illuminating the understudied fungal communities inhabiting these valleys, these findings offer valuable insights into fungal adaptations, enrich global biodiversity inventories, and support conservation strategies. Given global environmental changes, understanding fungal life in these harsh ecosystems has become increasingly pertinent, holding significant implications for the sustainable management and conservation of arid and semi-arid regions worldwide.

Table of contents

Ascomycota R.H. Whittaker
Dothideomycetes O.E. Erikss & Winka
Botryosphaeriales C.L. Schoch, Crous & Shoemaker
Aplosporellaceae Slippers, Boissin & Crous
Aplosporella Speg.
Aplosporella artocarpi Trakun., L. Lombard & Crous
Aplosporella hesperidica Speg.
Dyfrolomycetales K.L. Pang, K.D. Hyde & E.B.G. Jones
Pleurotremataceae Walt. Watson
Longiascospora Wanas., Phookamsak & J.C. Xu, **gen. nov.**
Longiascospora hongheensis Wanas., L.S. Dissan., Phookamsak & J.C. Xu, **sp. nov.**
Hysteriales Lindau
Hysteriaceae Chevall.
Rhytidhysteron Speg.
Rhytidhysteron neorufulum Thambug. & K.D. Hyde
Mycosphaerellales (Nannf.) P.F. Cannon
Mucomycosphaerellaceae Wanas., Phookamsak, L.S. Dissan. & J.C. Xu, **fam. nov.**
Mucomycosphaerella Quaedvl. & Crous
Mucomycosphaerella hongheensis Wanas., Phookamsak, L.S. Dissan. & J.C. Xu, **sp. nov.**
Patellariales D. Hawksw. & O.E. Erikss.
Patellariaceae Corda
Patellaria Fr.
Patellaria microspora Ekanayaka & K.D. Hyde
Pleosporales
Anteagloniaceae K.D. Hyde & A. Mapook
Anteaglonium Mugambi & Huhndorf
Anteaglonium hongheense Wanas., Phookamsak, L.S. Dissan. & J.C. Xu, **sp. nov.**
Didymellaceae Gruyter, Aveskamp & Verkley
Gruyteromyces Wanas., Phookamsak, L.S. Dissan. & J.C. Xu, **gen. nov.**
Gruyteromyces hongheensis Wanas., Phookamsak, & J.C. Xu, **sp. nov.**
Didymosphaeriaceae Munk
Chromolaenicola Mapook & K.D. Hyde
Chromolaenicola clematidis Phukhams. & K.D. Hyde
Chromolaenicola hongheensis Wanas., Phookamsak, L.S. Dissan. & J.C. Xu, **sp. nov.**
Paraphaeosphaeria O.E. Erikss.
Paraphaeosphaeria jaguarinae Y.P. Tan & R.G. Shivas
Tremateia Kohlm., Volkm.-Kohlm. & O.E. Erikss.
Tremateia guiyangensis J.F. Zhang, J.K. Liu, K.D. Hyde & Z.Y. Liu
Lophiostomataceae Sacc.
Neovaginatispora A. Hashim., K. Hiray. & Kaz. Tanaka
Neovaginatispora fuckelii (Sacc.) A. Hashim., K. Hiray. & Kaz. Tanaka
Pseudocapulatispora Mapook & K.D. Hyde
Pseudocapulatispora hongheensis Wanas., Phookamsak, L.S. Dissan. & J.C. Xu, **sp. nov.**
Pseudocapulatispora Mapook & K.D. Hyde
Pseudocapulatispora longiappendiculata Mapook & K.D. Hyde
Macrodiplodiopsidaceae Voglmayr, Jaklitsch & Crous
Pseudochaetosphaeronema Punith.
Pseudochaetosphaeronema hongheense Wanas., Phookamsak & J.C. Xu, **sp. nov.**
Pseudochaetosphaeronema punithalingamii Wanas., Phookamsak & J.C. Xu, **sp. nov.**
Mangifericomitaceae Wanas., Phookamsak, L.S. Dissan. & J.C. Xu, **fam. nov.**
Mangifericomes E.F. Yang & Tibpromma
Mangifericomes yunnanensis Wanas., Phookamsak, L.S. Dissan. & J.C. Xu, **sp. nov.**
Massarinaceae Munk
Helminthosporium Link
Helminthosporium hongheense Wanas., Phookamsak, L.S. Dissan. & J.C. Xu, **sp. nov.**
Parabambusicolaceae Kaz. Tanaka & K. Hiray.
Neomultiseptospora N. Xie, Phookamsak & Hongsanan
Neomultiseptospora hongheensis Wanas., Phookamsak, L.S. Dissan. & J.C. Xu, **sp. nov.**
Neomultiseptospora yunnanensis Phookamsak, Hongsanan & N. Xie
Phaeosphaeriaceae M.E. Barr
Leptospora Rabenh.
Leptospora phraeana Mapook & K.D. Hyde
Murichromolaenicola Mapook & K.D. Hyde
Murichromolaenicola thailandensis Htet, Mapook & K.D. Hyde
Pseudostaurosphaeria Mapook & K.D. Hyde
Pseudostaurosphaeria hongheensis Wanas., Phookamsak & J.C. Xu, **sp. nov.**
Roussoellaceae J.K. Liu, Phookamsak, D.Q. Dai & K.D. Hyde
Neoroussoella Jian K. Liu, Phookamsak & K.D. Hyde
Neoroussoella bambusae Phookamsak, J.K. Liu & K.D. Hyde
Xenoroussoella Mapook & K.D. Hyde
Xenoroussoella triseptata Mapook & K.D. Hyde
Sulcatisporaceae Kaz. Tanaka & K. Hiray.
Anthosulcatispora Phukhams. & K.D. Hyde
Anthosulcatispora hongheensis Wanas., Phookamsak, L.S. Dissan. & J.C. Xu, **sp. nov.**
Teichosporaceae M.E. Barr
Magnibotryascoma Thambug. & K.D. Hyde
Magnibotryascoma hongheense Wanas., Phookamsak, L.S. Dissan. & J.C. Xu, **sp. nov.**
Paulkirkia Wijayaw., Wanas., Tangthir., Camporesi & K.D. Hyde
Paulkirkia hongheensis Wanas., Phookamsak, L.S. Dissan. & J.C. Xu, **sp. nov.**
Torulaceae Corda
Dendryphion Wallr.
Dendryphion hydei J.F. Li, Phookamsak & Jeewon

Materials and methods

Specimens and isolates

Fresh fungal materials were collected from dead woody litter and twigs of deciduous plants in Honghe (Yunnan Province, China)

during both the dry season (March, April, December) and the rainy season (June, August). The local environment was characterized by poor eroded soils, steep valleys (Fig. 1), and a subtropical monsoon climate. The specimens were examined using standard protocols described in Dissanayake et al.[29], Gao et al.[34], and Xu et al.[35]. Single-spore isolations were performed following the approaches of Li et al.[36,37] and Mapook et al.[38], with slight modifications, including overnight incubation at 16–25 °C in darkness. Germinated spores were examined under a Motic SMZ 168 Stereo Zoom microscope, and then transferred to potato dextrose agar [PDA; potato extract 4 g/L (equivalent to 200g of infusion from potatoes), glucose 20 g/L, agar 15 g/L] or malt extract agar (MEA; malt extract 30 g/L, mycological peptone 5 g/L, agar 15 g/L) for further analysis, such as DNA extraction, growth rate measurements and cultural characterization. Isolates with the prefix KUNCC were preserved at the Culture Collection of the Kunming Institute of Botany, Chinese Academy of Sciences. Corresponding voucher specimens were deposited in the Cryptogamic Herbarium of the same institute (KUN-HKAS), Kunming, China. Nomenclatural data for fungal novelties were deposited in the https://gmsmicrofungi.org[39] and MycoBank[40].

Morphological classification

Digital images of reproductive structures were obtained using a Canon 450D camera mounted on a Nikon ECLIPSE 80i compound microscope. To examine micro-morphological features, squash mounts and hand-cut sections of fruiting bodies were prepared, allowing observation of ascomata/conidiomata and peridial structure. Morphological measurements were taken at the widest points of each structure. Dimensions were recorded using the Tarosoft® Image Framework software, and image plates were compiled using Adobe Photoshop CS3 Extended (version 10.0; Adobe Systems, USA). Each isolate was cultured in triplicate on PDA to assess colony morphology under light conditions at 16–20 °C. Colony dimensions and pigmentation were evaluated following the colour charts of Rayner[41], and mycelial zonation patterns were documented after a three-week incubation period. Descriptions of new taxa conform to the guidelines proposed by Jeewon & Hyde[42] and Maharachchikumbura et al.[43].

Fig. 1 The local environment showing steep valleys and eroded nutrient-poor soils that characterize the study area.

DNA extraction, PCR, and sequencing

DNA extraction, PCR amplification, and sequencing were carried out using the protocols outlined by Wanasinghe et al.[44], Wijesinghe et al.[45] and Htet et al.[46]. In cases where fungal isolates could not be obtained in culture, DNA was isolated directly from ascomycetous fruiting structures. Approximately 15–20 fruiting bodies (diameter > 500 μm; 10 per sample) were carefully detached from the host material using a sterilized needle and transferred into a drop of sterile water in a 1.5 mL sterile Eppendorf tube under aseptic conditions. Genomic DNA was then extracted using the E.Z.N.A.® Forensic DNA Kit (D3591-01, Omega Bio-Tek) in accordance with the manufacturer's guidelines.

Phylogenetic analyses

Sequences generated from this study were compared with homologous sequences retrieved from GenBank. Reference sequences were selected based on BLAST results and recently published studies. Multiple sequence alignments were carried out using MAFFT v.7 via the online platform[47,48], and the alignments were manually adjusted where necessary using BioEdit v.7.0.9[49]. Phylogenetic relationships were inferred from both single-locus and concatenated datasets using Maximum Likelihood (ML) and Bayesian Inference (BI) approaches. For both ML and Bayesian analyses, the best-fitting substitution models for each gene region were selected using MrModeltest v.2.3[50] under the Akaike Information Criterion (AIC), as implemented in PAUP v.4.0b10[51]. Phylogenetic analyses using both Maximum Likelihood (ML) and Bayesian Inference (BI) approaches were conducted via the CIPRES Science Gateway[52]. For ML analyses, RAxML-HPC2 on XSEDE v.8.2.10[53] was employed with default settings and 1,000 bootstrap replicates to assess branch support. Bayesian analyses were carried out using MrBayes on ACCESS[54], implementing the GTR+I+G substitution model. The MCMC algorithm was run for two to five million generations, with trees sampled every 1,000 generations. The run terminated automatically once the average standard deviation of split frequencies fell below 0.01, and the first 25% of trees were discarded as burn-in. ML bootstrap values (MLBS) ≥ 70% and Bayesian posterior probabilities (BYPP) ≥ 0.95 are reported above the corresponding branches in the phylogenetic trees. Final trees were visualized using FigTree v.1.4.0[55] and annotated using either Microsoft PowerPoint (2007) or Adobe Illustrator CS5 (Version 15.0.0, Adobe Systems, San Jose, CA). Accession numbers for all newly generated sequences are provided after "Material examined" section.

Results

Phylogenetic analyses

Comprehensive phylogenetic analyses were conducted across 18 families. Based on the phylogenetic evidence, coupled with morphological support, two new families, two new genera, and 15 new species were introduced and additional information was provided for 15 existing species. Phylogenetic results for each analysis are provided in the figure legends. Detailed discussions of the topologies related to our new strains are presented in the note sections of each respective taxonomic entry below.

Taxonomy

Ascomycota R.H. Whittaker

Dothideomycetes O.E. Erikss & Winka

Botryosphaeriales C.L. Schoch, Crous & Shoemaker

Aplosporellaceae Slippers, Boissin & Crous

Aplosporella Speg.

Notes: *Aplosporella* is a heterogeneous genus comprising over 275 species, typically associated with dead branches and twigs across diverse hosts and habitats[56–59]. Some species within *Aplosporella* are recognized as pathogens, causing branch and twig blight, canker, or dieback diseases in numerous plant hosts[60–63]. Recent taxonomic revision by Phillips et al.[64] formally synonymized *Bagnisiella* under *Aplosporella*. Although Hyde et al.[59] accepted approximately 275 species, phylogenetic positions based on molecular data have been confirmed for only 13 species. In this study, two new host records were reported for *Aplosporella artocarpi* and *A. hesperidica*.

Aplosporella artocarpi Trakun., L. Lombard & Crous, Persoonia 34: 91 (Figs 2 and 3).

MycoBank No: 810167

Saprobic on a dead twig of *Bougainvillea spectabilis*. Sexual morph: Undetermined. Asexual morph: *Conidiostromata* 300–350 μm high, 450–750 μm in diam., pycnidial, semi-immersed, erumpent through host epidermis, multilocular. *Disc* blackish brown, circular to ovoid, with one central ostiole per disc. *Ostioles* are inconspicuous, minute papillate, or with pore-like openings. *Locules* 180–220 μm high, 150–275 μm diam., multi-loculate, globose to ovoid, or irregular in shape, irregularly arranged, with three to five subdivided chambers separated by invaginations with common walls. *Pycnidial walls* 30–50 μm wide, composed of several cell layers, of large, broad, thick-walled, brown to dark brown pseudoparenchymatous cells, arranged in a *textura angularis*; interstitial walls of a locule composed of several cell layers of flattened, light brown to brown pseudoparenchymatous cells, arranged in *textura prismatica* or palisade-like cells. *Paraphyses* 20–30 × 2–3 μm ($\bar{x}$ = 25.9 × 2.5 μm), hyaline, filiform, with rounded apex, filamentous, smooth-walled, inconspicuous septate, unbranched, slightly tapering towards the apex. *Conidiophores* reduced to conidiogenous cells. *Conidiogenous* cells 5.5–7.5 × 3–6 μm ($\bar{x}$ = 6.3 × 4.1 μm, n = 20), raising from the inner cavity, holoblastic, phialidic, hyaline, ampulliform to

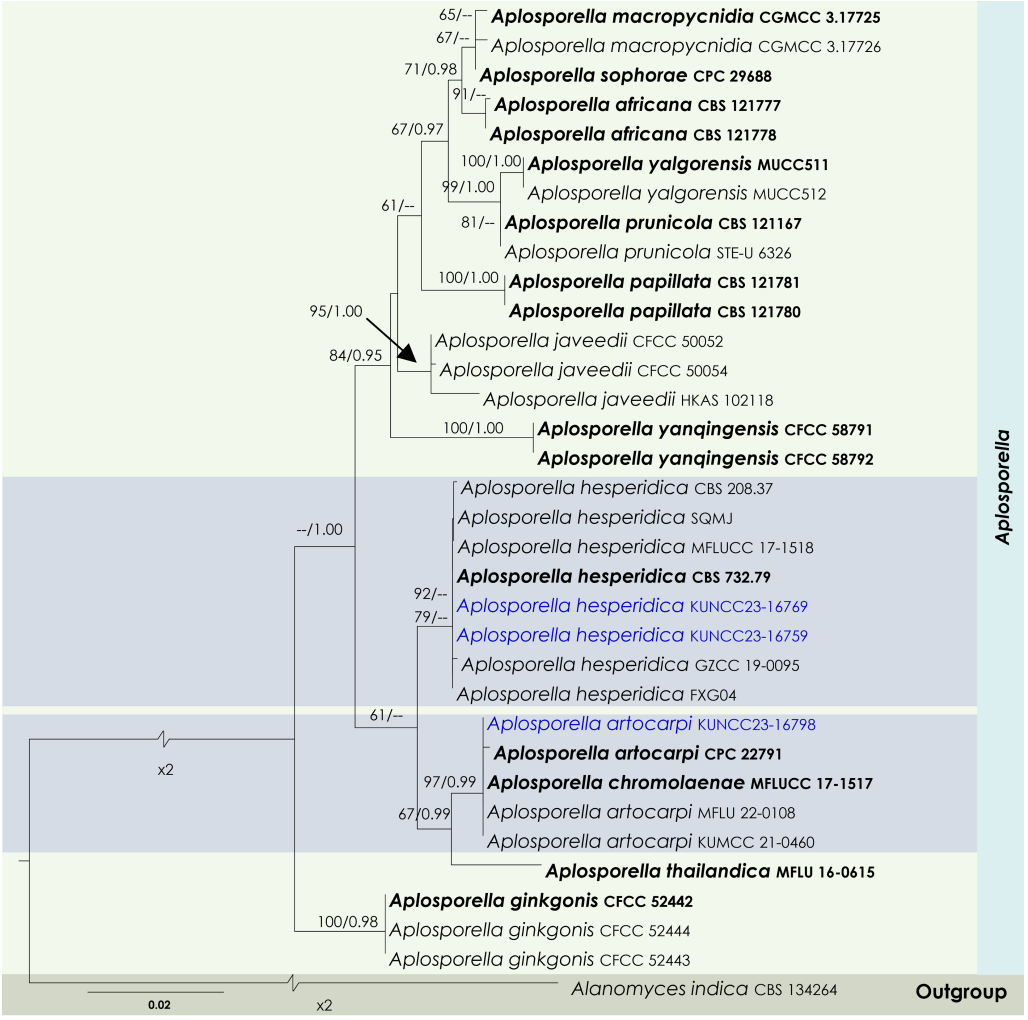

Fig. 2 Maximum Likelihood tree inferred from the concatenated dataset of partial LSU, ITS, and *tef*1-α sequences representing members of *Aplosporellaceae*. The phylogeny is rooted with *Alanomyces indica* (CBS 134264). The final likelihood value is –4,051.526624. The final alignment included 303 unique site patterns, with approximately 25.96% of the positions comprising gaps or ambiguous characters. The estimated nucleotide frequencies were as follows: A = 0.230562, C = 0.245552, G = 0.282555, T = 0.241332. The substitution model yielded the following relative rates: AC = 5.894305, AG = 6.724706, AT = 4.532426, CG = 4.107660, CT = 15.165187 and GT = 1.000000. The proportion of invariable sites (I) was estimated at 0.7274, and the gamma distribution shape parameter (α) was 0.6476. Bayesian inference reached convergence after 623,000 generations, when the average standard deviation of split frequencies dropped below 0.01 (observed value: 0.009918). A total of 3,116 trees were sampled, and 2,337 of these were retained for the final analysis after discarding the initial 25% as burn-in. The alignment also revealed 304 distinct informative sites. In the resulting phylograms, sequences generated in this study are highlighted in blue, while ex-type or type strains are indicated in boldface.

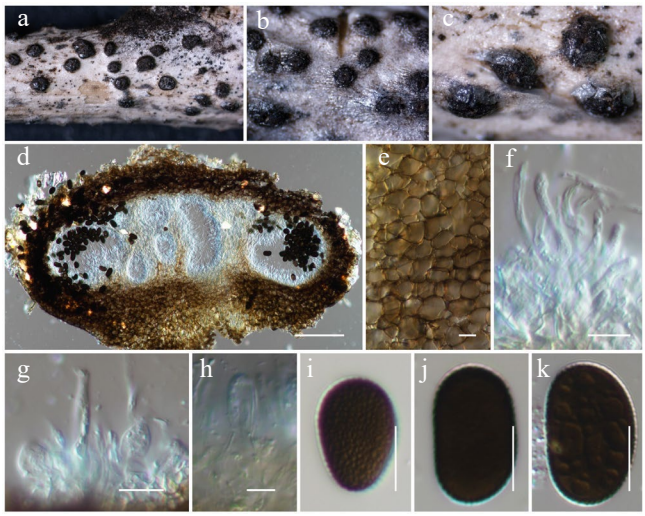

Fig. 3 *Aplosporella artocarpi* (HKAS146009). (a)–(c) Conidiostromata on host. (d) Cross-section of the conidiostroma. (e) Pycnidial wall. (f) Paraphyses. (g), (h) Conidiogenous cells and developing conidia. (i)–(k) Conidia. Scale bars: (d) = 100 μm, (e)–(k) = 10 μm.

subcylindrical, aseptate, smooth-walled. *Conidia* 18–22 × 10–14 μm ($\bar{x}$ = 19.3 × 12.4 μm, n = 30), aseptate, smooth, ovoid to ellipsoidal, broad oblong, brown to dark brown when mature, rough-walled, reticulate.

Material examined: China, Yunnan, Honghe Hani and Yi Autonomous Prefecture, Honghe County, 23.421524° N, 102.227973° E, 730 m, on dead twigs of *Bougainvillea spectabilis* (*Nyctaginaceae*), 10 June 2021, D.N. Wanasinghe, HH22-07 (HKAS146009), living culture, KUNCC23-16798.

GenBank numbers: KUNCC23-16798: ITS = PV742884, LSU = PV742940, *tef*1-α = PV738667.

Known hosts and distribution: Asymptomatic twigs of *Artocarpus heterophyllus*[65], dead stems of *Chromolaena odorata*[66], and dead woody twigs of *Hevea brasiliensis*[67] in Thailand; on asymptomatic leaves of *Stoechospermum marginatum* and *Caulerpa taxifolia* in India[68]; on dead branches of *Mangifera indica*[26] and *Bougainvillea spectabilis* in Yunnan, China (this study).

Notes: Phylogenetic analyses of a combined LSU, ITS and *tef*1-α DNA sequence demonstrated that the new strain KUNCC23-16798 shares the same branch length with the type strains of *Aplosporella artocarpi* (CPC 22791) and *A. chromolaenae* (MFLUCC 17-1517) and other two representative strains of *A. artocarpi* (MFLU 22-0108 and KUMCC 21-0460) with 97% MLBS and 0.99 BYPP supports (Fig. 2). Morphologically, the new isolate is similar to the type of *A. artocarpi* (CPC 22791) in having similar size range of conidiostromata, and conidia that are ellipsoid to ovoid, brown to dark brown, reticulate rough-walled when mature[65]. Additionally, the new isolate is also similar to *A. chromolaenae* (MFLUCC 17-1517) but slightly differs in having smaller conidiostromata (450–750 μm diam. vs 685–780 μm diam.) and larger conidia (18–22 × 10–14 μm vs 13–20 × 8.5–12 μm)[69]. Therefore, the new isolate is identified as *Aplosporella artocarpi* based on morphological resemblance and phylogenetic evidence. The species is reported on *Bougainvillea spectabilis* in Yunnan, China, for the first time. Notably, the conspecific status of *A. artocarpi* and *A. chromolaenae* is needed to be solved.

Aplosporella hesperidica Speg., Anales de la Sociedad Científica Argentina 13 (1): 18 (Figs 2 and 4).

MycoBank No: 218239

Saprobic on dead twigs of an unknown deciduous host. Sexual morph: Undetermined. Asexual morph: *Conidiostromata* 400–600 μm in diam., pycnidial, semi-immersed, erumpent through host epidermis, raised, becoming superficial, multilocular, with 3–5 locules per disc. *Disc* blackish brown, circular to ovoid, with one central ostiole per disc. *Ostioles* inconspicuous pore-like opening at the same level of the disc surface. *Locules* 120–180 μm high, 160–240 μm diam., multiple, globose to ovoid, irregularly arranged, with two to three subdivided chambers separated by invaginations with common walls. *Pycnidial walls* 30–50 μm wide, of unequal thickness, slightly thick at the apex, composed of several cell layers, of large, broad, thick-walled, brown to dark brown pseudoparenchymatous cells, arranged in a *textura angularis* to *textura globulosa*; interstitial walls of a locule composed of several cell layers of flattened, hyaline to light brown pseudoparenchymatous cells, arranged in *textura prismatica* or palisade-like cells. *Paraphyses* 28–44 × 2–3 μm ($\bar{x}$ = 34.1 × 2.2 μm), hyaline, filiform, with rounded apex, filamentous, smooth-walled, septate, unbranched, associated with blastic conidiogenesis. *Conidiophores* reduced to conidiogenous cells. *Conidiogenous* cells 7–10 × 3–5 μm ($\bar{x}$ = 8.6 × 3.7 μm, n = 20), holoblastic, phialidic, hyaline, ampulliform to subcylindrical, aseptate, smooth-walled. *Conidia* 12–18 × 7–9 μm ($\bar{x}$ = 15.1 × 8.1 μm, n = 20), aseptate, ellipsoid to broad oblong, hyaline when young, becoming brown when mature, rough-walled, reticulate.

Materials examined: China, Yunnan, Honghe Hani and Yi Autonomous Prefecture, Honghe County, 23.421068° N, 102.229128° E, 735 m, on dead twigs of an unknown deciduous host, 03 December 2020, D.N. Wanasinghe, DWHH13-02 (HKAS146011), living culture, KUNCC23-16769; *ibid*., 23 April 2020, DWHH08-01 (HKAS146010), living culture, KUNCC23-16759.

GenBank numbers: KUNCC23-16769: ITS = PV742885, LSU = PV742941, SSU = PV742996, *tef*1-α = PV738668; KUNCC23-16759: ITS = PV742886, LSU = PV742942, SSU = PV742997, *tef*1-α = PV738669.

Known hosts and distribution (based on molecular data): isolated from soil in Cuba[70]; associated with early stem-end rot on *Citrus sinensis* in Zimbabwe[71]; on dead stems of *Chromolaena odorata* in Thailand[69]; associated with cowpea root rot disease in India[72]; on decaying woody host in Guizhou, China[73]; on branches of *Euonymus japonicus* in Beijing, China[62].

Notes: Phylogenetic analyses of a combined LSU, ITS, and *tef*1-α DNA sequence (Fig. 2) demonstrated that two new strains

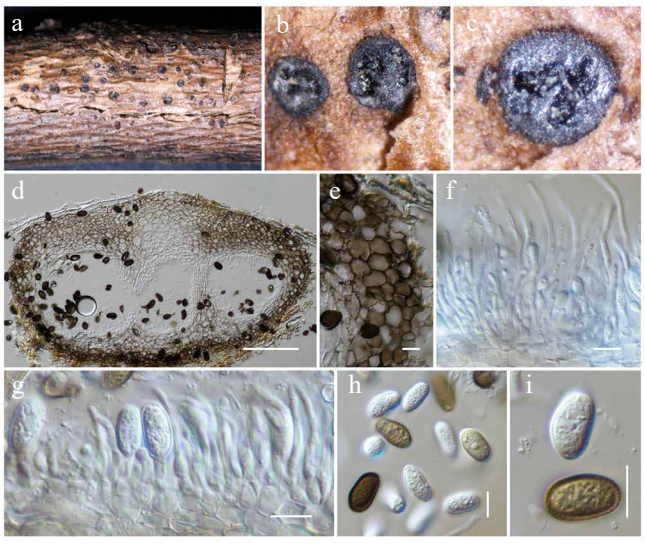

Fig. 4 *Aplosporella hesperidica* (HKAS146011). (a) Conidiostromata on host. (b)–(d) Cross sections of the conidiostromata. (e) Pycnidial wall. (f) Paraphyses. (g) Conidiogenous cells and developing conidia. (h), (i) Conidia. Scale bars: (d) = 100 μm, (e)–(i) = 10 μm.

(KUNCC23-16769 and KUNCC23-16759) group within the subclade of *Aplosporella hesperidica* with 79% MLBS support. Morphologically, the new isolates are typical of *A. hesperidica* in having multilocular, blackish brown, circular to ovoid conidiostromata and aseptate, ellipsoid to broad oblong, brown, rough-walled, reticulate conidia. However, the new isolates differ from the type of *A. hesperidica* in having smaller conidia (12–18 × 7–9 μm vs 22–25 × 9–11 μm)[74] and the number of locules (3–5 locules vs 3–7 locules of the type)[74]. Based on phylogenetic evidence, the study therefore identified the new isolates as *Aplosporella hesperidica* herein, and the species is reported from Yunnan, China, for the first time.

Dyfrolomycetales K.L. Pang, K.D. Hyde & E.B.G. Jones, Fungal Diversity 63 (1): 7.

Pleurotremataceae Walt. Watson, New Phytologist 28: 113.

Notes: The family *Pleurotremataceae* currently comprises three genera, *viz*. *Dyfrolomyces*, *Melomastia*, and *Pleurotrema*[59]. In this study, a fourth genus is introduced to this family: *Longiascospora*. Phylogenetically, *Longiascospora* is nested as the basal lineage within *Pleurotremataceae* (Fig. 5).

Longiascospora Wanas., Phookamsak & J.C. Xu, **gen. nov.**

MycoBank No: 859350

Etymology: The generic epithet referring to the long ascospores.

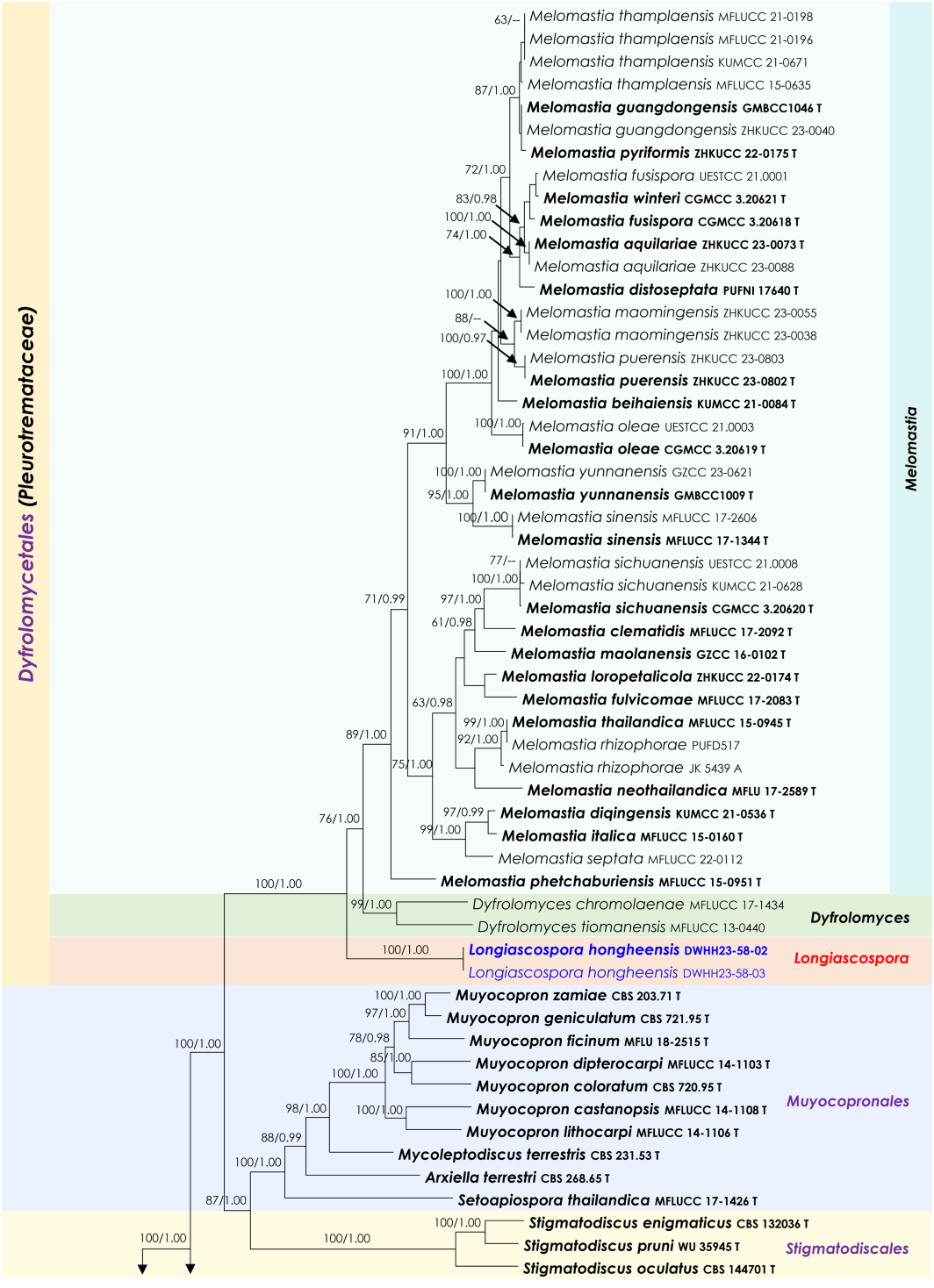

Fig. 5 (to be continued)

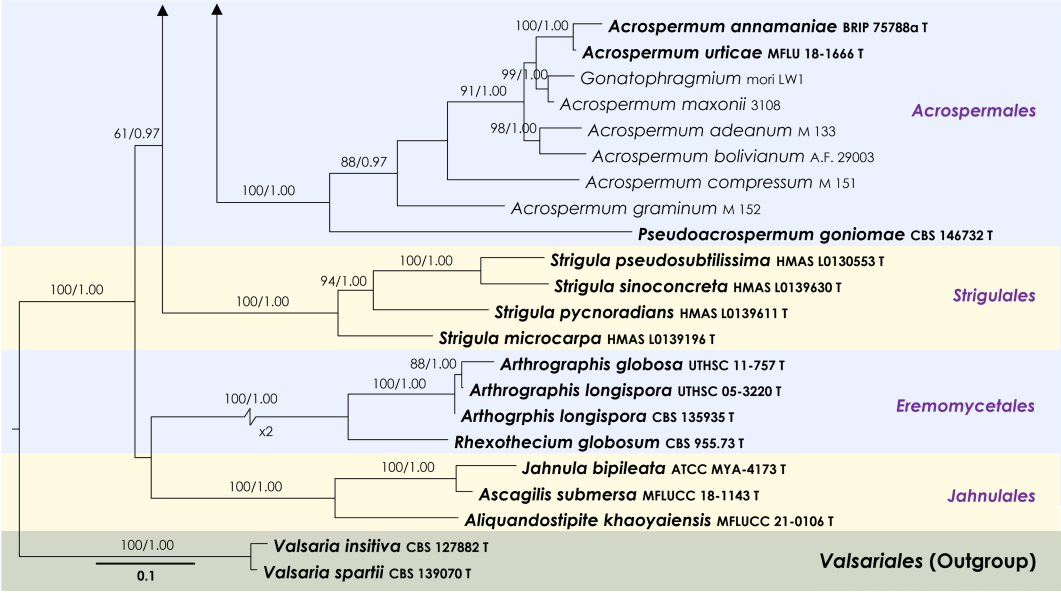

Fig. 5 Maximum Likelihood tree inferred from the concatenated dataset of partial LSU, ITS and *rpb*2 sequences. The phylogeny is rooted with *Valsaria insitiva* (CBS 126882) and *V. spartii* (CBS 139070). The final likelihood value is –48,977.732994. The final alignment included 2,750 unique site patterns, with approximately 44.21% of the positions comprising gaps or ambiguous characters. The estimated nucleotide frequencies were as follows: A = 0.236572, C = 0.265016, G = 0.288031, T = 0.21038. The substitution model yielded the following relative rates: AC = 1.574678, AG = 3.286228, AT = 1.515809, CG = 1.482881, CT = 7.546116, GT = 1.000000. The proportion of invariable sites (I) was estimated at 0.329292 and the gamma distribution shape parameter (α) was 0.554771. Bayesian inference reached convergence after 336,000 generations, when the average standard deviation of split frequencies dropped below 0.01 (observed value: 0.00998). A total of 1,681 trees were sampled, and 1,261 of these were retained for the final analysis after discarding the initial 25% as burn-in. The alignment also revealed 2,751 distinct informative sites. In the resulting phylograms, sequences generated in this study are highlighted in blue, while ex-type or type strains are indicated in boldface.

Saprobic on dead twigs of an unknown deciduous host. Sexual morph: *Ascomata* solitary, semi-immersed, black, subglobose to ampulliform, glabrous, papillate, ostiolate. *Ostiolar neck* clypeate, central, elongated, papillate, with periphyses, central, made up of pigmented, pseudoparenchymatous cells. *Peridium* thick-walled, composed of several celled layers of small, pigmented, pseudoparenchymatous cells of *textura angularis*, outer layers composed of brown to dark brown cells, fused with host tissues, lighter towards the inside of ascomata. *Hamathecium* comprises numerous filamentous, unbranched, aseptate, trabeculate pseudoparaphyses observed between and above the asci, and embedded in a gelatinous matrix. *Asci* 8-spored, bitunicate, cylindrical, short-pedicellate, with rounded apex. *Ascospores* multi-seriate, tightly fasciculate, straight or slightly curved, filiform, multi-septate, without constrictions at the septa, rounded at both ends, apical end broader than the basal end, hyaline, smooth-walled, guttulate in most cells. Asexual morph: Undetermined.

Type species: *Longiascospora hongheensis* Wanas., Phookamsak & J.C. Xu

Notes: *Longiascospora* is introduced as a monotypic genus herein to accommodate *Longiascospora hongheensis* sp. nov. This new genus can be distinguished from the other three genera in *Pleurotremataceae* by its spore arrangement in asci and filiform ascospores. Whereas *Dyfrolomyces*, *Melomastia,* and *Pleurotrema* have ellipsoid to fusiform, or elongate fusiform ascospores[75–77]. Phylogenetic analyses of a combined LSU, ITS, and *rpb*2 DNA sequence demonstrated that the new genus formed an independent monophyletic clade basal to *Dyfrolomyces* and *Melomastia* with 100% MLBS and 1.00 BYPP support values (Fig. 5). Therefore, the new genus is introduced based on morphological distinctiveness and phylogenetic evidence.

Longiascospora hongheensis Wanas., L.S. Dissan., Phookamsak & J.C. Xu, **sp. nov.** (Figs 5 and 6)

MycoBank No: 859351

Etymology: The specific epithet 'hongheensis' refers to Honghe, Yunnan Province, where the holotype was collected.

Holotype: HKAS146012

Saprobic on dead twigs of an unknown deciduous host. Sexual morph: *Ascomata* 370–520 μm high × 290–400 μm diam. ($\bar{x}$ = 448.1 × 324.4 μm, n = 5), solitary, semi-immersed, black, subglobose to ampulliform, glabrous, papillate, and ostiolate. *Ostiolar neck* 120–150 μm long and 50–70 μm wide, clypeate, elongated, papillate, with periphyses, central, made up of pigmented, pseudoparenchymatous cells. *Peridium* 20–50 μm wide, of equal thickness, composed of several celled layers of small, brown to dark brown, pseudoparenchymatous cells of *textura angularis*, outer layers composed of brown to dark brown cells, fused with host tissues, lighter towards the inside of ascomata, peripheral cells are darker. *Hamathecium* comprising 1.5–2 μm wide, numerous, filamentous, unbranched, aseptate, trabeculate pseudoparaphyses, observed between and above the asci, embedded in a gelatinous matrix. *Asci* 150–210 × 8–12 μm ($\bar{x}$ = 186.2 × 10.1 μm, n = 20), 8-spored, bitunicate, cylindrical, short-pedicellate, with rounded apex. *Ascospores* 110–180 × 3–4 μm ($\bar{x}$ = 141.9 × 3.4 μm, n = 20), multi-seriate, tightly fasciculate, hyaline, filiform, straight or slightly curved, multi-septate, up to 20 septa, without constrictions at the septa, rounded at both ends, apical end broader than the basal end, smooth-walled, guttulate in most cells. Asexual morph: Undetermined.

Materials examined: China, Yunnan, Honghe Hani and Yi Autonomous Prefecture, Honghe County, 23.421068 N, 102.229128 E, 735 m, on dead twigs of an unknown deciduous host, 22 April 2020, D.N. Wanasinghe, DWHH23-58-02 (holotype, HKAS146012); *ibid*., 23 April 2020, DWHH23-58-03 (HKAS146013).

GenBank numbers: HKAS146012: ITS = PV742887, LSU = PV742943, SSU = PV742998, *tef*1-α = PV700626, *rpb*2 = PV700675;

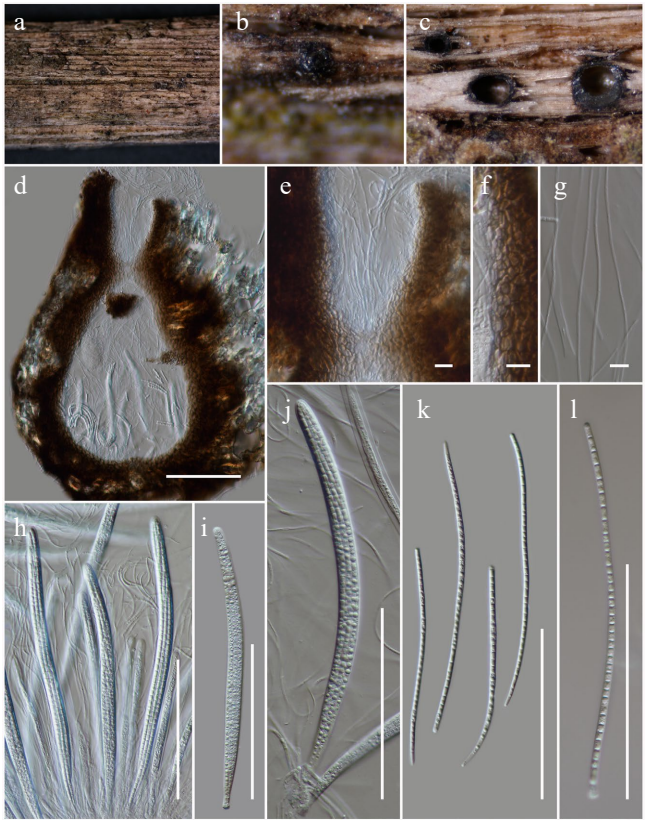

Fig. 6 *Longiascospora hongheensis* (HKAS146012, holotype). (a), (b) Ascomata on dead woody twigs. (c), (d) Sections of ascomata. (e) Close up of ostiole. (f) Peridium. (g) Pseudoparaphyses. (h)–(j) Asci. (k), (l) Ascospores. Scale bars: (d), (h)–(l) = 100 μm, (e)–(g) = 10 μm.

HKAS146013: ITS = PV742888, LSU = PV742944, SSU = PV742999, *tef*1-α = PV700627, *rpb*2 = PV700676.

Notes: The ascomata, peridium, pseudoparaphyses, and asci characteristics of this species resemble those found in *Pleurotremataceae*. However, the ascospore features are unique, as they are filiform. Phylogenetically, this species constitutes a basal lineage within the family, forming a distinct clade, which warrants its placement in a new genus.

Hysteriales Lindau, Die Natürlichen Pflanzenfamilien nebst ihren Gattungen und wichtigeren Arten 1 (1): 265.

Hysteriaceae Chevall., Flore Générale des Environs de Paris 1: 432.

Rhytidhysteron Speg., Anales de la Sociedad Científica Argentina 12 (4): 188.

Notes: *Rhytidhysteron* is commonly known as a saprobic fungi that occur on a wide range of hosts in terrestrial and marine habitats[78–81]. However, some species have been reported as endophytes and weak pathogens on woody plants as well as a human pathogen causing subcutaneous phaeohyphomycosis in immunocompetent patients in tropical regions[79–86]. The genus was introduced by Spegazzini[87], and later *Rhytidhysteron brasiliense* was designated as the type species by Clements and Shear[88]. Currently, 43 species epithets are listed in Index Fungorum[89]; however, Senwanna et al.[81]synonymized *R. erioi* under *R. bruguierae* and *R. mengziense* under *R. ligustrum*. Therefore, only 41 species are accepted in *Rhytidhysteron*, of which only about 24 species could be clarified in their phylogenetic placement in *Rhytidhysteron*. In the present study, the new host record for *R. neorufulum* was reported on dead twigs of an unknown deciduous host in Yunnan, China.

Rhytidhysteron neorufulum Thambug. & K.D. Hyde, Cryptog. Mycol. 37 (1): 110 (Figs 7 and 8).

MycoBank No: 551865

Saprobic on dead twigs of an unknown deciduous host. Sexual morph: *Ascomata* 1,000–2,000 μm long × 300–400 high × 350–450 μm diam. ($\bar{x}$ = 1,550 × 360.6 × 380.3 μm, n = 5), hysterothecial when young, becoming irregularly apothecioid when mature, superficial, coriaceous, erumpent, oblong or linear, rarely spherical, solitary or often gregarious, longitudinally striate and navicular in shape with tapering ends at maturity, black and carbonaceous when dry, arranged in parallel lines. *Excipulum* 40–80 μm wide, with the ectal excipulum narrow, layered, deep, and thick-walled, with black cells of *textura globulosa* to *textura angularis*, with *textura epidermoidea* at the base (hypothecium); the medullary excipulum composed of narrow, long, thin-walled, hyaline to brown cells of *textura angularis*. *Hamathecium* composed of 1.5–4 μm wide, numerous, propoloid, pseudoparaphyses, exceeding asci in length, apically swollen, branched, and reddish-orange pigmented; the branched apices form a layer on the hymenium to develop pseudo-epithecium. *Asci* 190–230 × 12.5–16 μm ($\bar{x}$ = 213.3 × 13.7 μm, n = 20), 8-spored, bitunicate, cylindrical, hyaline, short pedicellate, with a sinuous base, rounded apex with a well-developed ocular chamber. *Ascospores* 30–36 × 10–13 μm ($\bar{x}$ = 31.6 × 11.9 μm, n = 30), uni-seriate, light brown to yellowish brown when young, becoming dark brown when mature, ellipsoidal to fusiform, acute at both ends, 1–3-septate, rough-walled at immature stage, smooth-walled, guttules present at each cell upon maturity. Asexual morph: Undetermined.

Material examined: China, Yunnan, Honghe Hani and Yi Autonomous Prefecture, Honghe County, Dayangjiexiang, 23.390025° N, 102.225942° E, 1,186 m, on dead twigs of an unknown deciduous host, 13 March 2023, D.N. Wanasinghe, DWHH11 (HKAS146014), living culture, KUNCC23-16768.

GenBank numbers: KUNCC23-16768: ITS = PV742889, LSU = PV742945, SSU = PV743000, *tef*1-α = PV700628.

Known hosts and distribution: Saprobic on undetermined dead stem[83]; *Hevea brasiliensis*[90,91], *Tectona grandis*[92], *Magnolia* sp.[93], and *Rosa damascena*[81] in Thailand; on undetermined hosts in Brazil[94], Europe, and Ghana[95]; on *Bursera* sp. in Mexico[96]; on decaying wood of *Elaeagnus sarmentosa*[80], *Magnolia* sp.[93], and an unknown deciduous host (this study) in Yunnan, China.

Notes: Multigene phylogenetic analyses demonstrated that the new strain KUNCC23-16768 clustered within the monophyletic subclade of *Rhytidhysteron neorufulum* with 80% MLBS and 0.95 BYPP support (Fig. 7) and is closely related to *R. neorufulum* (MFLUCC 12-0567). The new isolate (KUNCC23-16768) resembles the type of *R. neorufulum* in having hysterothecial, navicular to lenticular or irregular in shape, with longitudinally slit, cylindrical asci and brown to dark brown, 3-septate ascospores. However, the new isolate has slightly longer ascomata (1,000–2,000 μm long vs 660–1,415 μm long), larger asci (190–230 × 12.5–16 μm vs 185–220 × 9.5–13 μm), and larger ascospores (30–36 × 10–13 μm vs 27–34 × (6.5–)7–10.6(–12.5))[83].

Mycosphaerellales (Nannf.) P.F. Cannon, Ainsworth & Bisby's Dictionary of the fungi, Ed. 9: X.

Mucomycosphaerellaceae Wanas., Phookamsak, L.S. Dissan. & J.C. Xu, **fam. nov.**

MycoBank No: 859352

Etymology: Referring to the name of the type genus

Saprobic on leaves and twigs. Sexual morph: *Ascomata* pseudothecial, solitary or in clusters of two or more joined together, immersed to erumpent, brown to dark brown, globose, ellipsoid to greatly elongated, or depressed ellipsoidal uni- to multi-locular, ostiolate, lacking periphyses. *Peridium* thin- to thick-walled of unequal thickness, thicker at the side towards the apex, composed of several layers of brown cells of *textura angularis*, to *textura globulosa* or *textura epidermoidea*, poorly developed at the base.

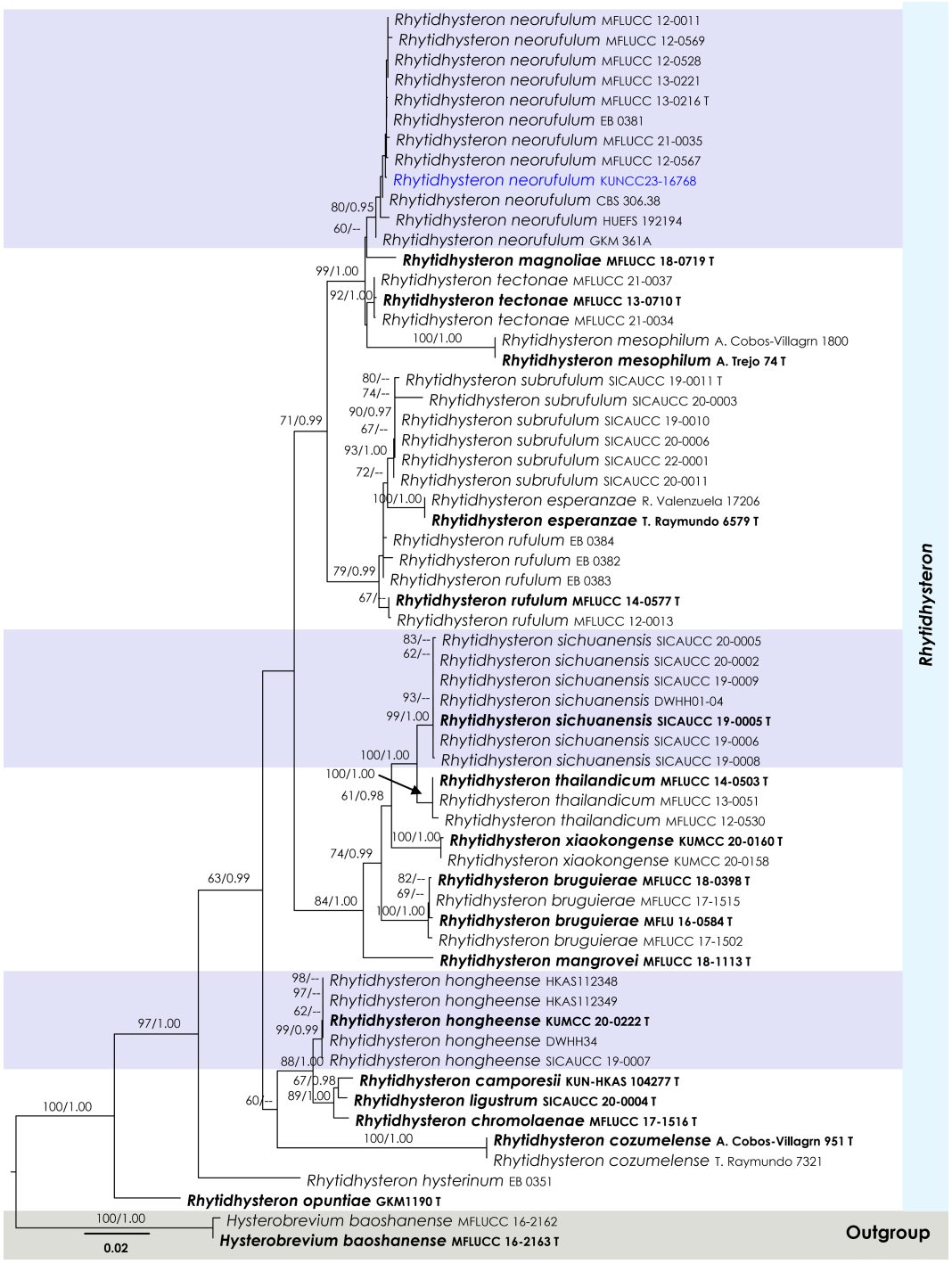

Fig. 7 Maximum Likelihood tree inferred from the concatenated dataset of partial SSU, LSU, ITS, and *tef*1-α sequences. The phylogeny is rooted with *Hysterobrevium baoshanense* (MFLUCC 16-2162, MFLUCC 16-2163). The final likelihood value is –10,916.669025. The final alignment included 813 unique site patterns, with approximately 23.31% of the positions comprising gaps or ambiguous characters. The estimated nucleotide frequencies were as follows: A = 0.240255, C = 0.247157, G = 0.276188, T = 0.236399. The substitution model yielded the following relative rates: AC = 1.376740, AG = 2.437005, AT = 1.147691, CG = 0.904034, CT = 5.839891, GT = 1.000000. The proportion of invariable sites (I) was estimated at 0.618399, and the gamma distribution shape parameter (α) was 0.641873. Bayesian inference reached convergence after 761,000 generations, when the average standard deviation of split frequencies dropped below 0.01 (observed value: 0.009903). A total of 7,611 trees were sampled, and 5,709 of these were retained for the final analysis after discarding the initial 25% as burn-in. The alignment also revealed 814 distinct informative sites. In the resulting phylograms, sequences generated in this study are highlighted in blue, while ex-type or type strains are indicated in boldface.

Hamathecium lacking pseudoparaphyses; if present, composed of sparse, branched, and anastomosing septate pseudoparaphyses. *Asci* 8-spored, bitunicate, fissitunicate, fasciculate, ellipsoidal to ovoid, or ampulliform, apedicellate, or with a short pedicel, apically rounded with distinct ocular chamber. *Ascospores* overlapping multi-seriate, hyaline, oblong to narrowly fusiform, or elongate ellipsoidal, sometimes inequilateral, rounded apex and acute at the bottom, septate, constricted at the septa, deeply constricted at the central septum, rough-walled, guttulate, surrounded by a thick mucilaginous sheath. Asexual morph: Undetermined.

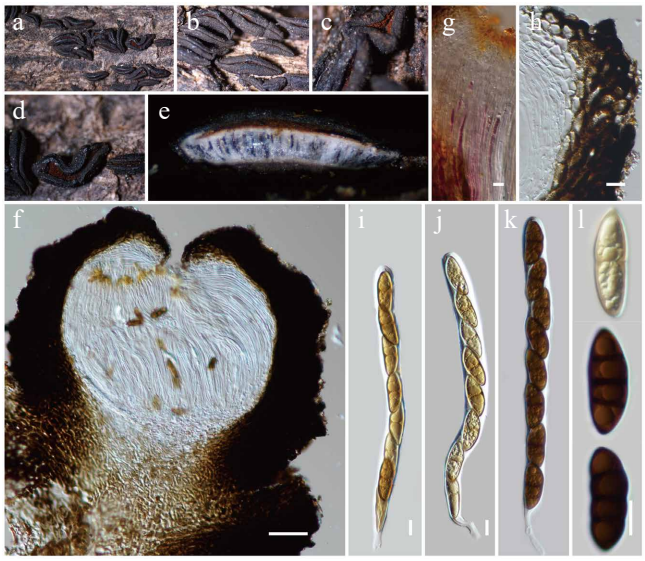

Fig. 8 *Rhytidhysteron neorufulum* (HKAS146014). (a)–(d) Appearance of hysterothecia on the dead woody twigs. (e) Horizontal section of hysteriothecium. (f) Cross-section of an ascoma. (g) Pseudoparaphyses. (h) Excipulum. (i)–(k) Asci. (l) Ascospores. Scale bars: (f) = 100 μm, (g)–(l) = 10 μm.

Type genus: *Mucomycosphaerella* Quaedvl. & Crous.

Notes: Quaedvlieg et al.[97] introduced *Mucomycosphaerella* to accommodate *M. eurypotami* (≡*Mycosphaerella eurypotami*). In this study, *Mucomycosphaerellaceae* is proposed as a novel family within *Mycosphaerellales* to accommodate *Mucomycosphaerella*. The genus *Mucomycosphaerella* is distinguished from *Mycosphaerella sensu stricto* by the presence of persistent mucoid sheaths surrounding the ascospores and the absence of *Ramularia* asexual states. *Mucomycosphaerella* ascomata are typically depressed with a pale, thin-walled lower half and the hamathecium consists of loosely branched, anastomosing hyphae embedded in a hymenial gel. Ascospores are hyaline. *Mucomycosphaerella eurypotami* was provisionally included in *Mycosphaerella* pending a formal genus revision, a process initiated with the epitypification of the type species[98] and subsequent segregation of allied genera and families[99,100]. Quaedvlieg et al.[97] suggested *Mucomycosphaerella* represents a distinct family within *Capnodiales*, closely related to *Schizothyriaceae*. However, with the addition of another species to *Mucomycosphaerella*, phylogenetic analyses have now placed it outside *Capnodiales* and instead within *Mycosphaerellales*, allied closely with *Aeminiaceae*, *Cystocoleaceae*, *Extremaceae,* and *Neodevriesiaceae*. *Aeminiaceae*, established by Trovão et al.[101], includes the monotypic genus *Aeminium*, known only from its hyphomycetous asexual morph characterized by dark brown, thick-walled, septate conidia forming in meristematic chains. *Cystocoleaceae* accommodates the lichenized genus *Cystocoleus*, distinguished by its dense filamentous thallus with *Trentepohlia* photobionts and a unique hyphal sheath composed of jigsaw puzzle-shaped cells[102]. *Extremaceae* was introduced by Quaedvlieg et al.[97] to accommodate lichenicolous or yeast-like taxa, with *Extremus* designated as the type genus. The family is characterized by solitary to sporodochial conidiophores that proliferate sympodially or possess a terminal rachis that may be subdenticulate; conidia are brown, solitary or in short, mostly unbranched chains, subcylindrical to narrowly fusoid-ellipsoidal or obclavate, rarely with 1–2 transverse septa, often surrounded by a mucoid sheath, and exhibit non- to slightly darkened hila. *Neodevriesiaceae* was also introduced by Quaedvlieg et al.[97], with *Neodevriesia* as the type genus. This family is known for having both sexual and asexual morphs and is characterized in the sexual morph by black, immersed, substromatic ascomata; 8-spored, bitunicate, subsessile, obovoid to broadly ellipsoid asci that are aparaphysate; and hyaline, thick-walled, fusoid-ellipsoidal, 1-septate ascospores. The asexual morph features pigmented, sympodially proliferating conidiophores, and brown, solitary or short unbranched chains of subcylindrical to narrowly fusoid-ellipsoidal or obclavate conidia, which are rarely septate. Morphologically, *Mucomycosphaerella* resembles taxa in *Neodevriesiaceae* in having solitary or stromatic ascomata, ellipsoidal to ovoid asci, and hyaline, fusoid-ellipsoidal, septate ascospores. However, the ascospores of *Mucomycosphaerella* are often covered by a thick mucilaginous sheath, a feature absent in *Neodevriesiaceae*. Previously, *Mucomycosphaerella* was treated as a genus *incertae sedis* within *Mycosphaerellales*[59]. Rather than leaving it orphaned, *Mucomycosphaerellaceae* fam. nov. was formally introduced to accommodate *Mucomycosphaerella*. Phylogenetic analyses confirm *Mucomycosphaerellaceae* as a monophyletic lineage basal to *Aeminiaceae* (Fig. 9).

Mucomycosphaerella Quaedvl. & Crous, Persoonia 33: 22.

Notes: *Mucomycosphaerella* has been a monotypic genus for the past decade, and in this study, the second species is introduced to the genus from Yunnan, China. Phylogenetically, the generic clade forms an independent lineage within *Mycosphaerellales*, suggesting that it warrants recognition as a separate family.

Mucomycosphaerella hongheensis Wanas., Phookamsak, L.S. Dissan. & J.C. Xu, **sp. nov.** (Figs 9 and 10)

MycoBank No: 859353

Etymology: The specific epithet 'hongheensis' refers to Honghe, Yunnan Province, where the holotype was collected.

Holotype: HKAS146015

Saprobic on dead twigs of an unknown deciduous host. Sexual morph: *Ascomata* 300–400 μm high × 70–100 μm diam. ($\bar{x}$ = 353 × 88 μm, n = 5), solitary, or in clusters, immersed, raised, becoming superficial, stomatic, globose, ellipsoid to greatly elongated, uni- to multi-locular, with a blunt opening ostiole of each locule. *Peridium* 20–30 μm wide, of unequal thickness, poorly-developed at the base, comprises several layers of brown to dark brown pseudoparenchymatous cells of *textura angularis* to *textura globulosa*, or *textura epidermoidea* at sides towards the apex, inner layer composed of 1 to 2 layers of flattened, hyaline cells. *Hamathecium* lacks pseudoparaphyses. *Asci* 50–90 × 25–40 μm ($\bar{x}$ = 62.7 × 31.2 μm, n = 20), 8-spored, bitunicate, fasciculate, ovoid to ampulliform, sessile to subsessile, or short pedicel, apically rounded with a distinct ocular chamber. *Ascospores* 18–25 × 6.5–9.5 μm ($\bar{x}$ = 21.7 × 7.4 μm, n = 40) overlapping multi-seriate, hyaline, oblong, with rounded ends, (2–)3-septate, constricted at septa, deeply constricted at the central septum, smooth-walled, guttulate at each cell, surrounded by a thick mucilaginous sheath (10–15 μm diam.). Asexual morph: Undetermined.

Culture characteristics: Colonies growing fast on PDA at room temperature (25 °C) under normal light, reaching 55 mm diam. after two weeks. Colonies dense at the center, sparse at the margin, circular, flat, slightly raised, with convex edge separating the margin, surface smooth, with edge entire, cottony at the center, feathery at the margin, smooth aspect, colonies white from above and below, do not produce pigmentation in PDA.

Materials examined: China, Yunnan, Honghe Hani and Yi Autonomous Prefecture, Honghe County, 23.421068° N, 102.229128° E, 735 m, on dead twigs of an unknown deciduous host, 22 April 2020, D.N. Wanasinghe, DWHH19-02 (holotype, HKAS146015), ex-type, KUNCC23-16782; *ibid*., 23 April 2020, DWHH19-02-01 (paratype, HKAS146016), ex-paratype, KUNCC25-19458.

GenBank numbers: KUNCC23-16782: ITS = PV742890, LSU = PV742946, *rpb2* = PV738665, ACT = PV738670, CAL = PV738674; HKAS146016: ITS = PV742891, LSU = PV742947, *rpb2* = PV738666, ACT = PV738671, CAL = PV738675.

Notes: Phylogenetic analyses of a combined LSU, ITS and *rpb2* sequence data demonstrated that two strains of *Mucomycosphaerella hongheensis* (KUNCC23-16782 and KUNCC25-19458) formed a robust subclade and clustered with *M. eurypotami* (JK 5586J) with 100% MLBS and 1.00 BYPP support (Fig. 9). *Mucomycosphaerella hongheensis* can be distinguished from *M. eurypotami* in having larger ascomata (300–400 μm high × 70–100 μm diam. vs 115–130 μm high, 190–300 μm diam.), lacking of pseudoparaphyses, and shorter and broader ascospores (18–25 μm × 6.5–9.5 μm vs 23–29 × 5.5–6.5 μm)[103] with (2–)3-euseptate, covered by irregular mucilaginous sheath. In contrast, ascospores of *M. eurypotami* are 1-euseptate, with one additional pseudoseptum in each cell, surrounded by a rounded mucilaginous sheath. Therefore, the new species, *M. hongheensis*, is introduced herein based on morphological distinctiveness and phylogenetic evidence.

Patellariales D. Hawksw. & O.E. Erikss., Systema Ascomycetum 5: 181.

Patellariaceae Corda, Icones fungorum hucusque cognitorum 2: 37.

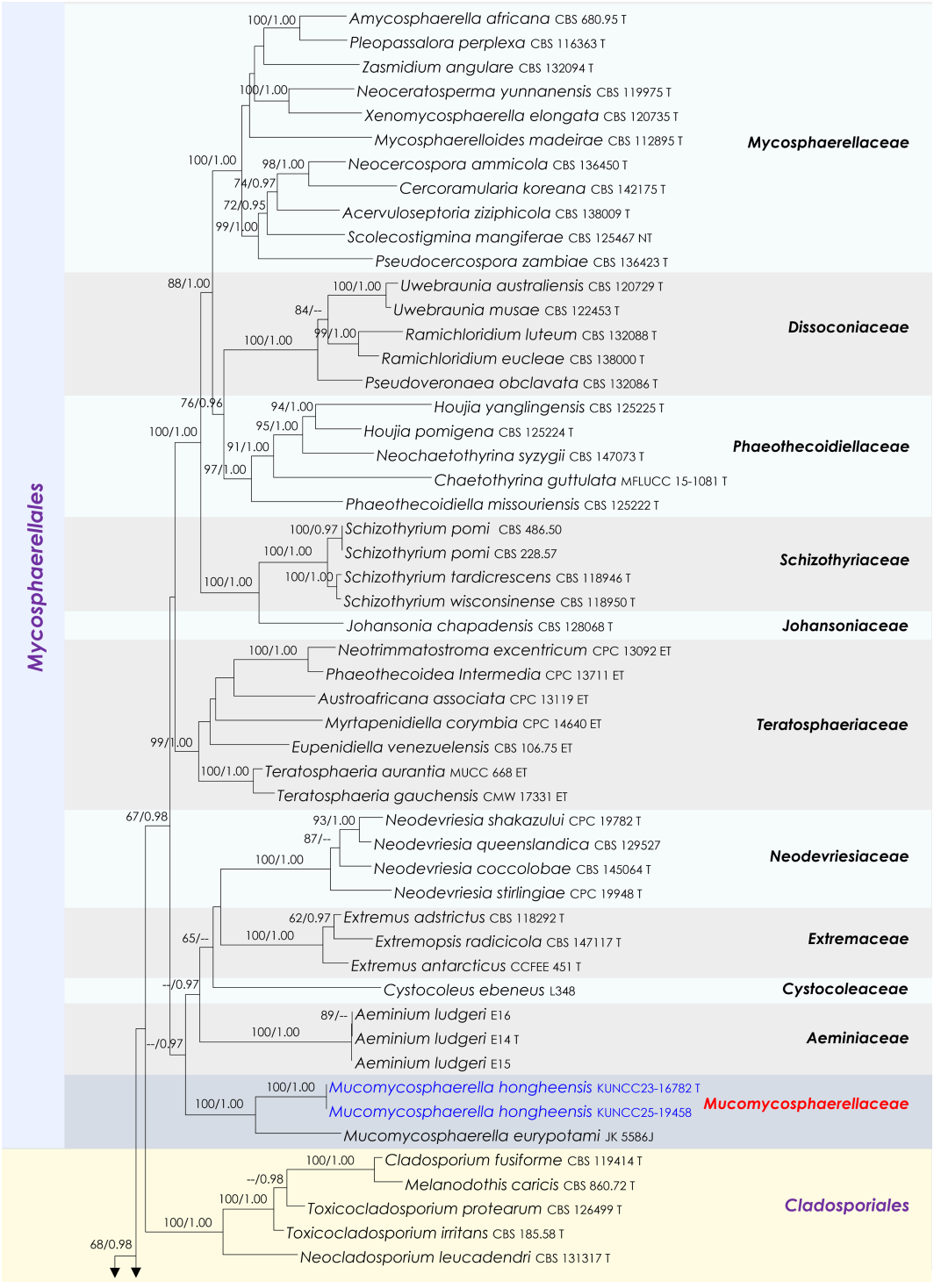

Fig. 9 (to be continued)

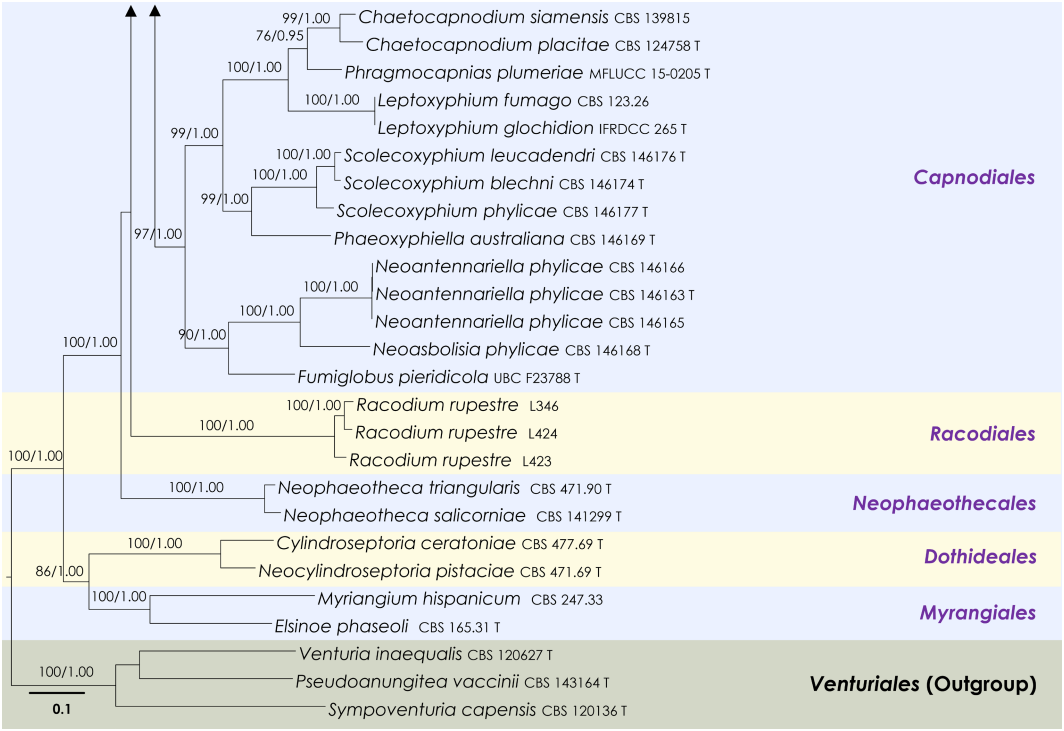

Fig. 9 Maximum Likelihood tree inferred from the concatenated dataset of partial LSU, ITS and *rpb*2 sequences. The phylogeny is rooted with *Pseudoanungitea vaccinii* (CBS 143164), *Sympoventuria capensis* (CBS 120136) and *Venturia inaequalis* (CBS 120627). The final likelihood value is –46,883.414087. The final alignment included 1,712 unique site patterns, with approximately 28.99% of the positions comprising gaps or ambiguous characters. The estimated nucleotide frequencies were as follows: A = 0.244142, C = 0.249865, G = 0.288498, T = 0.217496. The substitution model yielded the following relative rates: AC = 2.074748, AG = 3.272618, AT = 1.73051, CG = 1.485905, CT = 7.286184, GT = 1.000000. The proportion of invariable sites (I) was estimated at 0.36136 and the gamma distribution shape parameter (α) was 0.702452. Bayesian inference reached convergence after 467,000 generations, when the average standard deviation of split frequencies dropped below 0.01 (observed value: 0.009979). A total of 2,336 trees were sampled, and 1,752 of these were retained for the final analysis after discarding the initial 25% as burn-in. The alignment also revealed 1,714 distinct informative sites. Newly generated sequences are shown in blue. Ex-type and type strains are indicated with a 'T' at the end of the strain number.

Fig. 10 *Mucomycosphaerella hongheensis* (HKAS146015, holotype). (a) Ascomata on the dead woody twigs. (b), (c) Cross-section of ascomata. (d) Peridium. (e) Asci. (f)–(h) Ascospores. Scale bars: (b), (c) = 100 μm, (d)–(h) = 10 μm.

Patellaria Fr., Systema Mycologicum 2 (1): 158.

Notes: *Patellaria* is commonly known as sabprobe on decaying wood, stems, or bark in terrestrial and marine habitats[79,104]. The genus was introduced by Fries[105] with *P. atrata* as the type species and is characterized by apothecial, superficial, black, circular, flattened, sessile ascomata, with a carbonaceous rim, exposing the dark hymenium at the center; exciple composed of blue-black (hypothecium) or green-blue to colourless pseudoparenchymatous cells; 8-spored, bitunicate, fissitunicate, cylindrical to clavate, short pedicelate asci, embedded in septate, branched paraphyses, with slightly swollen and rounded apex, forming a dark and thick epithecium over the asci; and clavate to fusiform, or allantoid, hyaline, septate ascospores[75,104,106]. Presently, more than 1,400 species epithets are listed in Index Fungorum[89]. However, only about 50 morpho-species were accepted by Hyde et al.[59], of which 15 species have molecular data available in GenBank[104]. In this study, *Patellaria microspora* is reported on dead twigs of an unknown deciduous host in Yunnan, China, for the first time.

Patellaria microspora Ekanayaka & K.D. Hyde, Fungal Diversity 105: 131 (2020) (Figs 11 and 12).

MycoBank No: 557819

Saprobic on dead twigs of an unknown deciduous host. Sexual morph: *Ascomata* 160–220 high × 550–700 diam. μm ($\bar{x}$ = 180.4 × 601.2 μm, n = 5), apothecial, superficial, scattered, solitary or in groups, longitudinally wide, exposing the dark hymenium at the centre, circular, flattened, sessile, with a black, carbonaceous rim closed at first and open at maturity. *Receptacle* turbinate, slightly convex disc, with blue-black margin. *Exciple* 40–60 μm wide, composed of two-layered, thick-walled, pseudoparenchymatous cells, ectal excipulum comprised four to six celled layers, of black, thick-walled cells of *textura angularis* to *textura globulosa*, medullary excipulum composed of narrow, long, thin-walled, hyaline to brown cells of *textura prismatica*, blackish brown at the base (hypothecium) with cells of *textura angularis*. *Hamathecium* composed of 1.5–3 μm wide, hyaline, septate, branched paraphyses, swollen and rounded at the apex, forming a dark and thick epithecium over the asci. *Asci*

90–110 × 18–24 μm ($\bar{x}$ = 97.6 × 21.6 μm; n = 10), 8-spored, bituni-cate, fissitunicate, broadly cylindrical to cylindric-clavate, subsessile to short pedicel, apically rounded, with an inconspicuous ocular chamber. *Ascospores* 35–50 × 9–11 μm ($\bar{x}$ = 40.1 × 10.3 μm; n = 20), overlapping bi-seriate, cylindric-clavate to oblong, slightly curved, narrowed at the lower end, 7–9-septate, hyaline. Asexual morph: Undetermined.

Culture characteristics: Colonies grow slowly on PDA at room temperature (25 °C) under normal light, reaching 30–35 mm diam. after four weeks. Colonies dense, circular, raised, slightly umbonate, surface smooth, with edge entire, cottony, smooth aspect, do not produce pigmentation in PDA. Colonies from above grey to greenish grey, with darker greenish grey radiating near the margin, separated the margin from the center; colonies from below dark grey to black at the margin and paler greenish black towards the center.

Materials examined: China, Yunnan, Honghe Hani and Yi Autonomous Prefecture, Honghe County, 23.421013° N, 102.227243° E, 517 m, on dead twigs of an unknown deciduous host, 03 December 2020, D.N. Wanasinghe, DWHH18-01 (HKAS146017), living culture, KUNCC23-16777; *ibid*., DWHH18-01-2 (HKAS146018), living culture, KUNCC25-19457.

GenBank numbers: KUNCC23-16777: ITS = PV742892, LSU = PV742948, SSU = PV743001, *tef*1-α = PV700629; HKAS146018: ITS = PV742893, LSU = PV742949, SSU = PV743002, *tef*1-α = PV700630.

Known hosts and distribution: Saprobic on dead stems of unidentified plants in the UK[75]; on dead twigs of an unknown deciduous host in Yunnan, China (this study).

Notes: Phylogenetically, two new strains (KUNCC23-16777 and KUNCC25-19457) formed a subclade (100% MLBS, 1.00 BYPP; Fig. 11) with the type of *Patellaria microspora* (MFLU 16-0567) and clustered with *P. chromolaenae* (MFLUCC 17-1482, MFLUCC 17-1479 and MFLU 16-0567) with 100% MLBS and 1.00 BYPP support values (Fig. 11). Morphologically, the new isolates are similar to the type of *P. microspora* (MFLU 16-0567) in having apothecial, sessile ascomata with turbinate, convex disc of receptacle, cylindric-clavate asci and hyaline, cylindric-clavate, smooth-walled, 7–9-septate ascospores. However, there are some dimensional differences observed in the apothecia (550–700 μm diam. vs 396–402 μm diam.) and ascospores (35–50 × 9–11 μm vs 19.2–20.3 × 8.7–9.5 μm)[75]. These variations may have arisen as a result of the species adapting to distinctly different ecological zones. It is also noteworthy that the ascus measurements provided by Hongsanan et al.[75] appear to be inconsistent with the scale bars shown in their Fig. 65, suggesting a

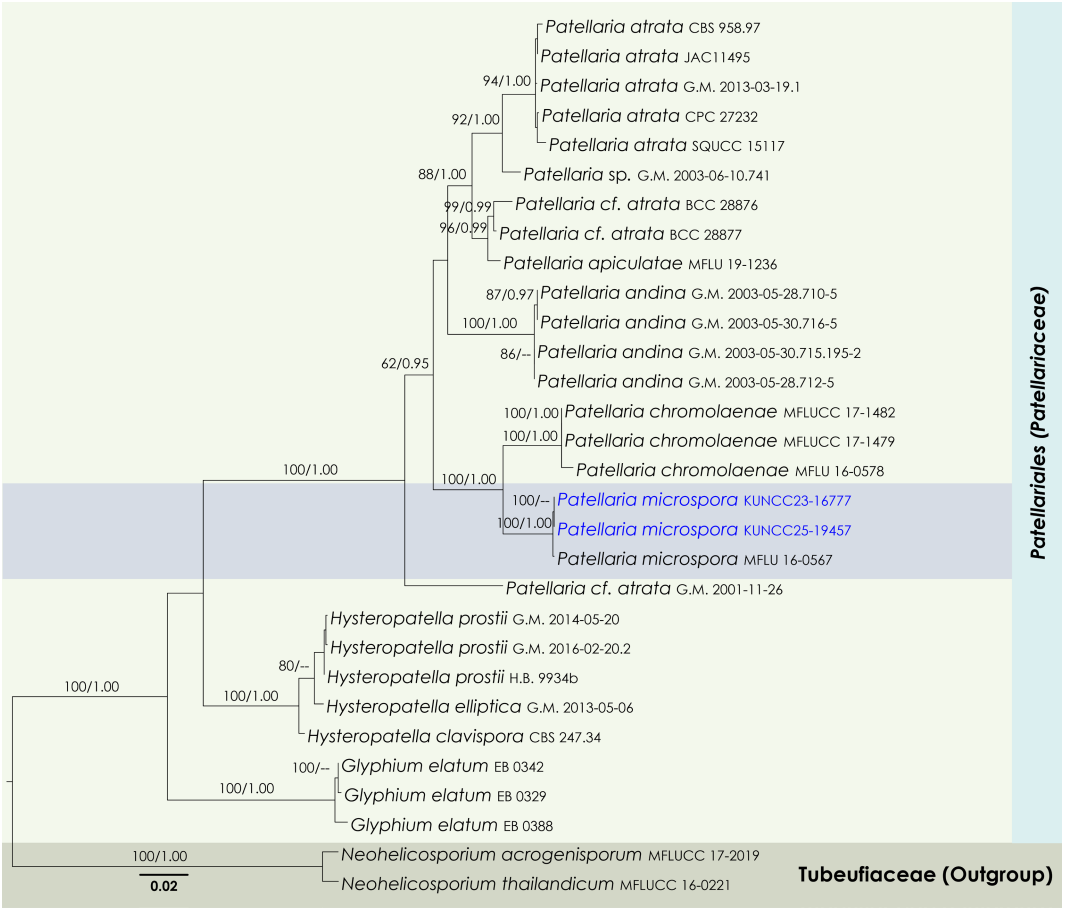

Fig. 11 Maximum Likelihood tree inferred from the concatenated dataset of partial SSU, LSU, ITS, and *tef*1-α sequences. The phylogeny is rooted with *Neohelicosporium acrogenisporum* (MFLUCC 17-2019) and *N. thailandicum* (MFLUCC 16-0221). The final likelihood value is –9911.771441. The final alignment included 749 unique site patterns, with approximately 42.67% of the positions comprising gaps or ambiguous characters. The estimated nucleotide frequencies were as follows: A = 0.245832, C = 0.243333, G = 0.273432, T = 0.237402. The substitution model yielded the following relative rates: AC = 2.866237, AG = 3.728289, AT = 2.673312, CG = 1.344539, CT = 15.427322, GT = 1.000000. The proportion of invariable sites (I) was estimated at 0.580820, and the gamma distribution shape parameter (α) was 0.704216. Bayesian inference reached convergence after 176,000 generations, when the average standard deviation of split frequencies dropped below 0.01 (observed value: 0.009992). A total of 881 trees were sampled, and 661 of these were retained for the final analysis after discarding the initial 25% as burn-in. The alignment also revealed 754 distinct informative sites. In the resulting phylograms, sequences generated in this study are highlighted in blue.

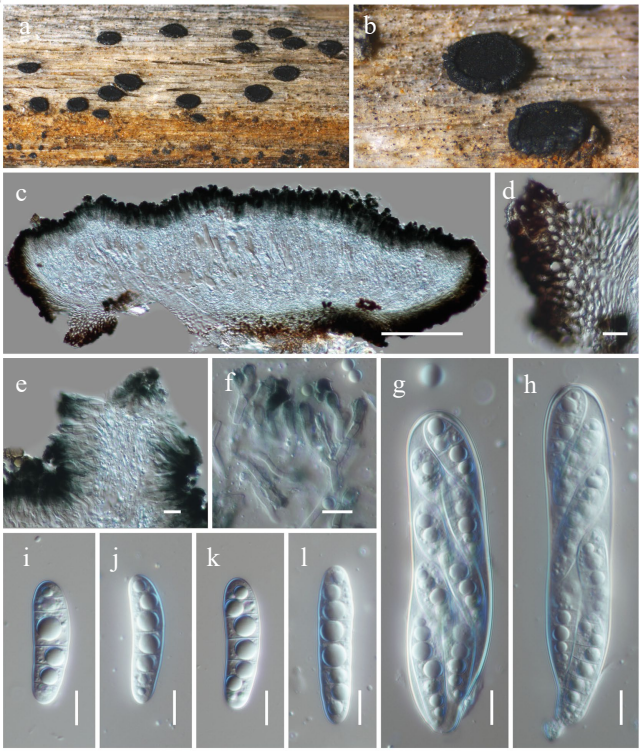

Fig. 12 *Patellaria microspora* (HKAS146017). (a), (b) Apothecia on host substrate. (c) Cross-section of an apothecial ascoma. (d) Exciple. (e) Paraphyses. (f) Branched paraphyses, with swollen and rounded at the apex. (g), (h) Asci. (i)–(l) Ascospores. Scale bars: (c) = 100 μm, (d)–(h) = 10 μm.

potential error in the original description. Nucleotide comparison between *Patellaria microspora* (MFLU 16-0567) and our new strains revealed only a two-base pair difference in the ITS region, while other regions were identical.

Pleosporales Luttr. ex M.E. Barr, Prodromus to class Loculoascomycetes: 67

Anteagloniaceae K.D. Hyde & A. Mapook, Fungal Diversity 63 (1): 33

Anteaglonium Mugambi & Huhndorf, Systematics and Biodiversity 7 (4): 460

Notes: *Anteaglonium* is commonly known as saprobes and endophytes on barks, branches, leaves, twigs, and wood of a wide range of shrubs and tree plants, as well as inhabiting rock[107–112]. *Anteaglonium* was introduced by Mugambi & Huhndorf[113], and is typified by *A. abbreviatum*. The genus is known for both sexual and asexual morphs that are characterized by hysterothecial, superficial, carbonaceous ascomata, with slit-like opening ostiolar, 8-spored, bitunicate, fissitunicate, elongate, cylindric-clavate to cylindrical asci, with short pedicellate, and hyaline, fusiform to oblong, 1-septate ascospores[110]. Coelomycetous asexual morph of *Anteaglonium* is characterized by pycnidial, subglobose to globose, superficial to subperidermal, uni- to multi-loculate conidiomata, cylindrical, unbranched conidiophores, phialidic, globose, smooth-walled conidiogenous cells, and hyaline, oblong to ellipsoidal or oval, aseptate, smooth-walled conidia[110,112]. Presently, there are 12 species accepted in this genus. In this study, the new species, *Anteaglonium hongheense*, is introduced on dead twigs of *Quercus* sp. in Yunnan, China based on morphological characteristics and phylogenetic evidence.

Anteaglonium hongheense Wanas., Phookamsak, L.S. Dissan. & J.C. Xu, **sp. nov.** (Figs 13 and 14).

MycoBank No: 859354

Etymology: The specific epithet 'hongheense' refers to Honghe, Yunnan Province, where the holotype was collected.

Holotype: HKAS146019

Saprobic on dead twigs of *Quercus* sp. Sexual morph: *Hysterothecia* 350–500 μm long × 150–180 μm high × 170–220 μm diam. ($\bar{x}$ = 419.2 × 169.3 × 191.2 μm, n = 10), superficial, carbonaceous, black, subglobose to oblong, straight, smooth or slightly striate laterally, with a longitudinal slit, sulcus shallow, gregarious, lying at irregular angles, occurring on a black thin crust, tending to darken the substratum. *Peridium* 20–40 μm wide, carbonaceous, brittle with age, longitudinally striated at the margins, equally thickened, the inner layer compressed and pallid, the outer layer thickened, comprising pigmented cells of *textura angularis*. *Hamathecium* 1–2 μm wide, comprising numerous, aseptate pseudoparaphyses, branched above the asci. *Asci* 40–50 × 3.5–4.5 μm ($\bar{x}$ = 45.6 × 4.2 μm; n = 20), 8-spored, bitunicate, cylindrical, short pedicellate, apically rounded, with an ocular chamber. *Ascospores* 6.5–7.2 × 3–3.3 μm ($\bar{x}$ = 6.9 × 3.2 μm; n = 30), obliquely to irregularly uni- to bi-seriate, hyaline, fusiform, straight, 1-septate, constricted at the middle septum, smooth-walled, guttulate. Asexual morph: Undetermined.

Materials examined: China, Yunnan, Honghe Hani and Yi Autonomous Prefecture, Jianshui County, Puxiongxiang 23.521432° N, 103.039049° E, 1,917 m, on dead twigs of *Quercus* sp., 15 March 2019, D.N. Wanasinghe, DW0528-09 (holotype, HKAS146019); *ibid*., DW1176-02 (HKAS146020).

GenBank numbers: HKAS146019: ITS = PV742894, LSU = PV742950, SSU = PV743003; HKAS146020: ITS = PV742895, LSU = PV742951, SSU = PV743004.

Notes: Multigene phylogenetic analyses revealed that *Anteaglonium hongheense* (HKAS146019 and HKAS146020) formed a sister subclade with *A. saxicola* (SDBR-CMU481 and SDBR-CMU482) (97% MLBS and 1.00 BYPP; Fig. 13). However, *Anteaglonium hongheense* is not morphologically comparable to *A. saxicola*, as the two species exhibit distinct morphs. *Anteaglonium saxicola* forms a coelomycetous asexual morph, characterized by pycnidial, dark brown to black, stromatic, globose to subglobose, ostiolate conidiomata; hyaline, ampulliform to subcylindrical, aseptate conidiogenous cells; and hyaline, subglobose to broadly ellipsoid, aseptate, smooth-walled conidia[112]. In contrast, *Anteaglonium hongheense* develops a sexual morph typical of *Anteaglonium*, with black, carbonaceous, hysterothecial ascomata and hyaline, fusiform, 1-septate ascospores[110,113]. Based on its distinct phylogenetic placement and morphological features, *Anteaglonium hongheense* is introduced here as a new species.

Didymellaceae Gruyter, Aveskamp & Verkley, Mycological Research 113 (4): 516.

Notes: *Didymellaceae* is one of the largest families in *Pleosporales* (*Dothideomycetes*), comprising approximately 50 genera and over 850 accepted species[59]. *Didymellaceae* species are cosmopolitan and inhabit a wide range of hosts and ecological niches, including terrestrial and aquatic environments[110,114–119]. Many taxa within this family have been documented as plant pathogens, endophytes, fungicolous fungi, lichenicolous fungi, or saprobes[110,114,115,118,120,121]. The family *Didymellaceae* was formally introduced by de Gruyter et al.[122], with *Didymella* designated as the type genus and *Didymella exigua* as the type species. In the present study, the most recent taxonomic treatments of *Didymellaceae* were followed followed Hongsanan et al.[110] and Hou et al.[118,119]. Based on a combination of multigene phylogenetic analyses and detailed morphological observations, the study introduces *Gruyteromyces* as a novel monophyletic genus within *Didymellaceae* to accommodate *G. hongheensis* sp. nov.

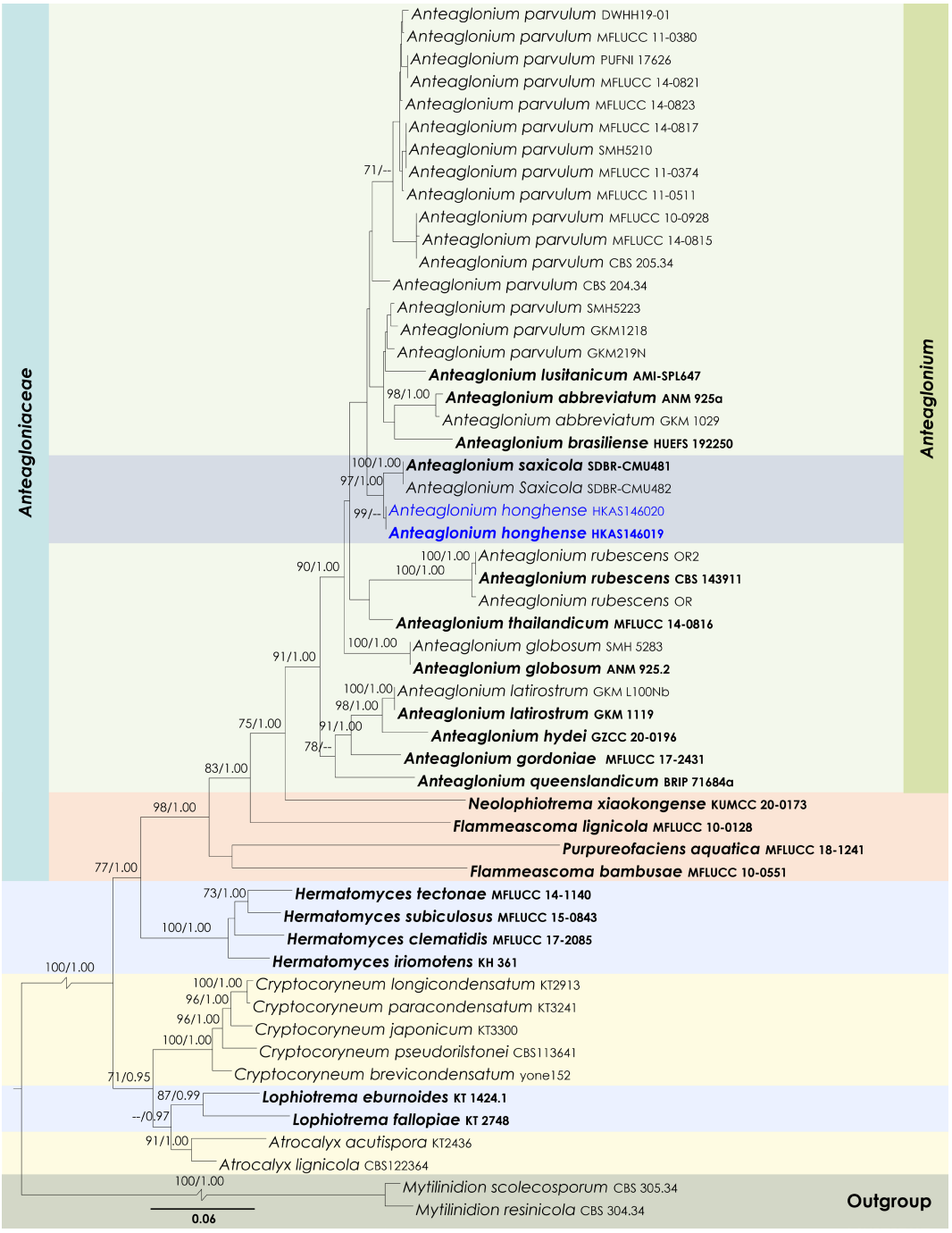

Fig. 13 Maximum Likelihood tree inferred from the concatenated dataset of partial SSU, LSU, ITS, *tef*1-α, and *rpb*2 sequences. The phylogeny is rooted with *Mytilinidion resinicola* (CBS 304.34) and *M. scolecosporum* (CBS 305.34). The final likelihood value is –24165.625703. The final alignment included 1,579 unique site patterns, with approximately 41.67% of the positions comprising gaps or ambiguous characters. The estimated nucleotide frequencies were as follows: A = 0.244857, C = 0.256513, G = 0.274249, T = 0.224381. The substitution model yielded the following relative rates: AC = 1.294483, AG = 3.792940, AT = 1.360675, CG = 1.200289, CT = 9.762669, GT = 1.000000. The proportion of invariable sites (I) was estimated at 0.455208, and the gamma distribution shape parameter (α) was 0.434309. Bayesian inference reached convergence after 2,141,000 generations, when the average standard deviation of split frequencies dropped below 0.01 (observed value: 0.009965). A total of 21,411 trees were sampled, and 16,059 of these were retained for the final analysis after discarding the initial 25% as burn-in. The alignment also revealed 1,580 distinct informative sites. In the resulting phylograms, sequences generated in this study are highlighted in blue, while ex-type or type strains are indicated in boldface.

Gruyteromyces Wanas., Phookamsak, L.S. Dissan. & J.C. Xu, **gen. nov.**
MycoBank No: 859355

Etymology: The generic epithet was given in honour of Johannes De Gruyter.

Saprobic on dead twigs of an unknown host. Sexual morph: Undetermined. Asexual morph: Coelomycetous. *Conidiomata* pycnidial, black, solitary, scattered, immersed to slightly erumpent, subglobose, uni-loculate, visible as small black dots on host surface, glabrous, with inconspicuous ostioles. *Pycnidial wall* composed of brown to dark brown pseudoparenchymatous cells of *textura angularis*. *Conidiophores* reduced to conidiogenous cells. *Conidiogenous cells* monoblastic, hyaline, smooth, phalidic, ampulliform, lining the conidiomatal cavity. *Conidia* ellipsoidal to oblong, hyaline, thin-walled, smooth to slightly rough, aseptate.

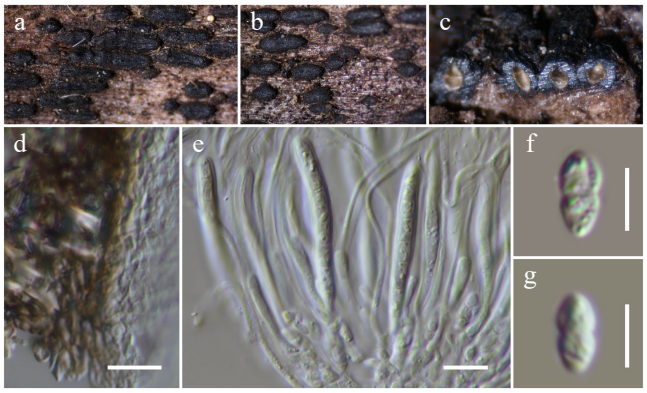

Fig. 14 *Anteaglonium hongheense* (HKAS146019, holotype). (a), (b) Hysterothecia on substrate. (c) Cross-section through hysterothecia. (d) Peridium. (e) Asci with pseudoparaphyses. (f), (g) Ascospores. Scale bars: (d), (e) = 10 μm, (f), (g) = 5 μm.

Type species: *Gruyteromyces hongheensis* Wanas. Phookamsak, & J.C. Xu

Notes: Multigene phylogenetic analyses revealed that *Gruyteromyces* forms a well-supported, monophyletic clade, representing an independent lineage within *Didymellaceae*. The genus is phylogenetically closely related to *Ectodidymella*, *Ectophoma,* and *Longididymella* (Fig. 15). Morphologically, *Gruyteromyces* exhibits characteristics typical of *Didymellaceae*, forming phoma-like asexual morphs similar to those observed in *Ectodidymella*, *Ectophoma,* and *Longididymella*[118]. However, *Gruyteromyces* can be distinguished from *Ectodidymella* by its small, subglobose conidiomata with inconspicuous ostioles, and ellipsoidal to oblong, hyaline, aseptate conidia that are smooth to slightly rough-walled. In contrast, *Ectodidymella* produces larger, globose to depressed-globose conidiomata, typically with a conspicuous neck, and oblong to subcylindrical conidia[118]. *Ectophoma* differs in having solitary to confluent conidiomata, each bearing one or more short ostiolar necks[116]. *Longididymella* is characterized by solitary to confluent, flask-shaped or irregular conidiomata with elongated ostiolar necks, variable conidiogenous cell morphology, and ellipsoidal to allantoid, smooth- and thin-walled, 0–1-septate conidia. As *Gruyteromyces* constitutes an independent lineage that is not strongly affiliated with any existing genus within *Didymellaceae*, *Gruyteromyces* gen. nov. is introduced in this study to accommodate this distinct lineage.

Gruyteromyces hongheensis Wanas. Phookamsak, & J.C. Xu, **sp. nov.** (Figs 15 and 16).

MycoBank No: 859356

Etymology: The specific epithet 'hongheensis' refers to Honghe, Yunnan Province, where the holotype was collected.

Holotype: HKAS146022

Saprobic on the dead sheath of a *Poaceae* host. Sexual morph*:* Undetermined. Asexual morph: Coelomycetous. *Conidiomata* 130–170 μm high × 220–280 μm diam. ($\overline{x}$ = 155.2 × 253.7 μm, n = 5), pycnidial, black, solitary, scattered, immersed to slightly erumpent, subglobose, uni-loculate, glabrous, visible as small black dots on host surface, glabrous, with inconspicuous ostiolate. *Pycnidial wall* 10–20 μm wide, comprising a few layers of dark brown to hyaline, thick-walled, pseudoparenchymatous cells of *textura angularis*. *Conidiophores* reduced to conidiogenous cells. *Conidiogenous cells* 3.5–4.5 × 3.5–4.7 μm ($\overline{x}$ = 3.9 × 4.1 μm, n = 30), monoblastic, hyaline, smooth, phalidic, ampulliform, lining the conidiomatal cavity. *Conidia* 5–8 × 2.5–4 μm ($\overline{x}$ = 6.7 × 3.3 μm, n = 30), ellipsoidal to oblong, hyaline, thin-walled, smooth to slightly rough, aseptate.

Culture characteristics: Colonies on PDA, 25–30 mm diam after one week, margin irregular, covered by velvety, sparse, flat mycelia, pinkish white, iron-grey ring patterns are visible near the centre and at peripheral areas. Sporulation has started after 45 d under light conditions at 25 °C. Reverse; orangish white, notable iron-grey ring was visible at the periphery.

Materials examined: China, Yunnan, Honghe Hani and Yi Autonomous Prefecture, Honghe County, 23.421013° N, 102.227243° E, 517 m, on dead sheath of a *Poaceae* sp., 03 December 2020, D.N. Wanasinghe, DWHH06-01 (holotype, HKAS146022), ex-type, KUNCC23-16758; *ibid*., DWHH06-02 (paratype, HKAS146023), ex-paratype KUNCC25-19455.

GenBank numbers: KUNCC23-16758: ITS = PV742896, LSU = PV742952, SSU = PV743005, *tef*1-α = PV700631, *rpb*2 = PV700677, *tub*2 = PV738672; HKAS146023: ITS = PV742897, LSU = PV742953, SSU = PV743006, *tef*1-α = PV700632, *rpb*2 = PV700678, *tub*2 = PV738673.

Notes: Multigene phylogenetic analyses demonstrated that two new strains (KUNCC23-16758 and KUNCC25-19455) of *Gruyteromyces hongheensis* formed a distinct subclade (60% MLBS; Fig. 15) basal to *Ectodidymella nigrificans* (CBS 100190). *Gruyteromyces hongheensis* can be distinguished from *E. nigrificans* in having subglobose conidiomata with an inconspicuous ostiole and slightly smaller conidia (5–8 × 2.5–4 μm vs 6–9 × 2–3 μm). On the other hand, *E. nigrificans* has globose to depressed globose conidiomata, usually with a conspicuous neck[118].

Didymosphaeriaceae Munk, Dansk botanisk Arkiv 15 (2): 128 (1953)

Chromolaenicola Mapook & K.D. Hyde, Fungal Diversity 101: 20 (2020)

Notes: *Chromolaenicola* is a well-defined genus in *Didymosphaeriaceae*, characterized by both sexual and asexual morphs, and supported by morphological features and multigene phylogenetic analyses. The genus was established by Mapook et al.[69] to accommodate four new species and one new combination, with *Chromolaenicola nanensis* designated as the type species. Most species of *Chromolaenicola* are saprobic, commonly found on hosts such as *Ananas comosus*, *Bidens pilosa*, *Chromolaena odorata*, *Clematis subumbellata*, and *Leucaena* sp. in Thailand[46,69,108,123,124]. To date, only *Chromolaenicola sapindi* has been recorded outside Thailand, collected from dead woody twigs of *Sapindus rarak* in Yunnan, China[125]. Currently, eight species are listed under *Chromolaenicola* in Index Fungorum[89]. The sexual morph of *Chromolaenicola* is characterized by immersed to semi-immersed, solitary, coriaceous, globose to subglobose ascomata with a protruding ostiolar neck; 6–8-spored, bitunicate, cylindrical asci; and reddish brown to brown, ellipsoid to broadly fusiform, muriform ascospores[69]. The coelomycetous asexual morph produces solitary, pycnidial, globose to obpyriform conidiomata with a papillate ostiole, and hyaline, unbranched, broadly filiform to ampulliform conidiogenous cells. Conidia are oblong to ellipsoid, globose to subglobose, hyaline to brown, 0–1-septate, and finely verruculose[69]. Notably, some species of *Chromolaenicola* have demonstrated antimicrobial activity against *Mucor plumbeus* and *Bacillus subtilis*[46,69]. In the present study, *Chromolaenicola hongheensis* sp. nov., a saprobe isolated from *Citrus australasica*, was introduced, marking the first report of this genus from this host and the second record of *Chromolaenicola* from Yunnan Province, China. In addition, *C. clematidis* was reported from dead twigs of an unidentified deciduous host in Yunnan, China, for the first time.

Chromolaenicola clematidis Phukhams. & K.D. Hyde, Fungal Diversity 102: 31 (Figs 17 and 18).

MycoBank No: 557133

Saprobic on dead wood of an unknown deciduous host. Sexual morph: Undetermined. Asexual morph: Coelomycetous. *Conidiomata* 75–110 × 100–140 μm ($\bar{x}$ = 87.3 × 118.2 μm, n = 20), pycnidial, black, solitary, scattered, immersed to slightly erumpent, subglobose to globose, uni-loculate, glabrous, visible as black dots on host surface, with protruding ostiole. *Pycnidial wall* 8–12 μm wide, thin-walled of equal thickness, comprising 1–3 layers of hyaline to brown, thick-walled, pseudoparenchymatous cells of *textura angularis* to *textura prismatica*. *Conidiophores* reduced to conidiogenous cells. *Conidiogenous cells* 6–7.2 × 3.8–4.5 μm ($\bar{x}$ = 6.7 × 4.2 μm, n = 30), enteroblastic, phialidic, determinate, discrete, hyaline, cylindrical or ampulliform, sometimes narrow at the apex and wider from the bottom, smooth-walled, unbranched, lining the conidiomatal cavity. *Conidia* 7.5–9.5 × 6.5–7.7 μm ($\bar{x}$ = 8.5 × 7.1 μm, n = 30), globose to subglobose, hyaline, aseptate, at immature stage, becoming brown, single or multi-guttulate, sometimes guttules not observed, aseptate to 1-septate, thick-walled, smooth-walled at maturity.

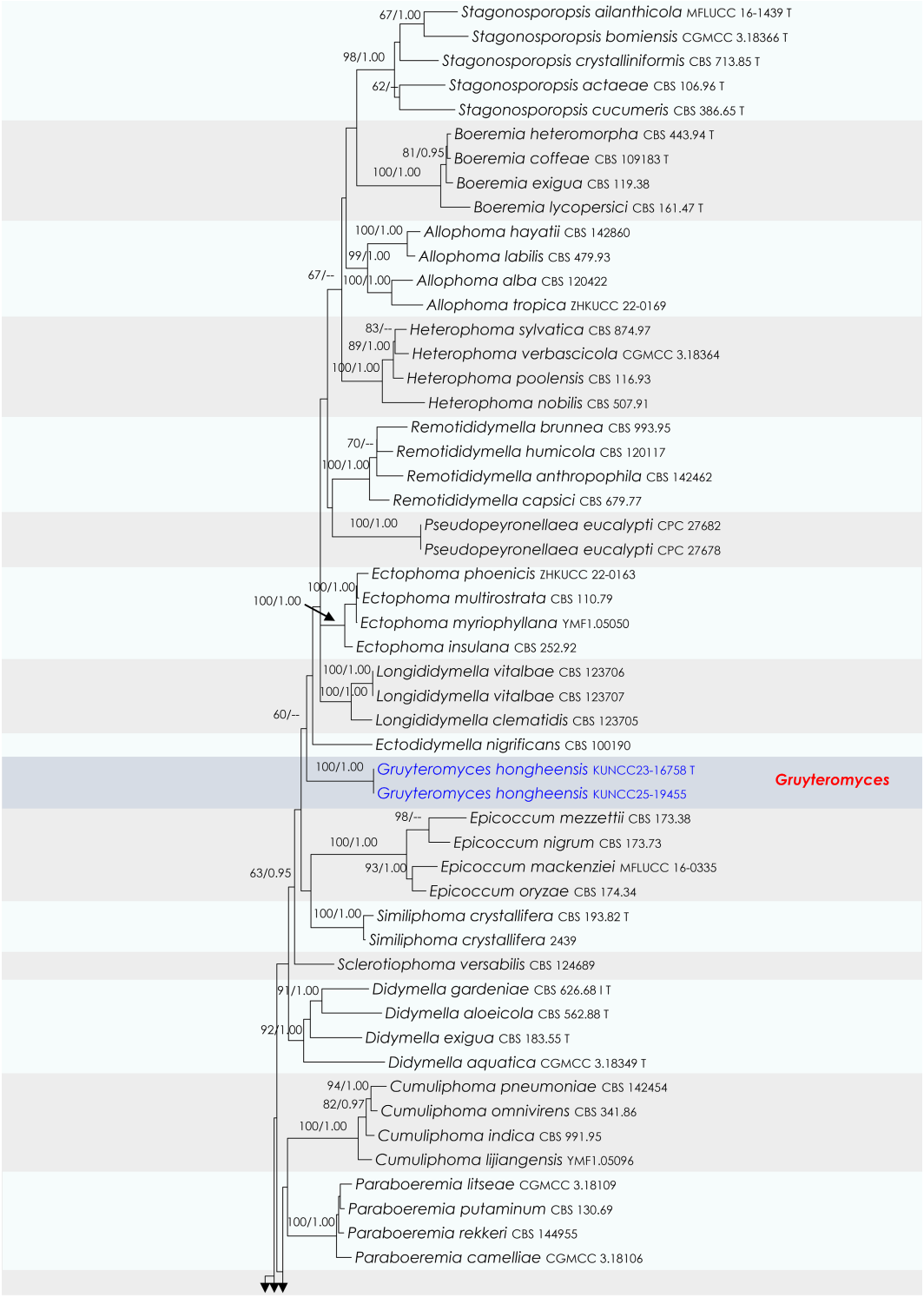

Fig. 15 (to be continued)

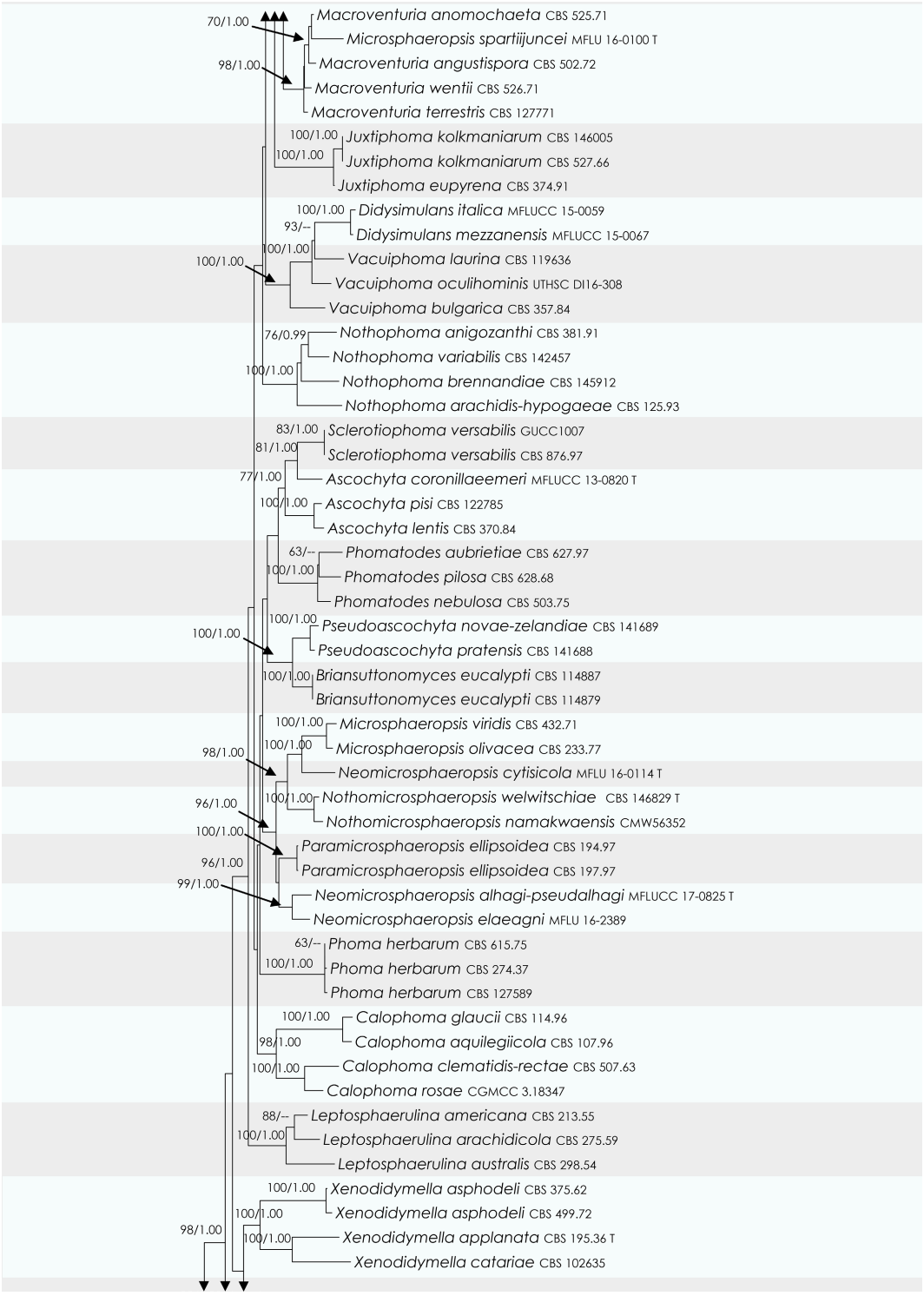

Fig. 15 (to be continued)

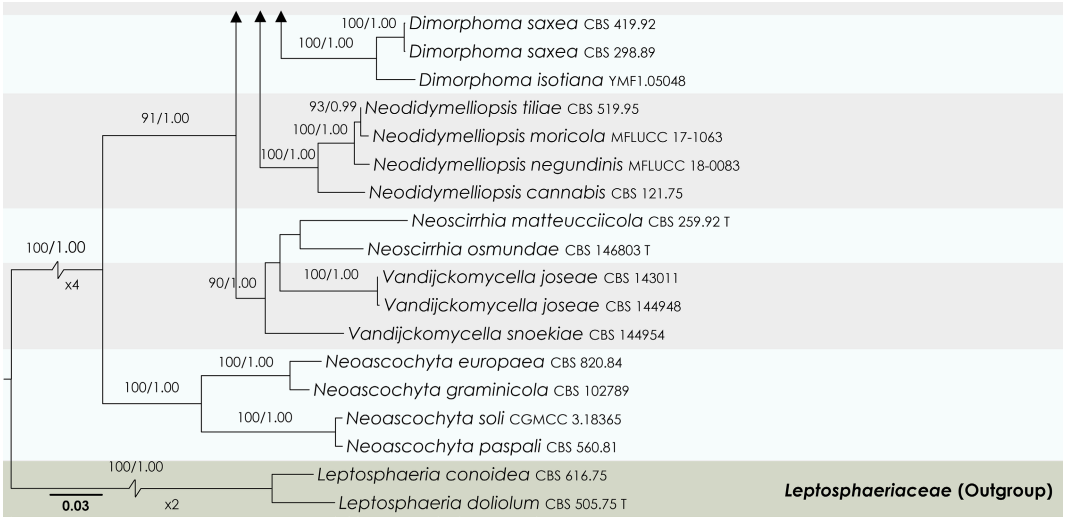

Fig. 15 Maximum Likelihood tree inferred from the concatenated dataset of partial LSU, ITS, *rpb2* and *tub2* sequences. The phylogeny is rooted with *Leptosphaeria conoidea* (CBS 616.75) and *L. doliolum* (CBS 505.75). The final likelihood value is –30,111.669487. The final alignment included 1,051 unique site patterns, with approximately 16.06% of the positions comprising gaps or ambiguous characters. The estimated nucleotide frequencies were as follows: A = 0.240399, C = 0.243000, G = 0.274422, T = 0.242180. The substitution model yielded the following relative rates: AC = 2.034753, AG = 7.468658, AT = 2.243260, CG = 1.095539, CT = 14.634190, GT = 1.000000. The proportion of invariable sites (I) was estimated at 0.633611, and the gamma distribution shape parameter (α) was 0.621330. Bayesian inference reached convergence after 1,476,000 generations, when the average standard deviation of split frequencies dropped below 0.01 (observed value: 0.009988). A total of 14,761 trees were sampled, and 11,071 of these were retained for the final analysis after discarding the initial 25% as burn-in. The alignment also revealed 1,053 distinct informative sites. In the resulting phylograms, sequences generated in this study are highlighted in blue, while ex-type or type strains are indicated with a 'T' at the end of the strain number.

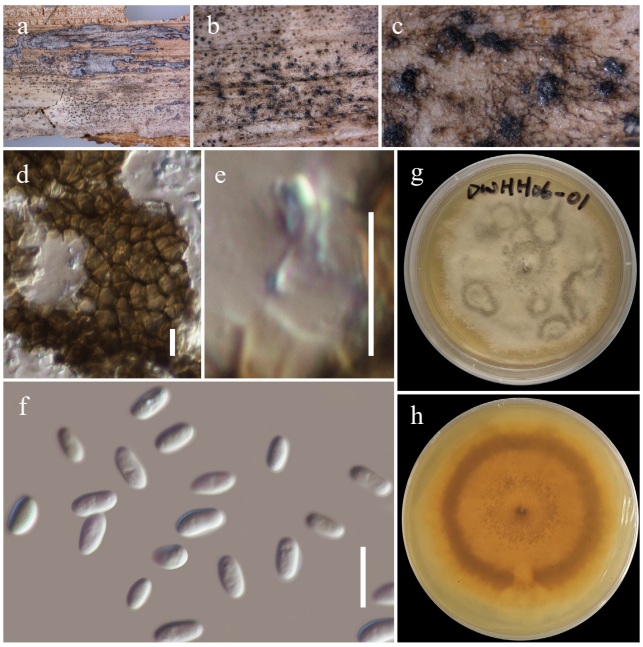

Fig. 16 *Gruyteromyces hongheensis* (HKAS146022, holotype). (a)–(c) Conidiomata on host. (d) Pycnidial wall. (e) Conidiogenous cell. (f) Conidia. (g), (h) Colony on PDA (h from the bottom). Scale bars: (d)–(f) = 10 μm.

Culture characteristics: Colonies on PDA, 35 mm diam. after one week, the margin is irregular, covered by velvety, puffy mycelium that sometimes condenses in the middle as patches, and the mouse gray. Reverse: grayish brown at the middle, grayish white at the periphery.

Material examined: China, Yunnan, Honghe Hani and Yi Autonomous Prefecture, Honghe County, 23.421013 N, 102.227243 E, 517 m, on dead twigs of an unknown deciduous host, 03 December 2020, D.N. Wanasinghe, DWHH14-04 (HKAS146029), living culture, KUNCC23-16771.

GenBank numbers: KUNCC23-16771: ITS = PV742898, LSU = PV742954, SSU = PV743007, *tef*1-α = PV700633, *rpb2* = PV700679.

Known hosts and distribution: Saprobic on dead stems of *Clematis subumbellata* in Thailand[123]; on dead twigs of an unknown deciduous host in Yunnan, China (this study).

Notes: Phylogenetically, the new strain (KUNCC23-16771) shared the same branch with the type of *Chromolaenicola clematidis* (MFLUCC 17-2075) and clustered with *C. nanensis*, *C. lampangensis*, *C. thailandensis*, *C. siamensis*, and *C. chiangraiensis* with 96% MLBS and 1.00 BYPP support values (Fig. 17). The new strain KUNCC23-16771 shares similar morphological characteristics with the type strain of *C. clematidis* in having black, subglobose to globose, uni-loculate conidiomata, and brown, 0–1-septate conidia. However, our collection (HKAS146029) has broader conidiomata (75–110 × 100–140 μm vs 76–145 × 107–128 μm), with inconspicuous ostioles, broader (7.5–9.5 × 6.5–7.7 μm vs 7–10 × 4.5–7 μm), globose to subglobose, and smooth-walled conidia. On the other hand, the type of *C. clematidis* has ostiolate, papillate conidiomata, and ellipsoidal to subglobose, verrucose conidia[123]. Despite these slight dimensional differences, based on phylogenetic results and other morphological similarities, the new isolate is identified as *Chromolaenicola clematidis* and is reported from Yunnan, China, for the first time.

Chromolaenicola hongheensis Wanas., Phookamsak, L.S. Dissan. & J.C. Xu, **sp. nov.** (Figs 17 and 19).

MycoBank No: 859357

Etymology: The specific epithet 'hongheensis' refers to Honghe, Yunnan Province, where the holotype was collected.

Holotype: HKAS146024

Saprobic on dead twigs of *Citrus australasica*. Sexual morph: Undetermined. Asexual morph: Coelomycetous. *Conidiomata* 150–200 μm high × 120–250 μm diam. ($\overline{x}$ = 180.5 × 172.7 μm, n = 5), pycnidial, black, solitary, or in a small group, immersed to slightly erumpent, globose to subglobose, uni-loculate, glabrous, visible as

gregarious black dots on host surface, with inconspicuous, central ostiole. *Pycnidial wall* 10–20 μm wide, thin-walled of equal thickness, comprising 2–5 layers of light brown, flattened pseudoparenchymatous cells of *textura angularis* to *textura prismatica*, slightly paler towards the inner layer. *Conidiophores* reduced to conidiogenous cells. *Conidiogenous cells* 5.5–6.5 × 3–3.5 μm ($\bar{x}$ = 5.9 × 3.3 μm, n = 30), monoblastic, phialidic, discrete, hyaline, ampulliform to doliform, unbrached, smooth-walled, lining the conidiomatal cavity. *Conidia* 10–14 × 5–8 μm ($\bar{x}$ = 11.6 × 6 μm, n = 30), ellipsoidal to oblong, hyaline, aseptate, at immature stage, becoming brown, 1-septate, guttulate, rough-walled, verruculose at maturity.

Culture characteristics: Colonies on PDA, 30 mm diam. after one week, margin irregular, covered by velvety, puffy mycelium that sometimes condenses in the middle as patches, and the mouse is gray. Reverse: grayish brown at the middle, grayish white at the periphery.

Materials examined: China, Yunnan, Honghe Hani and Yi Autonomous Prefecture, Honghe County, 23.421013° N, 102.227243° E,

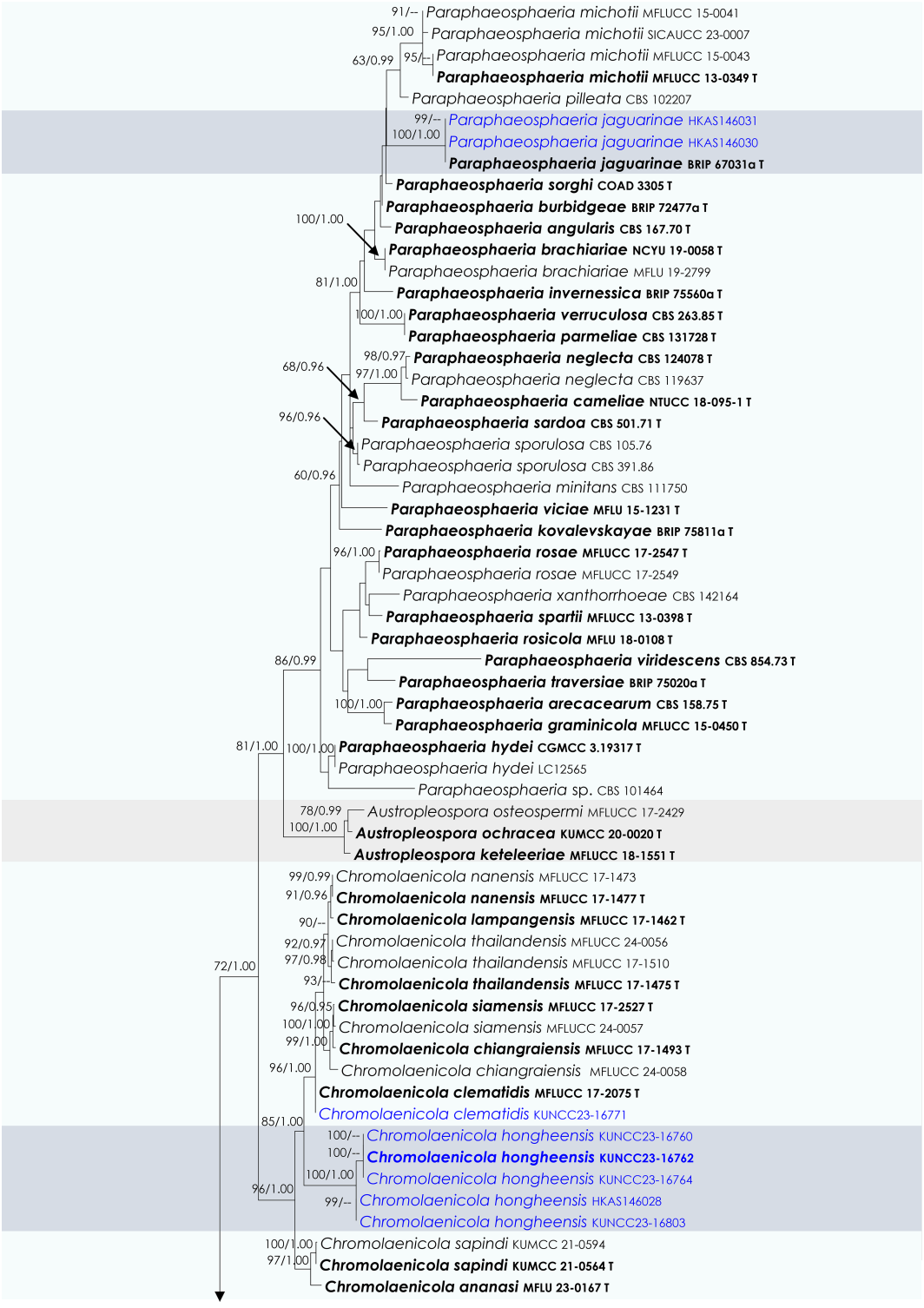

Fig. 17 (to be continued)

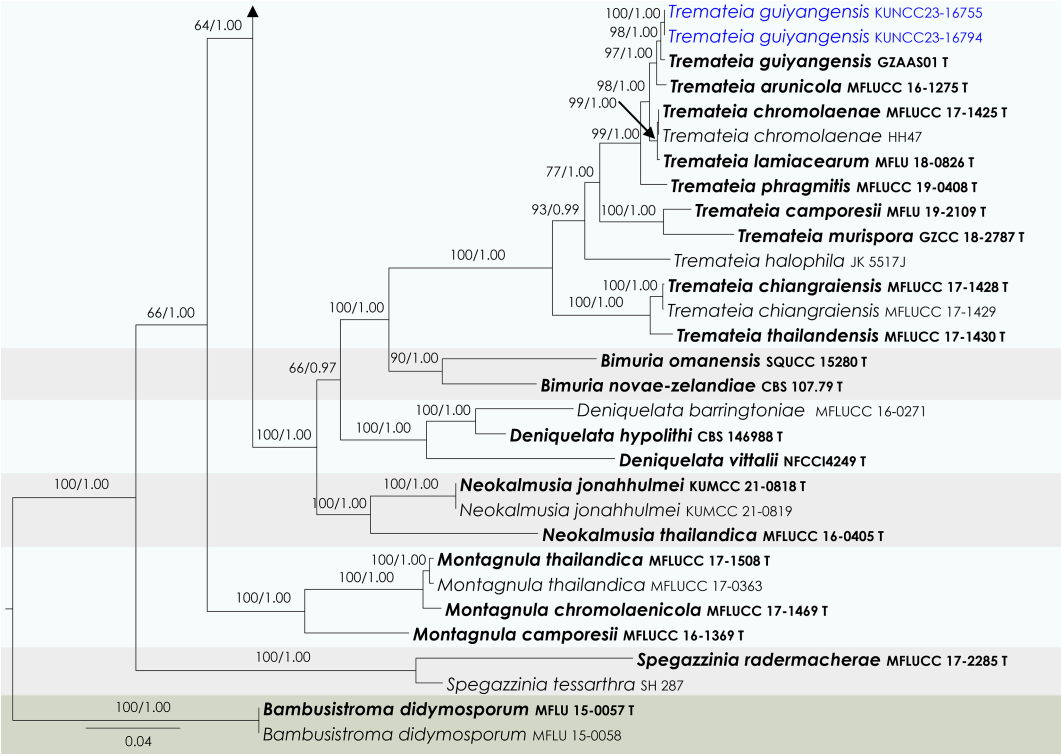

Fig. 17 Maximum Likelihood tree inferred from the concatenated dataset of partial SSU, LSU, ITS, *tef*1-α and *rpb*2 sequences. The phylogeny is rooted with *Bambusistroma didymosporum* (MFLU 15-0057, MFLU 15-0058). The final likelihood value is –29,800.793962. The final alignment included 1,978 unique site patterns, with approximately 36.43% of the positions comprising gaps or ambiguous characters. The estimated nucleotide frequencies were as follows: A = 0.238939, C = 0.255983, G = 0.270197, T = 0.234881. The substitution model yielded the following relative rates: AC = 1.677295, AG = 3.846144, AT = 1.480569, CG = 1.417310, CT = 8.251750, GT = 1.000000. The proportion of invariable sites (I) was estimated at 0.419546, and the gamma distribution shape parameter (α) was 0.473863. Bayesian inference reached convergence after 2,194,000 generations, when the average standard deviation of split frequencies dropped below 0.01 (observed value: 0.009957). A total of 21,941 trees were sampled, and 16,456 of these were retained for the final analysis after discarding the initial 25% as burn-in. The alignment also revealed 1,981 distinct informative sites. In the resulting phylograms, sequences generated in this study are highlighted in blue, while ex-type or type strains are indicated in boldface.

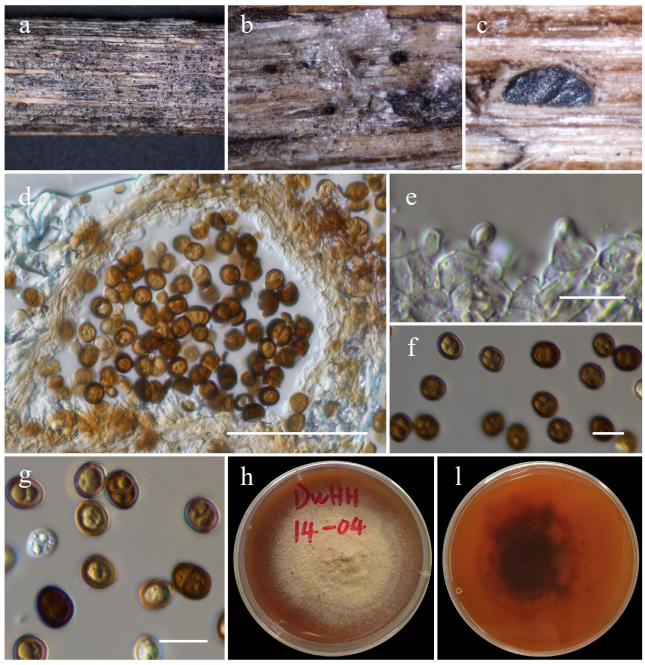

Fig. 18 *Chromolaenicola clematidis* (HKAS146029). (a), (b) Conidiomata on host. (c), (d) Sections of conidiomata. (e) Conidiogenous cells. (f), (g) Conidia. (h), (i) Colony on MEA (i from the bottom). Scale bars: (d) = 50 μm, (e)–(g) = 10 μm.

517 m, on dead twigs of *Citrus australasica*, 14 August 2022, D.N. Wanasinghe, DWHH08-06 (holotype, HKAS146024), ex-type, (KUNCC23-16762); *ibid*., DWHH08-05 (HKAS146025), living culture (KUNCC23-16760); *ibid*., DWHH08-08 (HKAS146026), living culture (KUNCC23-16764); *ibid*., DWHH22-18-01 (HKAS146027), living culture (KUNCC23-16803); *ibid*., DWHH22-18-02 (HKAS146028).

GenBank numbers: KUNCC23-16762: ITS = PV742899, LSU = PV742955, SSU = PV743008, *tef*1-α = PV700634, *rpb*2 = PV700680; KUNCC23-16760: ITS = PV742900, LSU = PV742956, SSU = PV743009, *tef*1-α = PV700635, *rpb*2 = PV700681; KUNCC23-16764: ITS = PV742901, LSU = PV742957, SSU = PV743010, *tef*1-α = PV700636; KUNCC23-16803: ITS = PV742902, LSU = PV742958, SSU = PV743011, *tef*1-α = PV700637, *rpb*2 = PV700682; HKAS146028: ITS = PV742903, LSU = PV742959, SSU = PV743012, *tef*1-α = PV700638, *rpb*2 = PV700683.

Notes: Multigene phylogenetic analyses based on a concatenated dataset of SSU, LSU, ITS, *tef*1-α, and *rpb*2 loci revealed that five strains of *Chromolaenicola hongheensis* (KUNCC 23-16762, KUNCC 23-16760, KUNCC 23-16764, KUNCC 23-16803, and HKAS 146028) formed a monophyletic subclade (100% MLBS and 1.00 BYPP; Fig. 17), positioned basally to *C. nanensis*, *C. lampangensis*, *C. thailandensis*, *C. siamensis*, *C. chiangraiensis*, and *C. clematidis*. Among these, *C. hongheensis* shows the closest phylogenetic affinity to *C. clematidis* (85% MLBS and 1.00 BYPP; Fig. 17). Morphologically, *C. hongheensis* is comparable to *C. clematidis* in conidial shape but can be distinguished by its larger conidiomata (150–200 × 120–250 μm vs 76–145 × 107–128 μm) and larger, ellipsoidal to oblong

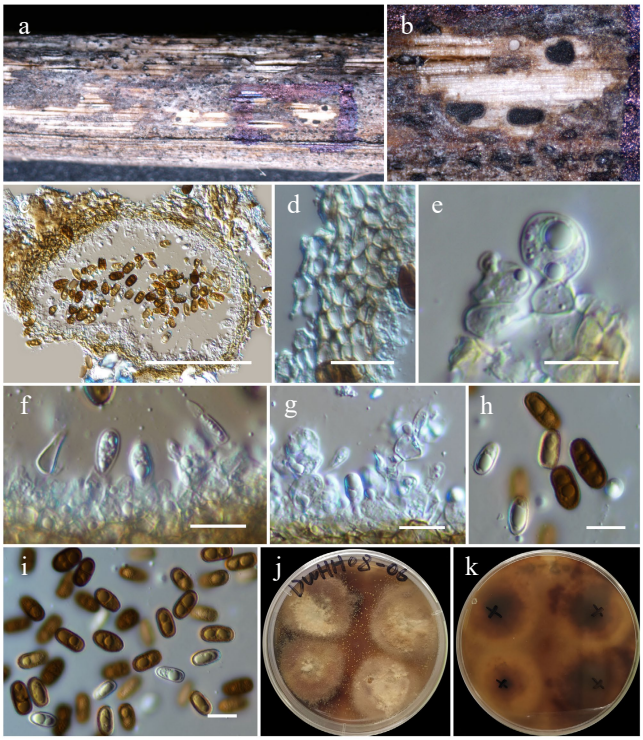

Fig. 19 *Chromolaenicola hongheensis* (HKAS146024, holotype). (a) Conidiomata on host. (b), (c) Sections of conidiomata. (d) Pycnidial wall. (e)–(g) Conidiogenous cells. (h), (i) Conidia. (j), (k) Colony on PDA (k from the bottom). Scale bars: (c) = 100 μm, (d)–(i) = 10 μm.

conidia (10–14 × 5–8 μm vs 7–10 × 4.5–7 μm). In contrast, *C. clematidis* typically produces ellipsoidal to subglobose conidia[123]. These morphological and phylogenetic distinctions support the recognition of *C. hongheensis* as a novel species.

Paraphaeosphaeria O.E. Erikss., Ark. Bot. Ser. 2. 6 (4–5): 405.

Notes: *Paraphaeosphaeria* was introduced by Eriksson[126] with *P. michotii* as the type species. The genus was initially established to accommodate four sexual species, including *P. castagnei, P. michotii, P. obtusispora*, and *P. rusci*[110]. The genus is characterized by immersed to semi-immersed, globose to subglobose ascomata, with protruding ostiole, or a short beak, 8-spored, bitunicate, fissitunicate, broadly cylindrical asci, and brown to yellowish brown, oblong to cylindrical, tapering towards the lower end cell, septate ascospores[110,127]. *Paraphaeosphaeria* produces coniothyrium-like asexual morphs and is characterized by eustromatic or pycnidial conidiomata, phialidic or annellidic, discrete or integrated conidiogenous cells, and ellipsoid to obovoid-pyriform, hyaline to brown, 0–1-septate, smooth to verrucose conidia[128]. Presently, 52 epithets under *Paraphaeosphaeria* are available in Index Fungorum[89]. In this study, the new host record for *P. jaguarinae* in Yunnan, China, was reported for the first time.

Paraphaeosphaeria jaguarinae Y.P. Tan & R.G. Shivas, Index Austral. Fungi 19: 5 (Figs 17 and 20).

MycoBank No: 901285

Saprobic on dead leaf blades of *Poaceae* hosts. Sexual morph: Undetermined. Asexual morph: Coelomycetous. *Conidiomata* 40–60 μm high × 55–70 μm diam. ($\bar{x}$ = 47.6 × 61.5 μm, n = 5), pycnidial, solitary, scattered, immersed to slightly erumpent, uni-loculate, globose to subglobose, glabrous, ostiolate with central, minutely papillate. *Pycnidial wall* 5–10 μm wide, thin-walled of equal thickness, composed of 2–3 layers of large, light brown to golden brown, pseudoparenchymatous cells, of *textura angularis*, slightly paler brown to hyaline towards the inner layers. *Conidiophores* reduced to

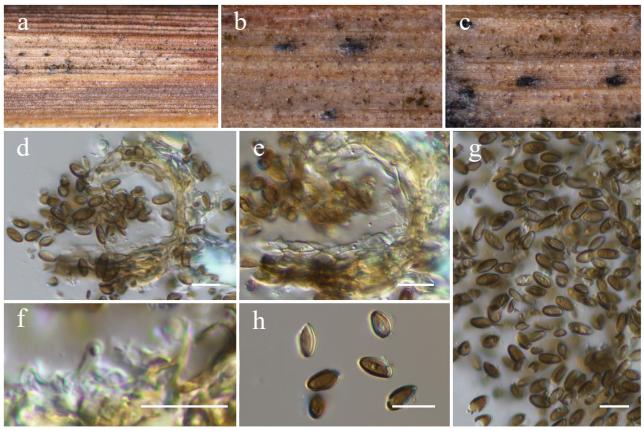

Fig. 20 *Paraphaeosphaeria jaguarinae* (HKAS146030). (a)–(c) Conidiomata on host. (d) Section of a conidioma. (e) Pycnidial wall. (f) Conidiogenous cells. (g), (h) Conidia. Scale bars: (d)–(h) = 10 μm.

conidiogenous cells. *Conidiogenous cells* 2.3–2.8 × 3.4–3.9 μm ($\bar{x}$ = 2.5 × 3.7 μm, n = 10), holoblastic, phialidic, determinate, discrete, hyaline, ampulliform, unbranched, smooth-walled. *Conidia* 5–9 × 3–4.5 μm ($\bar{x}$ = 6.9 × 3.4 μm, n = 30), elliptic to ellipsoidal, with acute or obtuse ends, initially hyaline to light brown with guttules, becoming brown, aseptate, thick-walled at maturity.

Materials examined: China, Yunnan, Honghe Hani and Yi Autonomous Prefecture, Honghe County, 23.390025 N, 102.225942 E, 1186 m, on dead leaf blades of *Poaceae* sp., 13 March 2023, D.N. Wanasinghe, DWHH23-38-1 (HKAS146030); *ibid*., DWHH23-38-2 (HKAS146031).

GenBank numbers: HKAS146030: ITS = PV742904, LSU = PV742960, SSU = PV743013, *tef*1-α = PV700639, *rpb*2 = PV700684; HKAS146031: ITS = PV742905, LSU = PV742961, SSU = PV743014, *tef*1-α = PV700640, *rpb*2 = PV700685.

Known hosts and distribution: Associated with leaf spot of *Arundienella* sp. in Queensland, Australia[129]; saprobic on dead leaf blades of *Poaceae* spp. in Yunnan, China (this study).

Notes: Multigene phylogenetic analyses based on a combined dataset of SSU, LSU, ITS, *tef*1-α, and *rpb*2 sequences revealed that two newly obtained strains (HKAS 146030 and HKAS 146031) clustered within the same branch as the type strain of *Paraphaeosphaeria jaguarinae* (BRIP 67031a), with 100% MLBS and 1.00 BYPP statistical support (Fig. 17). However, when *P. jaguarinae* was introduced by Tan & Shivas[129], no morphological data were provided for the type strain, rendering direct morphological comparison with our new isolates impossible. Based on robust phylogenetic evidence and their *Poaceae* host association, the new isolates were identified as *P. jaguarinae*. This study provides an updated morphological description and photographic illustrations of the species based on our collections.

Tremateia Kohlm., Volkm.-Kohlm. & O.E. Erikss., Bot. Mar. 38: 165.

Notes: *Tremateia* was introduced as a monotypic genus by Kohlmeyer et al.[130] and is typified by *T. halophila*. The genus was initially established to accommodate a facultative marine fungus occurring on senescent culms of *Juncus roemerianus* in North Carolina (USA). Ariyawansa et al.[127] recircumscribed the genus based on the isotype of the type species *T. halophila* that is characterized by solitary, scattered, brown to black, globose to subglobose ascomata, 4–8-spored, bitunicate, clavate to broadly clavate asci, embedded in cellular pseudoparaphyses, and ellipsoid to fusiform, light brown to brown, muriform, with phoma-like asexual morph. Subsequently, nine species were included in this genus[69,131–134]. These species were found as saprobes in both

marine and terrestrial habitats. In the present study, *T. guiyangensis* is reported on dead twigs of an unknown deciduous host in Yunnan, China, for the first time.

Tremateia guiyangensis J.F. Zhang, J.K. Liu, K.D. Hyde & Z.Y. Liu, Fungal Diversity 80: 48 (2016) (Figs 17 and 21).

MycoBank No: 552160

Saprobic on a dead twig of a deciduous host. Sexual morph: *Ascomata* 230–270 μm high × 250–280 μm diam. ($\bar{x}$ = 250.7 × 261.2 μm, n = 5), immersed to semi-immersed, solitary or gregarious, appearing as small dark spots, black, coriaceous, globose to subglobose, uni-loculate, glabrous, central ostiolate, with minutely papillate. *Peridium* 10–20 μm wide, thin-walled of equal thickness, comprising 2–3 layers, of large, flattened, light brown to brown, pseudoparenchymatous cells of *textura angularis* to *textura prismatica*, slightly paler brown to hyaline towards the inner layers. *Hamathecium* consisted of 2–3.5 μm wide, cylindrical, filamentous, septate, often unbranched, sometimes branched, hyaline pseudoparaphyses. *Asci* 80–100 × 16–22 μm ($\bar{x}$ = 90.9 × 18.9 μm, n = 20), 8-spored, bitunicate, fissitunicate, cylindric-clavate, short pedicellate, apically rounded with indistinct ocular chamber. *Ascospores* 19–23 × 9–11 μm ($\bar{x}$ = 21.2 × 10 μm, n = 30), overlapping, uni- or bi-seriate, ellipsoidal to broad fusiform, hyaline, thick-walled, 1-transversely septate at immature stage, golden-brown muriform, 2–7-transversely septate, with 1-longitudinal septum in each row at maturity, with Y septum at the apical cell, acute or obtuse ends, slightly constricted at the central septum, straight or slightly curved, guttulate at immaturity, surrounded by hyaline gelatinous sheath. Asexual morph: Undetermined.

Culture characteristics: Colonies on PDA, 20 mm diam. after one week, margin was irregular, covered by pinkish white cottony mycelium, and a notable partial groove was visible. Reverse: pinkish brown.

Materials examined: China, Yunnan, Honghe Hani and Yi Autonomous Prefecture, Honghe County, 23.421013° N, 102.227243° E, 517 m, on dead twigs of an unknown deciduous host, 03 December 2020, D.N. Wanasinghe, DWHH22-02 (HKAS146033), living culture, KUNCC23-16794; *ibid*., DWHH22-03 (HKAS146034), living culture, KUNCC23-16755.

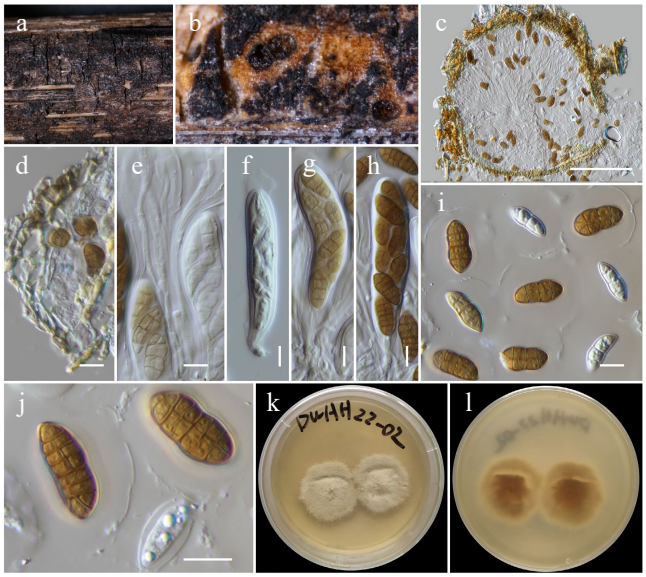

Fig. 21 *Tremateia guiyangensis* (HKAS146033). (a) Ascomata on the dead woody twigs. (b), (c) Cross-section of ascomata. (d) Peridium. (e) Pseudoparaphyses. (f)–(h) Asci. (i), (j) Ascospores. (k), (l) Colony on PDA (l from the bottom). Scale bars: (c) = 100 μm, (d)–(j) = 10 μm.

GenBank numbers: KUNCC23-16794: ITS = PV742906, LSU = PV742962, SSU = PV743015, *tef*1-α = PV700641; KUNCC23-16755: ITS = PV742907, LSU = PV742963, SSU = PV743016, *tef*1-α = PV700642.

Known hosts and distribution: Saprobic on dead herbaceous stems in Guizhou, China[131]; on dead twigs of an unknown deciduous host in Yunnan, China (this study).

Notes: Phylogenetic analyses based on a combined dataset of SSU, LSU, ITS, *tef*1-α, and *rpb*2 sequence data revealed that two new strains (KUNCC 23-16794 and KUNCC 23-16755) clustered with the type strain of *Tremateia guiyangensis* (GZAAS01) (98% MLBS and 1.00 BYPP; Fig. 17). This clade is sister to *T. arunicola* (MFLUCC 16-1275, type strain), also with 97% MLBS and 1.00 BYPP statistical support. Morphologically, the new isolates are consistent with *T. guiyangensis* in possessing coriaceous, subglobose ascomata with minutely papillate ostioles, cylindric-clavate asci and muriform, ellipsoidal to broadly fusiform and golden-brown ascospores. However, they exhibit smaller asci (80–100 × 16–22 μm vs 152–160 × 21–27 μm), and ascospores (19–23 × 9–11 μm vs 20–28 × 9–12 μm). Additionally, the ascospores of the new isolates have 2–7 transverse septa and a single longitudinal septum in each row, and are covered by a hyaline gelatinous sheath. In contrast, the type strain of *T. guiyangensis* typically has 3–5 transverse septa, one longitudinal septum per row, and lacks a mucilaginous sheath[131]. Based on the strong phylogenetic affinity and general morphological congruence, these two isolates are identified as *Tremateia guiyangensis*. This represents the first report of the species from dead twigs of an unidentified deciduous host in Yunnan, China.

Lophiostomataceae Sacc., Syll. Fung. 2: 672.

Neovaginatispora A. Hashim., K. Hiray. & Kaz. Tanaka, Stud. Mycol. 90: 188.

Notes: *Neovaginatispora* was introduced as a monotypic genus by Hashimoto et al.[135] to accommodate the type species, *N. fuckelii*. The genus is commonly known as saprobic fungi in terrestrial and freshwater habitats[135–138], as well as causing leaf spot on *Phoenix canariensis*[139]. The genus is characterized by solitary, coriaceous, black, subglobose ascomata, with rounded or slit-like ostioles, 8-spored, bitunicate, fissitunicate, cylindric-clavate asci, embedded in narrow cellular pseudoparaphyses, and fusiform, hyaline, 1–2-septate, smooth-walled ascospores, with appendages at both ends[136]. The coelomycetous asexual morph of *Neovaginatispora* has been reported for *N. aquadulcis* by Magaña-Dueñas et al.[140] and is characterized by pycnidial, brown to dark brown, semi-immersed, solitary, globose, ostiolate conidiomata, phialidic, determinate, hyaline, globose, conidiogenous cells, and, aseptate, hyaline, smooth-walled, guttulate, conidia. Chlamydospores are solitary or in chains, abundant, terminal, and intercalary, brown, globose to clavate, aseptate, thick-walled[140]. Presently, only four species are accommodated in this genus, of which the type species, *N. fuckelii* is cosmopolitan. In this study, *N. fuckelii* is reported as the new collection on dead twigs of an unknown deciduous host in Yunnan, China.

Neovaginatispora fuckelii (Sacc.) A. Hashim., K. Hiray. & Kaz. Tanaka, Stud. Mycol. 90: 188 (Figs 22 and 23).

MycoBank No: 823148

Saprobic on a dead twig of *Fabaceae* spiny host. Sexual morph: *Ascomata* 230–270 μm high × 250–280 μm diam. ($\bar{x}$ = 200.8 × 195.1 μm, n = 5), solitary, scattered to clustered, semi-immersed, carbonaceous to coriaceous, black, uni-loculate to multi-loculate, each locule is globose to subglobose, glabrous, ostiolate, papillate. *Ostiole* rounded or slit-like opening, central, periphyses. *Peridium* 10–20 μm wide, of unequal thickness, slightly thick at the apex (up to 40 μm), composed of several cell layers, of small, hyaline to brown or dark brown, pseudoparenchymatous cells of *textura angularis* to

textura prismatica, with carbonaceous cells at the apex towards the ostiolar, outer layers fused with the host tissues, composed of brown to dark brown, flattened cells, inner layers composed of hyaline cells. *Hamathecium* 2–2.5 μm wide, numerous, filiform, hyaline, branched, septate, anastomosed cellular pseudoparaphyses, embedded in a hyaline gelatinous matrix. *Asci* 100–140 × 14–20 μm ($\bar{x}$ = 118.3 × 16.9 μm, n = 20), 8-spored, bitunicate, cylindrical, short pedicellate with furcate or bulb pedicel, apically round with well-developed ocular chamber. *Ascospores* 30–38 × 7–8.2 μm ($\bar{x}$ = 34.6 × 7.8 μm, n = 20), overlapping uni- to bi-seriate, fusiform with acute

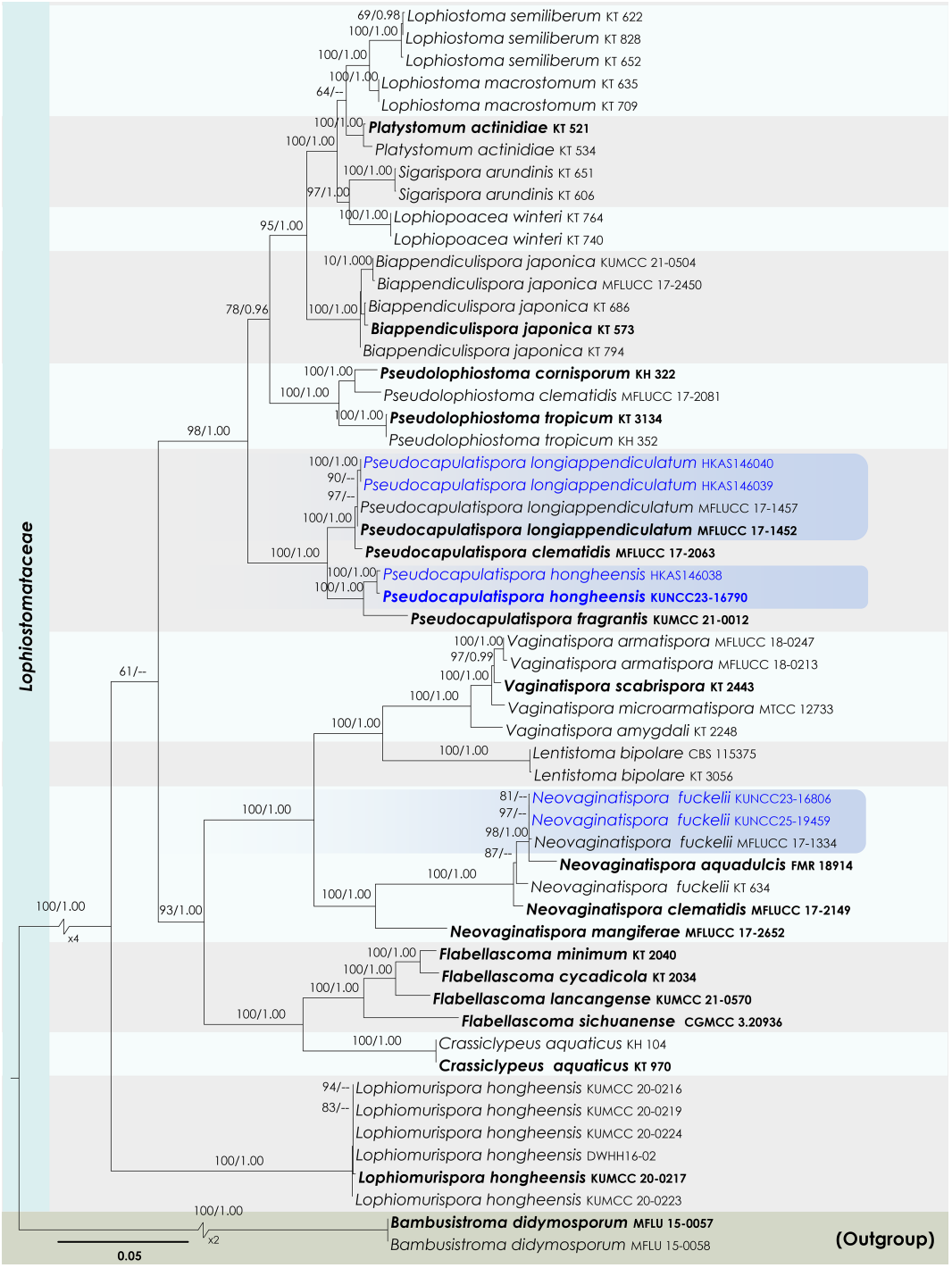

Fig. 22 Maximum Likelihood tree inferred from the concatenated dataset of partial SSU, LSU, ITS, *tef*1-*α*, and *rpb*2 sequences. The phylogeny is rooted with *Bambusistroma didymosporum* (MFLU 15-0057, MFLU 15-0058). The final likelihood value is −23,551.161444. The final alignment included 1,560 unique site patterns, with approximately 13.11% of the positions comprising gaps or ambiguous characters. The estimated nucleotide frequencies were as follows: A = 0.250154, C = 0.249645, G = 0.265412, T = 0.234790. The substitution model yielded the following relative rates: AC = 1.772887, AG = 4.441914, AT = 1.366252, CG = 1.518065, CT = 9.220171 and GT = 1.000000. The proportion of invariable sites (I) was estimated at 0.527527, and the gamma distribution shape parameter (α) was 0.567921. Bayesian inference reached convergence after 44,000 generations, when the average standard deviation of split frequencies dropped below 0.01 (observed value: 0.009691). A total of 441 trees were sampled, and 331 of these were retained for the final analysis after discarding the initial 25% as burn-in. The alignment also revealed 1,561 distinct informative sites. In the resulting phylograms, sequences generated in this study are highlighted in blue, while ex-type or type strains are indicated in boldface.

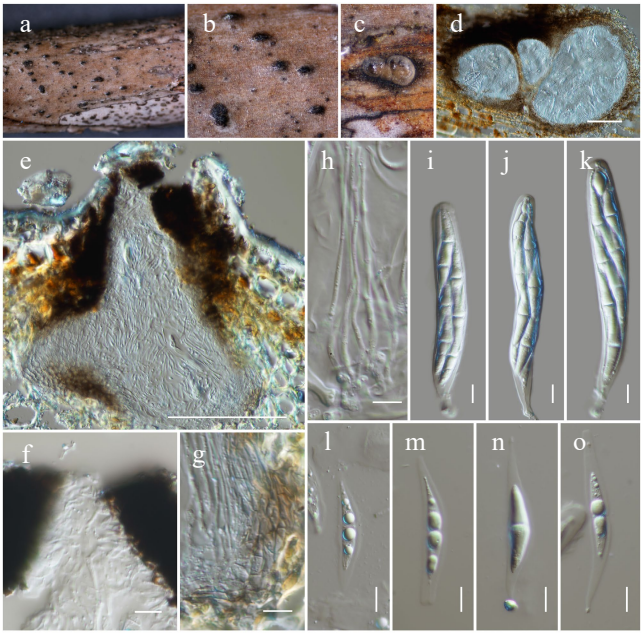

Fig. 23 *Neovaginatispora fuckelii* (HKAS146035). (a), (b) Ascomata on the dead woody twigs. (c) Transverse section of ascomata. (d), (e) Cross-section of ascomata. (f) Close up of ostiole. (g) Peridium. (h) Pseudoparaphyses. (i)–(k) Asci. (l)–(o) Ascospores. Scale bars: (d), (e) = 100 μm, (h)–(o) = 10 μm.

ends, hyaline, 1-septate, slightly constricted at the septum, upper cell slightly broader than the lower cell, with guttules at immature stage, smooth-walled, surrounded by conspicuous hyaline mucilaginous sheath, with tail-like at both ends (10–20 μm long), lacking appendages. Asexual morph: Undetermined.

Culture characteristics: Colonies on PDA at room temperature (25 °C) under normal light, reaching 28–30 mm diam. after two weeks. Colonies dense, circular, flattened, slightly raised, to low convex, surface smooth, with edge entire, floccose, smooth aspect, do not produce pigmentation in PDA. Colonies sectored, from above grey and white, slightly radiating with concentric ring, pale grey near the margin; colonies from below sectored, white to cream at the margin, dark greenish grey to black near the margin, paler grey to cream toward the center, another white to cream towards the center.

Materials examined: China, Yunnan, Honghe Hani and Yi Autonomous Prefecture, Honghe County, 23.390025° N, 102.225942° E, 1,186 m, on dead twigs of *Fabaceae* spiny sp., 13 March 2023, D.N. Wanasinghe, DWHH23-27A (HKAS146035), living culture, KUNCC23-16806; *ibid*., 23 April 2020, DWHH23-64 (HKAS146036), living culture, KUNCC25-19459.

GenBank numbers: KUNCC23-16806: ITS = PV742908, LSU = PV742964, SSU = PV743017, *tef*1-α = PV700643, *rpb*2 = PV700686; HKAS146036: ITS = PV742909, LSU = PV742965, SSU = PV743018, *tef*1-α = PV700644, *rpb*2 = PV700687.

Known hosts and distribution: Saprobic on stems of unknown herbaceous plant in Japan[136]; on dead stems of *Mangifera indica* in Taiwan[141], on decaying wood submerged in a stream in Yunnan[137], on decaying wood of *Prunus* sp. in Yunnan[132], on a branch of *Camellia oleifera*, *Idesia polycarpa*, *Juglans nigra* and *Paeonia suffruticosa* in Sichuan[142], pathogen causing leaf spot *Phoenix canariensis* in Sichuan[139], stem blight on *Rosa chinensis* in Yunnan, China[143], on dead twigs of *Fabaceae* sp. (this study).

Notes: Phylogenetic analyses of a combined SSU, LSU, ITS, *tef*1-α, and *rpb*2 demonstrated that the new strains (KUNCC23-16806 and KUNCC25-19459) shared the same branch with *Neovaginatispora fuckelii* (MFLUCC 17-1334) (98% MLBS and 1.00 BYPP; Fig. 22) and formed a subclade with *N. aquadulcis* (FMR 18914), *N. fuckelii* (KT 634) and *N. clematidis* (MFLUCC 17-2149) with 100% MLBS and 1.00 BYPP support (Fig. 22). Morphologically, the new isolates resemble *N. fuckelii* (MFLUCC 17-1334) in having semi-immersed, coriaceous, black, subglobose ascomata, with periphysate, rounded or slit-like ostiole, cylindrical asci, and hyaline, fusiform, 1-septate ascospores. However, the new isolates slightly differ from *N. fuckelii* (MFLUCC 17-1334) in having larger asci (100–140 × 14–20 μm vs 47–54 × 6.5–8.5 μm) and larger ascospores (30–38 × 7–8.2 μm vs 12–13 × 3–4 μm). Additionally, the ascospores of new isolates are surrounded by conspicuous hyaline mucilaginous sheath, with tail-like appendages at both ends, and lacking appendages, whereas *N. fuckelii* (MFLUCC 17-1334) is present with appendages at both ends lacks a mucilaginous sheath covering ascospores[137]. These isolates can be distinguished from *N. aquadulcis* (FMR 18914) in having smaller, carbonaceous to coriaceous, globose to subglobose ascomata, cylindrical asci, and 1-septate ascospores. At the same time, *N. aquadulcis* (FMR 18914) has larger (400–550 × 300–325 μm), pyriform ascomata, with conic-truncate necks, cylindrical to cylindrical-clavate asci, and 3-septate ascospores, with papillate to pulvinate appendages at each end[140]. Based on phylogenetic evidence and morphological characteristics, the new isolates are identified as *N. fuckelii* herein.

Pseudocapulatispora Mapook & K.D. Hyde, Fungal Diversity 101: 47.

Notes: *Pseudocapulatispora* was introduced by Mapook et al.[69] as a monotypic genus to accommodate the type species, *P. longiappendiculata*. The genus is characterized by immersed, coriaceous, solitary, ovoid, light brown to brown ascomata, with long, carbonaceous, crest-like, ostiolar necks, 8-spored, bitunicate, fissitunicate, cylindric-clavate asci, and hyaline, broadly fusiform, 1-septate ascospores, with narrow sheaths drawn out to form polar appendages at both ends. Andreasen et al.[144] synonymized this genus under *Lophiostoma*. Their treatment has not been followed by recent publications[145]. *Pseudocapulatispora* was also treated as a distinct genus from *Lophiostoma*, as it exhibits morphological differences from the latter, such as immersed, coriaceous ascomata, with long, carbonaceous, crest-like, ostiolar necks and hyaline, broad fusiform, 1-septate ascospores, with a long sheath drawn out to form polar appendages[69,123,145]. Whereas, *Lophiostoma* has immersed to semi-immersed, coriaceous to carbonaceous ascomata, with short, pore-like, or crest-like, papillate ostioles, and hyaline to yellowish brown, uni- to multi-septate ascospores, without or with terminal appendages, and lacking a mucilaginous sheath[136]. Currently, three species are accounted in this genus, *viz*. *Pseudocapulatispora clematidis*, *P. fragrantis,* and *P. longiappendiculata*. However, *Pseudocapulatispora fragrantis* is considered Nom. inval., Art. 40.7 (Shenzhen) in Index Fungorum[89]. In the present study, the new species *P. hongheensis* is introduced based on morphological characteristics and phylogenetic evidence.

Pseudocapulatispora hongheensis Wanas., Phookamsak, L.S. Dissan. & J.C. Xu, **sp. nov.** (Figs 22 and 24).

MycoBank No: 859358

Etymology: The specific epithet 'hongheensis' refers to Honghe, Yunnan Province, where the holotype was collected.

Holotype: HKAS146037

Saprobic on a dead twig of an unknown deciduous host. Sexual morph: *Ascomata* 320–380 μm high × 240–290 μm diam. ($\bar{x}$ = 351.9 × 269.7 μm, n = 5), immersed, solitary, scattered, coriaceous, pyriform to ovoid, brown to dark brown, uni-loculate, glabrous, ostiolate, visible as black knobs on host surface. *Ostiole* elongated cannel, carbonaceous, inverted crest-like, filled with periphyses, erumpent

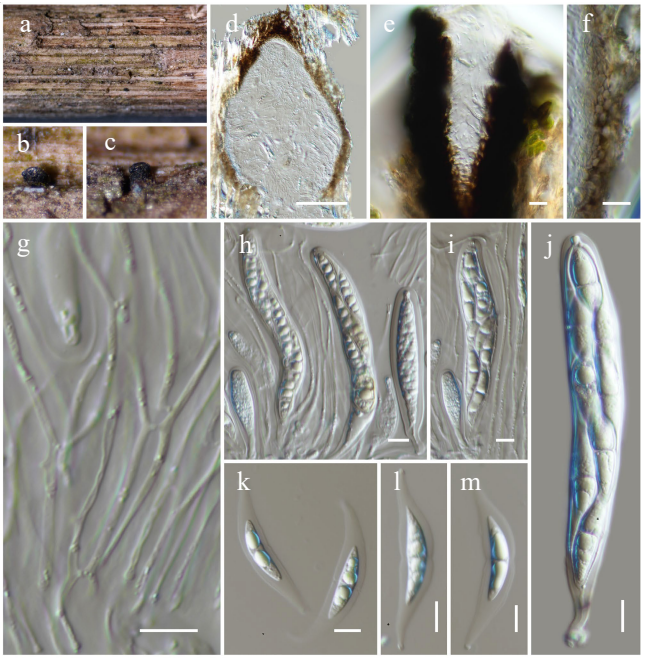

Fig. 24 *Pseudocapulatispora hongheensis* (HKAS146037, holotype). (a)–(c) Ascomata on the dead woody twigs. (d) Cross-section of ascoma. (e) Close up of ostiole. (f) Peridium. (g) Pseudoparaphyses. (h)–(j) Asci. (k)–(m) Ascospores. Scale bars: (d) = 100 μm, (e)–(m) = 10 μm.

through host surface. *Peridium* 10–20 μm wide, thin-walled of equal thickness, composed of 3–5 layers of brown to dark brown pseudoparenchymatous cells of *textura angularis* to *textura prismatica*, outer layers composed of brown to dark brown, somewhat compressed, thick-walled cells, fused with the host tissues, inner layers composed of pale brown to hyaline, flattened cells. *Hamathecium* consisted of 1.2–2 μm wide, numerous, filiform, branched, septate, anastomosed pseudoparaphyses, embedded in a hyaline gelatinous matrix. *Asci* 90–120 × 14–20 μm ($\bar{x}$ = 108.5 × 16.4 μm, n = 20), 8-spored, bitunicate, fissitunicate, cylindrical or cylindric-clavate, short pedicellate, apically rounded, with distinct ocular chamber. *Ascospores* 30–40 × 7–8 μm ($\bar{x}$ = 30.8 × 7.3 μm, n = 20), overlapping, uni- or bi-seriate, hyaline, fusiform, with acute ends, 1-septate, not constricted at the septum, with large guttules, surrounded by narrowly, distinct mucilaginous sheath, drawn out to form tail-like, hyaline appendages tapering towards at both ends of the ascospores (10–20 μm long), with a globose drop situated at the end of the appendages. Asexual morph: Undetermined.

Culture characteristics: Colonies on PDA at room temperature (25 °C) under normal light, reaching 18–20 mm diam. after two weeks. Colonies dense, circular, flattened, slightly raised, surface smooth, with curled to undulate edge, floccose to velvety, smooth aspect, slightly radiated, produce yellow pigmentation in PDA. Colonies from above dark greenish to black at the margin, white to pale grey at the center, with yellow droplets; colonies from below dark greenish to black at the margin towards the middle, cream to pale yellowish at the center.

Materials examined: China, Yunnan, Honghe Hani and Yi Autonomous Prefecture, Honghe County, 23.390025° N, 102.225942° E, 1,186 m, on dead twigs of an unknown deciduous host, 13 March 2023, D.N. Wanasinghe, DWHH23-06 (holotype, HKAS146037), ex-type, KUNCC23-16790: *ibid*., DWHH23-55 (HKAS146038).

GenBank numbers: KUNCC23-16790: ITS = PV742910, LSU = PV742966, SSU = PV743019, *tef*1-α = PV700645, *rpb*2 = PV700688; HKAS146038: ITS = PV742911, LSU = PV742967, SSU = PV743020, *tef*1-α = PV700646, *rpb*2 = PV700689.

Notes: Phylogenetic analyses of a combined SSU, LSU, ITS, *tef*1-α, and *rpb*2 sequence data demonstrated that two new strains (KUNCC23-16790 and HKAS146038) of *Pseudocapulatispora hongheensis* sp. nov. formed a robust subclade, sister to *P. fragrantis* with 100% MLBS and 1.00 BYPP support (Fig. 22). These two species constituted the base of *P. clematidis* and *P. longiappendiculata* with 100% MLBS and 1.00 BYPP support (Fig. 22), and are distant from *Lophiostoma*. Morphologically, *P. hongheensis* resembles *P. fragrantis* but can be distinguished by slightly smaller ascomata (320–380 μm high × 240–290 μm diam. vs 220–377 μm high × 162–325 μm diam.), shorter and broader asci (90–120 × 14–20 μm vs 58–127 × 8–15 μm), and ascospores (30–40 × 7–8 μm vs 29–36 × 4–8 μm) with shorter tail-like appendages (10–20 μm long vs 16–46 × 8–14 μm)[145]. *Pseudocapulatispora hongheensis* produced yellowish pigmentation on PDA, whereas *P. fragrantis* does not produce pigmentation on PDA. Therefore, *Pseudocapulatispora hongheensis* sp. nov. is introduced herein as a distinct species.

Pseudocapulatispora longiappendiculata Mapook & K.D. Hyde, Fungal Diversity 101: 48 (Figs 22 and 25).

MycoBank No: 557286

Saprobic on dead twigs of an unknown deciduous host. Sexual morph: *Ascomata* 220–280 μm high × 140–200 μm diam. ($\bar{x}$ = 239.1 × 169.6 μm, n = 5), solitary to gregarious, scattered, immersed, coriaceous to carbonaceous, black, often globose to subglobose, uniloculate, glabrous, ostiolate, papillate, visible as black knobs on the host surface. *Ostiolar canal* rounded, central carbonaceous papillate, sometimes with a pore-like ostiole, filled with periphyses. *Peridium* 10–20 μm thick, thin-walled of equal thickness, composed of 3–5 layers of flattened, brown to dark brown pseudoparenchymatous cells of *textura angularis* to *textura prismatica*, outer layers composed of dark brown cells, fused with the host tissues, slightly lighter to hyaline towards the inner layers, with compressed cells. *Hamathecium* composed of 1.5–2 μm wide, numerous, filiform, septate, branched, hyaline, anastomosed pseudoparaphyses, embedded in a gelatinous matrix. *Asci* 80–110 × 13–16 μm ($\bar{x}$ =

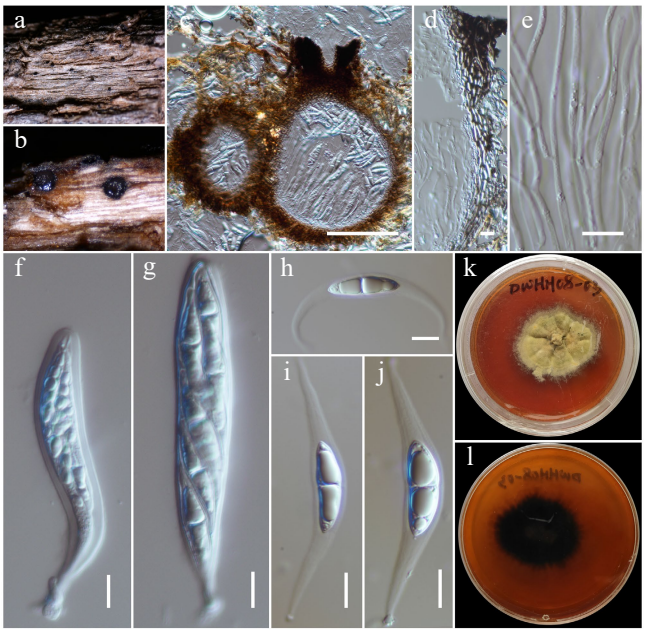

Fig. 25 *Pseudocapulatispora longiappendiculata* (HKAS146039). (a) Ascomata on the dead woody twigs. (b), (c) Cross-section of ascomata. (d) Peridium. (e) Pseudoparaphyses. (f), (g) Asci. (h)–(j) Ascospores. (k), (l) Colony on MEA (l from the bottom). Scale bars: (c) = 100 μm, (d)–(j) = 10 μm.

98.6 × 15.1 μm, n = 20), 8-spored, bitunicate, fissitunicate, cylindrical, cylindric-clavate or sometimes narrowly clavate, long-pedicellate, apex rounded, with a well-developed ocular chamber. *Ascospores* 23–29 × 7–9.5 μm ($\bar{x}$ = 27.2 × 7.9 μm, n = 20), partially overlapping uni- to bi-seriate, initially hyaline, becoming light brown at maturity, fusiform, 1-septate when young, becoming 1–3-septate at maturity, slightly constricted at septum when mature, smooth-walled, with guttules, surrounded by a narrow, conspicuous mucilaginous sheath, drawn out to form tubular, hyaline appendages at both ends. *Appendages* 15–25 μm long, elongated, smooth, thin-walled, tapering towards the apex, base of each appendage near the center cells are wider than the apex, terminating from a globose drop situated at the end of the appendages. Asexual morph: Undetermined.

Culture characteristics: Colonies on PDA at room temperature (25 °C) under normal light, reaching 24–26 mm diam. after two weeks. Colonies dense, irregular, flattened, slightly raised, surface rough, with erose to fimbriate, floccose to velvety, heaped and folded, slightly radiated outwards colony, produce brown pigmentation in PDA. Colonies from above dark olivaceous-brown; colonies from below black.

Materials examined: China, Yunnan, Honghe Hani and Yi Autonomous Prefecture, Honghe County, 23.390025° N, 102.225942° E, 1,186 m, on dead twigs of an unknown deciduous host, 13 March 2023, D.N. Wanasinghe, DWHH23-02 (HKAS146039); *ibid*., 23.421013° N, 102.227243° E, 517 m, 03 December 2020, DWHH08-03 (HKAS146040).

GenBank numbers: HKAS146039: ITS = PV742912, LSU = PV742968, SSU = PV743021, *tef*1-α = PV700647, *rpb*2 = PV700690; HKAS146040: ITS = PV742913, LSU = PV742969, SSU = PV743022, *tef*1-α = PV700648, *rpb*2 = PV700691.

Known hosts and distribution: Saprobic on dead stems of *Chromolaena odorata* in Thailand[69]; on dead twigs of an unknown deciduous host in Yunnan, China (this study).

Notes: Phylogenetic analyses of a combined SSU, LSU, ITS, *tef*1-α, and *rpb*2 sequence data demonstrated that two new strains (HKAS146039 and HKAS146040) clustered with two strains of *Pseudocapulatispora longiappendiculata* (MFLUCC 17-1457 and MFLUCC 17-1452, type strain) with 97% MLBS support (Fig. 22) and is sister to *P. clematidis* (MFLUCC 17-2063, type strain) with 100% MLBS and 1.00 BYPP support (Fig. 22). Morphologically, the new isolates resemble the type of *P. longiappendiculata* but slightly differ in having larger ascomata (220–280 μm high × 140–200 μm diam. vs 195–265 μm high × 105–150 μm diam.), overlapping in ascospore size range (23–29 × 7–9.5 μm vs 24–29 × 6–9 μm). Ascospores of the new isolates turn brown with 1–3-septate at maturity, whereas this character was not described for the type[69]. Furthermore, the new isolates can be distinguished from *P. clematidis* in having smaller ascomata (220–280 μm high × 140–200 μm diam. vs 197–386 μm high × 160–252 μm diam.), smaller asci (80–110 × 13–16 μm vs 68–117 × 12–22 μm), and slightly narrower ascospores (23–29 × 7–9.5 μm vs 22–28 × 7–12 μm)[123]. Therefore, the new isolates are identified as *P. longiappendiculata* based on phylogenetic evidence.

Macrodiplodiopsidaceae Voglmayr, Jaklitsch & Crous, IMA Fungus 6 (1): 178 (2015)

Pseudochaetosphaeronema Punith., Nova Hedwigia 31 (1-3): 126 (1979)

Notes: *Pseudochaetosphaeronema* was introduced by Punithalingam[146], with *P. larense* designated as the type species. Members of this genus have been reported as human pathogens, endophytes, and saprobes[147–149]. Both sexual and asexual morphs have been documented for species in this genus[93,108,132,142,148–154]. The sexual morph is characterized by immersed, uniloculate ascomata; a peridium composed of textura angularis cells; unbranched, septate pseudoparaphyses; 8-spored, bitunicate, fissitunicate asci with a short, distinct pedicel and rounded apex; and fusiform, 1-septate, guttulate ascospores with pointed ends[148]. The asexual morph features globose conidiomata; monophialidic, cylindrical conidiogenous cells; and hyaline, subglobose to oval, aseptate conidia[93,108]. Currently, 17 species are accepted within the genus[89]. The present study introduces two novel species of *Pseudochaetosphaeronema* collected from the Honghe region of Yunnan, China (Fig. 26).

Pseudochaetosphaeronema hongheense Wanas., Phookamsak & J.C. Xu, **sp. nov**. (Figs 26 and 27).

MycoBank No: 859359

Etymology: The specific epithet 'hongheense' refers to Honghe, Yunnan Province, where the holotype was collected.

Holotype: HKAS146045

Saprobic on a dead wood of an unknown host. Sexual morph: Undetermined. Asexual morph: *Conidiomata* 110–150 μm high × 130–200 μm diam. ($\bar{x}$ = 131.7 × 179.1 μm, n = 5), pycnidial, black, solitary or gregarious, scattered or clustered, immersed to semi-immersed, globose to subglobose uni-loculate, ostiolate, apapillate or minutely papillate, protruding from the host surface, with pore-like opening. *Pycnidial wall* 5–15 μm wide, thin-walled of unequal thickness, slightly thinner at the base, thicker towards the apex, composed of 2–3 celled layers of flattened, brown to dark brown, thick-walled, pseudoparenchymatous cells, of *textura angularis* to *textura prismatica*, slightly paler brown to hyaline towards the inner layer. *Conidiophores* reduced to conidiogenous cells. *Conidiogenous cells* 5–11 × 3.5–4.5 μm ($\bar{x}$ = 7.6 × 3.9 μm, n = 20), holoblastic, monoblastic, phialidic, hyaline, discrete, determine, cylindrical to ampulliform, unbranched, aseptate, thin-walled, guttulate and smooth, with a corn-shaped flat base and a cylindrical apex. *Conidia* 13–17 × 5–6.5 μm ($\bar{x}$ = 14.7 × 5.7 μm, n = 30), brown, elliptic to fusiform, thick- and smooth-walled at maturity, 3-septate, constricted at septa, acute or rounded at apex, often guttulate. *Immature conidia* hyaline, rough-walled, aseptate to 1-septate with guttules.

Culture characteristics: Colonies on PDA, 25 mm diam. after one week, dense, irregular, flattened, slightly raised at the center, surface rough at the center, smooth towards the margin, with erose to fimbriate edge, fairy fluffy to velvety, covered by pinkish brown and raised, cottony mycelium, profuse growth, with black conidiomata sporulated after 12 weeks; not produce pigmentation in PDA. Colonies from above brown; colonies from below black.

Materials examined: China, Yunnan, Honghe Hani and Yi Autonomous Prefecture, Honghe County, 23.421068° N, 102.229128° E, 735 m, on dead twigs of an unknown deciduous host, 03 December 2020, D.N. Wanasinghe, DWHH16-04 (holotype, HKAS146045), ex-type, KUNCC23-16774; *ibid*., 14 August 2022, DWHH09-01 (HKAS146046), living culture, KUNCC25-19456.

GenBank numbers: HKAS146045: ITS = PV742914, LSU = PV742970, SSU = PV743023, *tef*1-α = PV700649; HKAS146046: ITS = PV742915, LSU = PV742971, SSU = PV743024, *tef*1-α = PV700650.

Notes: Multigene phylogenetic analyses based on a combined SSU, LSU, ITS, *tef*1-α, and *rpb*2 DNA sequence dataset demonstrated that the two new strains (KUNCC 23-16774 and KUNCC25-19456) formed a subclade (94% MLBS and 1.00 BYPP; Fig. 26), closely related to *Pseudochaetosphaeronema kunmingense* (100% MLBS and 1.00 BYPP). Morphologically, the new isolates resemble *P. kunmingense* in possessing black, globose to subglobose conidiomata with apapillate ostioles, monoblastic phialidic conidiogenous cells, and ellipsoidal to fusiform, brown, 3-septate conidia. However, they can be distinguished by having smaller conidiomata (130–200 μm diam. vs 180–250 μm diam.) and slightly larger conidia (13–17 × 5–6.5 μm vs 10–15 × 4–6 μm)[132]. Although the new isolates are

morphologically similar to *P. kunmingense*, their distinct phylogenetic placement supports their recognition as a separate species. Therefore, *Pseudochaetosphaeronema hongheense* is introduced herein as a new species.

Pseudochaetosphaeronema punithalingamii Wanas., Phookamsak & J.C. Xu, **sp. nov.** (Figs 26 and 28).

MycoBank No: 859360

Etymology: The species epithet was given in honour of Eliyathamby Punithalingam, who introduced the genus *Pseudochaetosphaeronema*.

Holotype: HKAS146048

Saprobic on the dead wood of an unknown host. Sexual morph: Undetermined. Asexual morph: *Conidiomata* 150–230 μm high × 200–300 μm diam. ($\overline{x}$ = 188.3 × 259.7 μm, n = 5), pycnidial, black, solitary or gregarious, scattered, semi-immersed to slightly erumpent, globose to subglobose, uni-loculate, glabrous, with inconspicuous ostiolate. *Pycnidial wall* 10–20 μm wide, thin-walled of equal thickness, composed of 3–6 celled layers, of flattened, light brown to brown, pseudoparenchymatous cells, of *textura angularis* to *textura prismatica*, with hyaline cells towards the inner layer. *Conidiophores* reduced to conidiogenous cells. *Conidiogenous cells* 3–7 × 1.5–2.2 μm ($\overline{x}$ = 4.6 × 1.8 μm, n = 20), holoblastic, monoblastic, phialidic, hyaline, discrete, determinate, cylindrical to ampulliform, aseptate, unbranched, thin, and smooth-walled. *Conidia* 12–16.5 × 5–6.5 μm ($\overline{x}$ = 14.4 × 5.9 μm, n = 30), ellipsoidal, hyaline at immature stage, brown at maturity, thick-walled, 3-septate, slightly constricted at septa, smooth-walled.

Materials examined: China, Yunnan, Honghe Hani and Yi Autonomous Prefecture, Honghe County, 23.390025° N, 102.225942° E, 1,186 m, on dead twigs of an unknown deciduous host, 13 March 2023, D.N. Wanasinghe, DWHH23-60 (holotype, HKAS146048); *ibid.*, DWHH23-61 (HKAS146047).

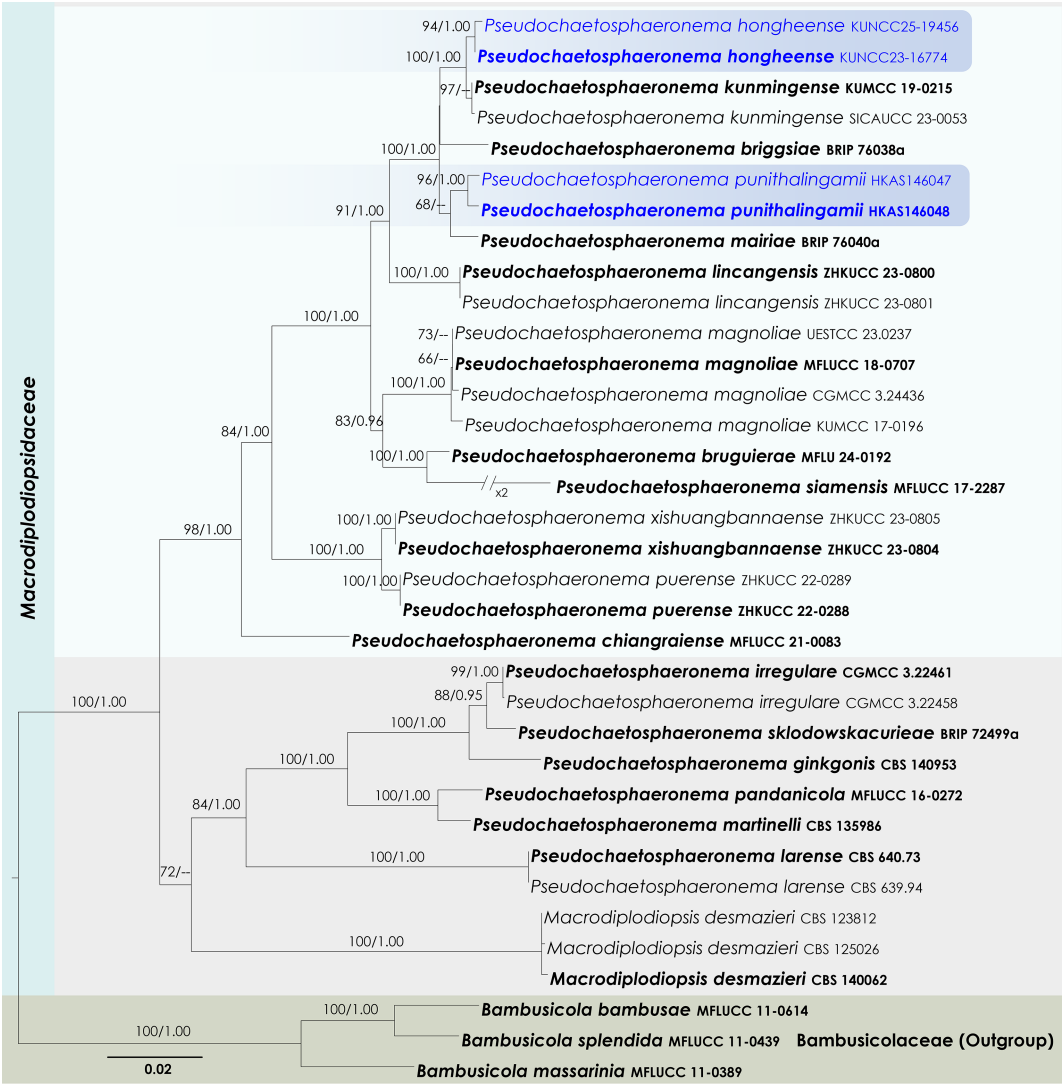

Fig. 26 Maximum Likelihood tree inferred from the concatenated dataset of partial SSU, LSU, ITS, *tef*1-*α*, and *rpb*2 sequences. The phylogeny is rooted with *Bambusicola bambusae* (MFLUCC 11-0614), *B. massarinia* (MFLUCC 11-0389), and *B. splendida* (MFLUCC 11-0439). The final likelihood value is –14,837.504911. The final alignment included 1,020 unique site patterns, with approximately 30.06% of the positions comprising gaps or ambiguous characters. The estimated nucleotide frequencies were as follows: A = 0.238962, C = 0.252036, G = 0.270241, T = 0.238761. The substitution model yielded the following relative rates: AC = 1.527778, AG = 4.223035, AT = 1.623867, CG = 1.375339, CT = 9.995702, GT = 1.000000. The proportion of invariable sites (I) was estimated at 0.569470, and the gamma distribution shape parameter (α) was 0.582697. Bayesian inference reached convergence after 34,000 generations, when the average standard deviation of split frequencies dropped below 0.01 (observed value: 0.009637). A total of 341 trees were sampled, and 256 of these were retained for the final analysis after discarding the initial 25% as burn-in. The alignment also revealed 1,022 distinct informative sites. In the resulting phylograms, sequences generated in this study are highlighted in blue, while ex-type or type strains are indicated in boldface.

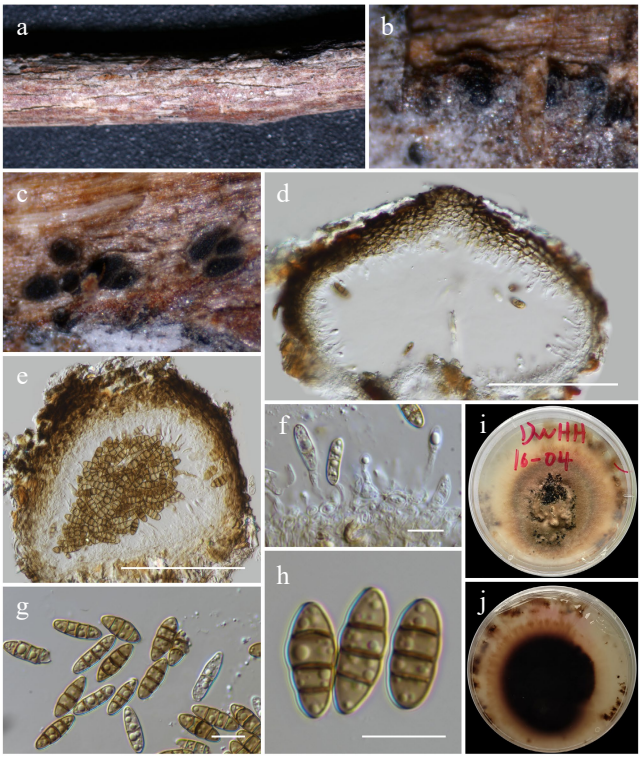

Fig. 27 *Pseudochaetosphaeronema hongheense* (HKAS146045, holotype). (a), (b) Conidiomata on host. (c)–(e) Sections of conidiomata. (f) Conidiogenous cells. (g), (h) Conidia. (i), (j) Colony on PDA (j from below). Scale bars: (d), (e) = 100 μm, (f)–(h) = 10 μm.

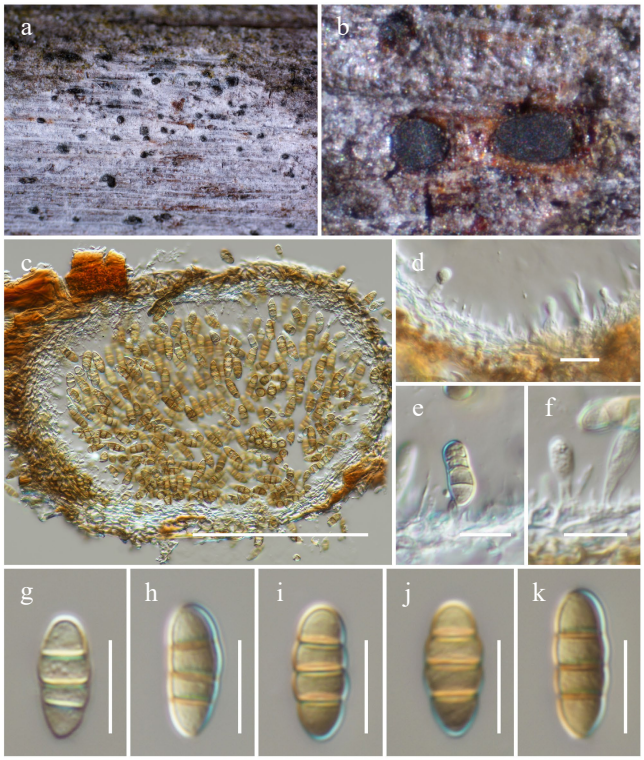

Fig. 28 *Pseudochaetosphaeronema punithalingamii* (HKAS146048, holotype). (a) Conidiomata on host. (b), (c) Sections of conidiomata. (d)–(f) Conidiogenous cells. (g)–(k) Conidia. Scale bars: (c) = 100 μm, (d)–(k) = 10 μm.

GenBank numbers: HKAS146048: ITS = PV742916, LSU = PV742972, SSU = PV743025, *tef*1-α = PV700651; HKAS146047: ITS = PV742917, LSU = PV742973, SSU = PV743026, *tef*1-α = PV700652.

Notes: Multigene phylogenetic analyses based on a combined SSU, LSU, ITS, *tef*1-α, and *rpb*2 DNA sequence dataset revealed that two new strains (HKAS 146048 and HKAS 146047) formed a subclade (96% MLBS and 1.00 BYPP; Fig. 26), and clustered as sister to *Pseudochaetosphaeronema mairiae* (68% MLBS). However, morphological comparison with *P. mairiae* is not possible, as no morphological description was provided when Tan & Shivas[155] introduced the species as an endophyte associated with *Geijera salicifolia* in Queensland, Australia. Only ITS and LSU sequence data of this species are currently available in GenBank. Based on phylogenetic evidence, the new species *Pseudochaetosphaeronema punithalingamii* is introduced herein. *Pseudochaetosphaeronema punithalingamii* also clusters with *P. briggsiae*, *P. kunmingense,* and *P. hongheense*. However, morphological data for *P. briggsiae* are also unavailable[155]. In contrast, *P. punithalingamii*, *P. kunmingense,* and *P. hongheense* share similar morphological features, particularly ellipsoidal to fusiform, brown, 3-septate conidia. *Pseudochaetosphaeronema punithalingamii* differs from *P. kunmingense* and *P. hongheense* in having larger conidiomata (200–300 μm diam. vs 180–250 μm and 130–200 μm, respectively). Its conidial dimensions (12–16.5 × 5–6.5 μm) are larger than those of *P. kunmingense* (10–15 × 4–6 μm), but overlap with *P. hongheense* (13–17 × 5–6.5 μm). Despite some morphological similarities, the phylogenetic distinctiveness of these taxa clearly supports their recognition as separate species.

Mangifericomitaceae Wanas., Phookamsak, L.S. Dissan. & J.C. Xu, **fam. nov.**

MycoBank No: 859361

Etymology: Referring to the name of the type genus, *Mangifericomes*

Saprobic on dead or decaying branches, leaves, or wood in terrestrial habitats. Sexual morph: *Ascomata* immersed to semi-immersed, solitary to gregarious, scattered to clustered, dark brown to black, globose to subglobose, uni-loculate to multi-loculate, emerging in a unique small epidermal clypeus, glabrous, with or without ostiolate, penetrating the host. *Peridium* thin- to thick-walled of equal thickness, composed of several cell layers of light brown to dark brown, pseudoparanchymatous cells of *textura angularis* to *textura globulosa*, or *textura prismatica*. *Hamathecium* numerous, composed of filiform, filamentous, hyaline, septate, branched, anastomosed, broad cellular pseudoparaphyses. *Asci* 8-spored, bitunicate, broadly cylindrical to cylindrical-clavate, pedicellate, apically rounded with an ocular chamber. *Ascospores* muriform, ellipsoid to broad fusoid, or clavate, brown to dark brown, asymmetrical, multi-septate, sectored, slightly constricted at the central septum, surrounded by a thick, distinct mucilagenous sheath. Asexual morph: Undetermined.

Type genus: *Mangifericomes* E.F. Yang & Tibpromma.

Notes: The new family *Mangifericomitaceae* is introduced herein to accommodate the monotypic genus *Mangifericomes*, with *M. hongheensis* designated as the type species. Previously, *Mangifericomes* was treated as a genus *incertae sedis* within *Pleosporales*[59,156,157]. In earlier phylogenetic analyses, *Mangifericomes* formed an unstable lineage: clustering with *Brunneoclavispora bambusae* (*Halotthiaceae*) in Yang et al.[156], and forming a separate lineage basal to *Pleomonodictydaceae* in Du et al.[157]. Although Hyde et al.[59] noted morphological similarities between *Mangifericomes* and botryosphaeria-like genera, they emphasized their distinction based on muriform ascospores. However, the tree topology in Yang et al.[156] has limitations, particularly due to the unstable placement of *Brunneoclavispora bambusae*, which appeared distinct from *Halotthiaceae*, warranting further phyloge-

netic reassessment[59]. In the present study, phylogenetic analyses based on a concatenated dataset of SSU, LSU, 5.8s, *tef*1-α, and *rpb*2 sequences confirmed that *Mangifericomes* forms a monophyletic clade, distinct from both *Halotthiaceae* and *Pleomonodictydaceae*, and clusters as a sister lineage to *Corynesporascaceae*. Rather than retaining *Mangifericomes* as an *incertae sedis* genus within *Pleosporales*, *Mangifericomitaceae* fam. nov. is also formally introduced to accommodate this taxon. Morphologically, *Mangifericomitaceae* differs from *Corynesporascaceae* in having immersed to semi-immersed, uni- to multi-loculate ascomata emerging beneath a distinct small epidermal clypeus, broadly cylindrical to cylindric-clavate asci embedded in broad cellular pseudoparaphyses, and muriform, sectored, multi-septate ascospores occurring in terrestrial habitats. In contrast, *Corynesporascaceae* features cleistothecioid, spherical ascomata; obovoid asci surrounded by deliquescent paraphysoids; and 1–3-septate ascospores, or spores with indistinct distosepta, typically found as pathogens or saprobes on leaves[110]. *Halotthiaceae* is distinguished by its semi-immersed to superficial ascomata, occasionally formed beneath a pseudoclypeus, cylindrical to clavate or subclavate asci embedded in narrowly cellular pseudoparaphyses, and predominantly didymosporous or phragmosporous, thick-walled, septate ascospores. An exception is *Brunneoclavispora*, which has muriform ascospores with 7–8 transverse and 1–4 longitudinal septa. Members of *Halotthiaceae* are found in terrestrial, freshwater, and marine habitats as saprobes or pathogens[110,158]. *Pleomonodictydaceae*, on the other hand, is known solely from hyphomycetous asexual morphs characterized by micro- to semi-macronematous conidiophores (sometimes reduced to mono- or polyblastic conidiogenous cells) and solitary or short-chained, dark brown to black, muriform, verrucose to tuberculate conidia[110]. Therefore, the molecular and morphological evidence supports the establishment of *Mangifericomitaceae* as a distinct family within *Pleosporales*.

Mangifericomes E.F. Yang & Tibpromma, Journal of Fungi 8 (2, no. 152): 10.

Notes: *Mangifericomes* was introduced by Yang et al.[156] as a monotypic genus to accommodate a saprobic fungus occurring on mango (*Mangifera indica*) in Yunnan, China, and is typified by *M. hongheensis*. The genus is characterized by immersed or semi-immersed, dark brown to black, globose to subglobose ascomata, sometimes visible apical black neck effuses to host surface, with or without ostiolate, 8-spored, bitunicate, cylindrical-clavate asci, and muriform, ellipsoid, asymmetrical, sectored, multi-transverse and longitudinal septa ascospores, surrounded by mucilaginous sheath[156]. The asexual morph of this genus has not yet been described. Presently, two species are accommodated in this genus[156,157]. In this study, the new species, *M. yunnanensis,* is introduced as the third species of this genus, of which was collected from different hosts in Yunnan, China.

Mangifericomes yunnanensis Wanas., Phookamsak, L.S. Dissan. & J.C. Xu, **sp. nov.** (Figs 29 and 30).

MycoBank No: 859362

Etymology: The specific epithet 'yunnanensis' refers to Yunnan Province, where the holotype was collected.

Holotype: HKAS146058

Saprobic on dead twigs of an unknown deciduous host. Sexual morph: *Ascomata* 250–430 μm high, 390–650 μm diam. ($\bar{x}$ = 346.2 × 490.3 μm, n = 5), immersed, visible as raised regions on host surface, solitary to gregarious, scattered to clustered, dark brown to black, globose to subglobose, uni-loculate to multi-loculate, emerging in a unique small epidermal clypeus, glabrous, non-ostiolate. *Peridium* 10–20 μm wide, thin-walled, of equal thickness, composed of 3–5-layers of hyaline to pale brown, thick cell walls, pseudoparenchymatous cells of *textura angularis* to *textura prismatica*, or *textura globulosa*. *Hamathecium* 2–3.5 μm wide, numerous, hyaline, filamentous, septate, branched, anastomosed, cellular pseudoparaphyses, embedded in a hyaline gelatinous matrix. *Asci* 160–220 × 34–50 μm ($\bar{x}$ = 193 × 44.6 μm, n = 15), 8-spored, bitunicate, fissitunicate, cylindrical-clavate, with long or short pedicel, rounded at the apex, with a small ocular chamber. *Ascospores* 45–57 × 18–27 μm ($\bar{x}$ = 52.4 × 23.1 μm, n = 25), overlapping uni- to tri-seriate, brown to golden brown, muriform, ellipsoidal to broad fusoid, or clavate, straight to slightly bent, multi-septate, sectored, 11–12-transversely septate, 2–5 longitudinally septate at each row, slightly constricted at the central septum, asymmetrical, slightly wider above the central septum, with rounded ends, surrounded by a thick (12–15 μm) mucilaginous sheath. Asexual morph: Undetermined.

Culture characteristics: Colonies on PDA at room temperature (25 °C) under normal light, reaching 22–25 mm diam. after two weeks. Colonies dense, circular, flattened, slightly raised, surface rough, with erose to fimbriate, fluffy, with hyphal tufts, produced small, black droplets, did not produce pigmentation in PDA. Colonies from above are white, with brown hyphae at the edge; colonies from below are cream at the margin, and brown to dark brown towards the center.

Materials examined: China, Yunnan, Honghe Hani and Yi Autonomous Prefecture, Honghe County, 23.421013° N, 102.227243° E, 517 m, on dead twigs of an unknown deciduous host, 03 December 2020, D.N. Wanasinghe, DWHH18-02 (holotype, HKAS146058), ex-type, KUNCC23-16778; *ibid*., DWHH18-02-2 (HKAS146059).

GenBank numbers: KUNCC23-16778: ITS = PV742918, LSU = PV742974, SSU = PV743027, *tef*1-α = PV700653, *rpb*2 = PV700692; HKAS146059: ITS = PV742919, LSU = PV742975, SSU = PV743028, *tef*1-α = PV700654, *rpb*2 = PV700693.

Notes: Phylogenetically, two new strains (KUNCC 23-16778 and HKAS 146059) formed a subclade (100% MLBS and 1.00 BYPP; Fig. 29), positioned basal to *Mangifericomes aquilariae* and *M. hongheensis*. Morphologically, the new isolates resemble *M. aquilariae* and *M. hongheensis* in producing muriform, multi-septate ascospores. However, they can be clearly distinguished from both species based on differences in the dimensions of ascomata, asci, and ascospores, as well as peridial structure and ascospore septation patterns. The new isolates differ from *M. aquilariae* in having larger ascomata (250–430 μm high × 390–650 μm diam. vs 280–460 μm high × 250–510 μm diam.), non-ostiolate ascomata with a hyaline to pale brown peridium composed of thick-walled cells of textura angularis to textura prismatica or textura globulosa, smaller asci (160–220 × 34–50 μm vs 170–265 × 32–50 μm), and ascospores with 11–12 transverse septa and 2–5 longitudinal septa. In contrast, *M. aquilariae* has ostiolate ascomata and ascospores with 10–13 transverse septa and 3–6 longitudinal septa[157]. Compared to *M. hongheensis*, the new isolates have larger ascomata (250–430 × 390–650 μm vs 160–230 × 220–300 μm), non-ostiolate and pale peridia (vs ostiolate, dark brown to black), larger asci (160–220 × 34–50 μm vs 90–120 × 8–12 μm), and larger ascospores (45–57 × 18–27 μm vs 14–17 × 4–8 μm), with distinct septation (11–12 transverse and 2–5 longitudinal septa vs 7–11 transverse and 5–8 longitudinal septa)[156]. Based on phylogenetic evidence and clear morphological distinctiveness, *Mangifericomes yunnanensis* is introduced as a novel species in the present study.

Massarinaceae Munk, Friesia 5 (3-5): 305.

Helminthosporium Link, Mag. Neuesten Entdeck. Gesammten Naturk. Ges. Naturf. Freunde Berlin 3 (1): 10.

Notes: *Helminthosporium* was established by Link[159], with *H. velutinum* designated as the type species. The genus is characterized by immersed ascomata, an inconspicuous ostiole that

does not protrude above the cortical surface, clavate to fusoid asci, and large, hyaline to dark brown, fusoid, subellipsoid to obovoid ascospores surrounded by a thick gelatinous sheath. The asexual morph is distinguished by effuse to punctiform colonies and subhyaline to brown, obclavate, obpyriform to lageniform conidia[159]. *Helminthosporium* species have been reported as saprobes and plant pathogens on various hosts and are widely distributed worldwide[148,160–167]. Currently, 225 species are

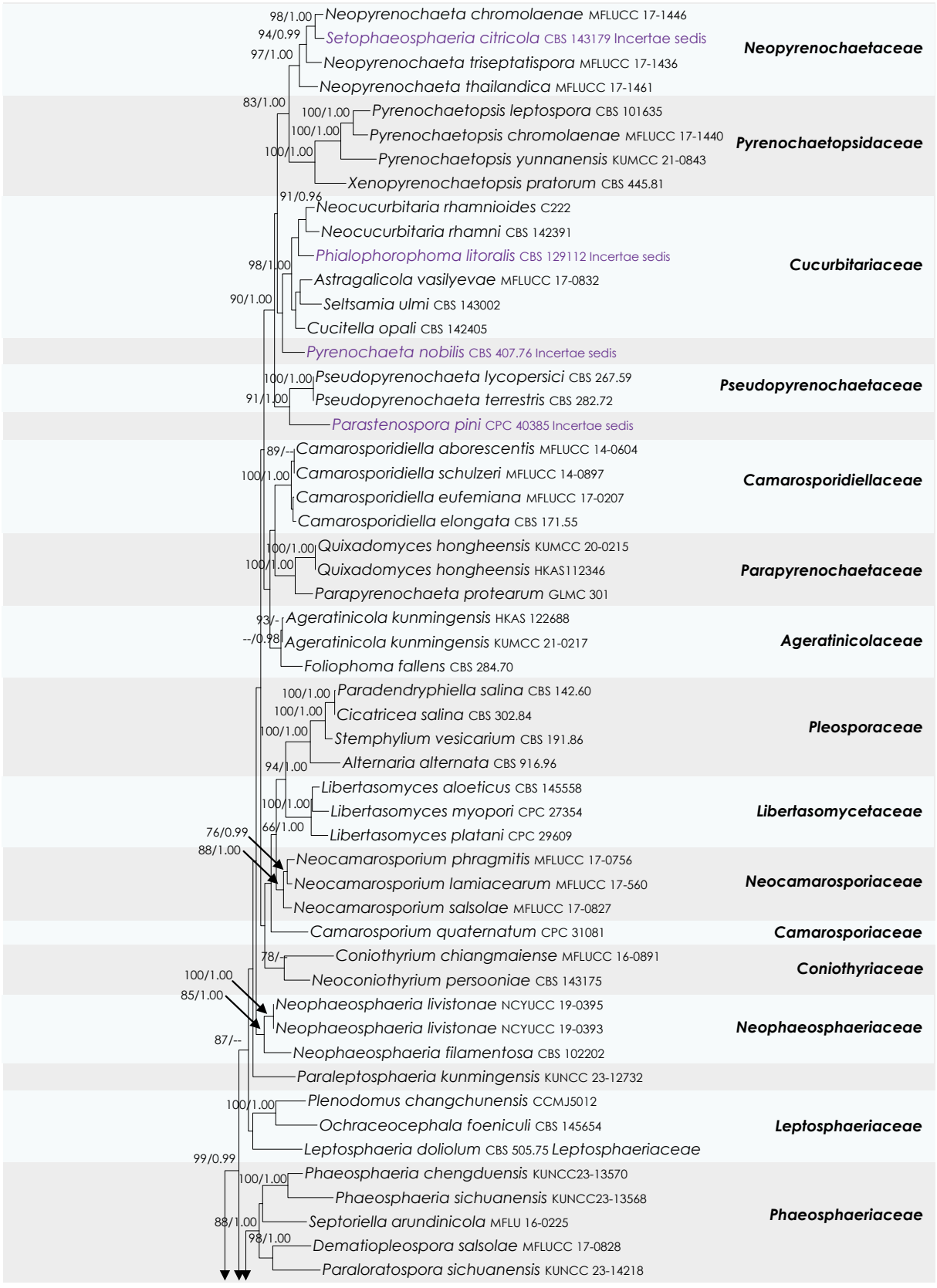

Fig. 29 (to be continued)

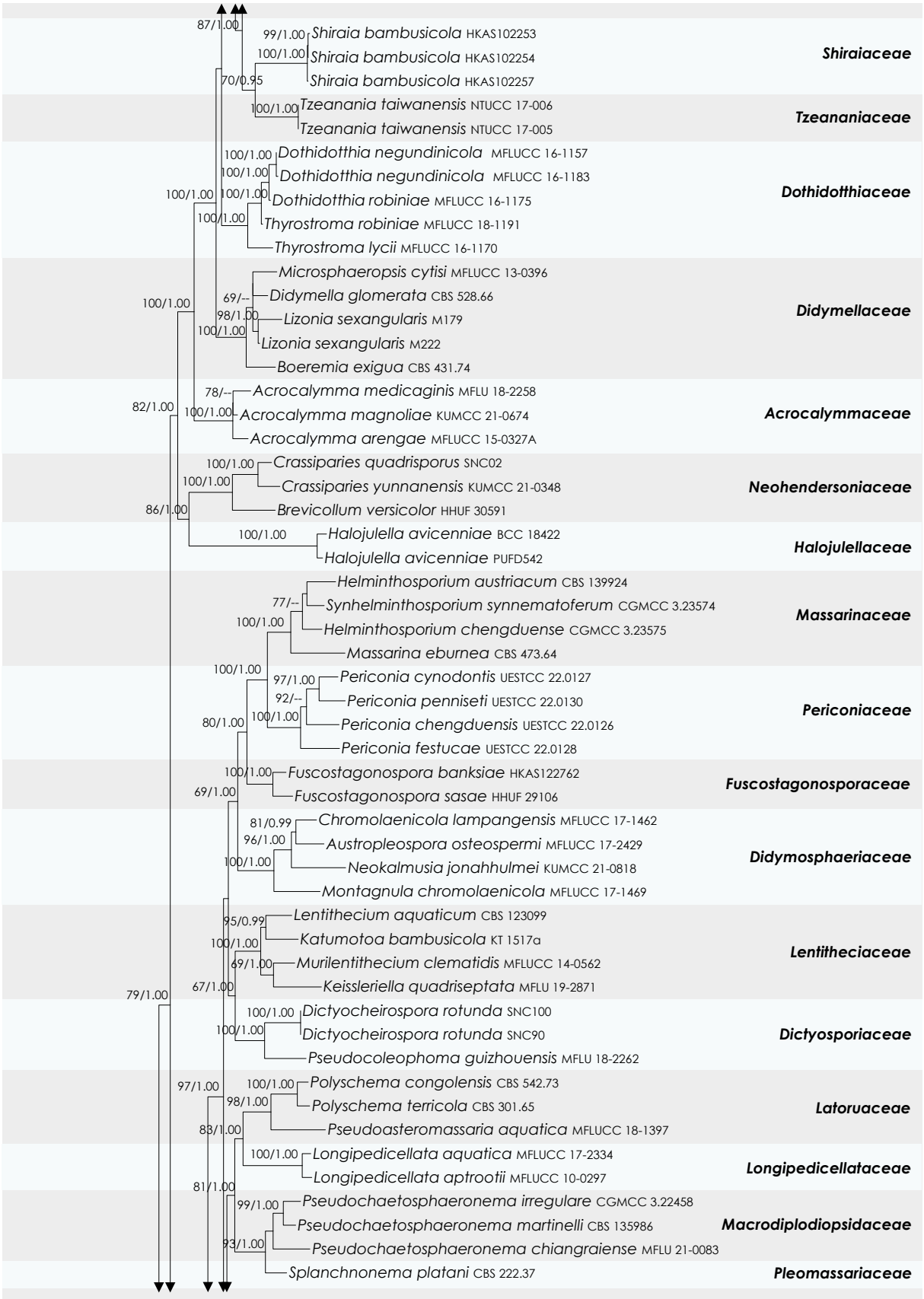

Fig. 29 (to be continued)

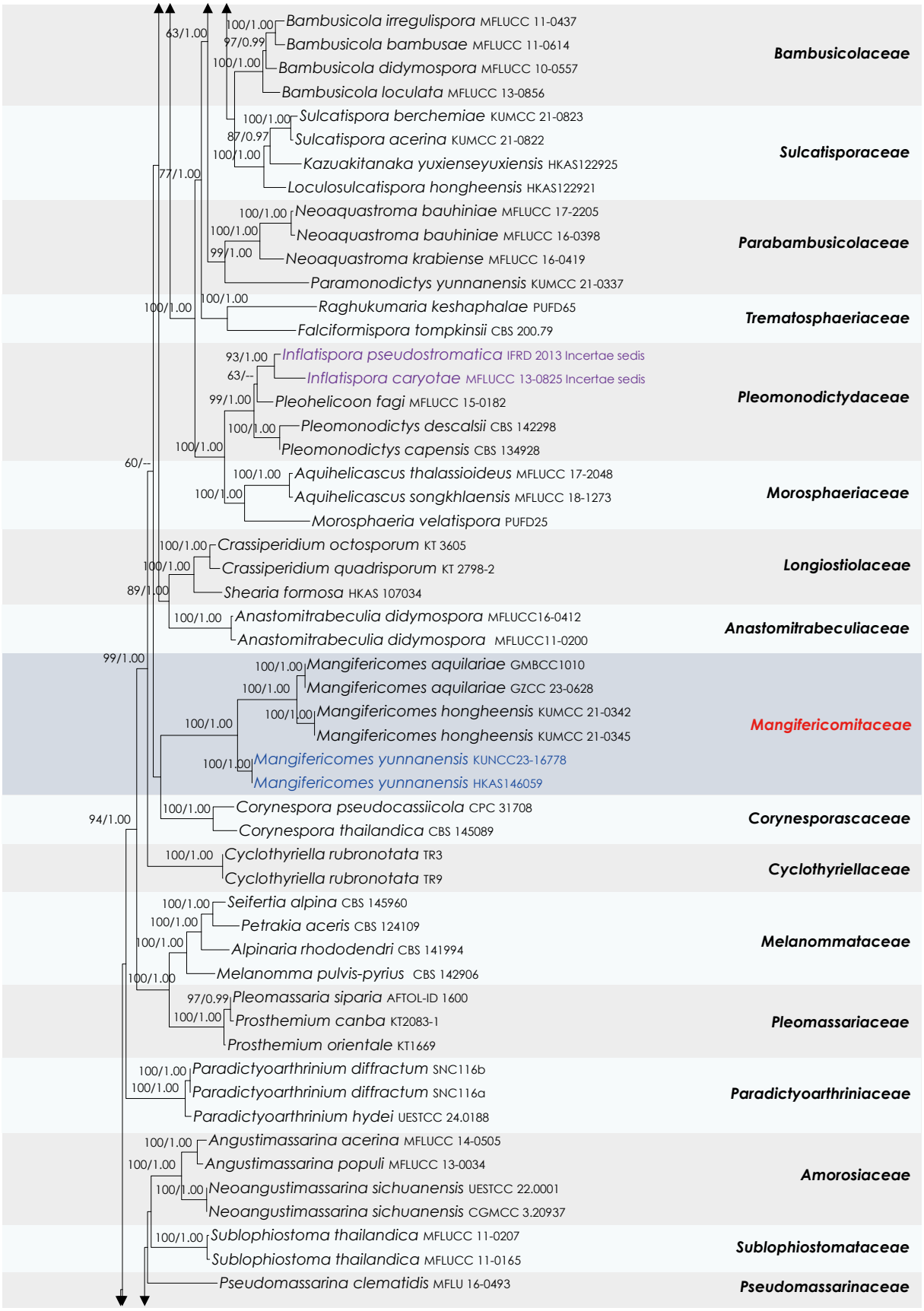

Fig. 29 (to be continued)

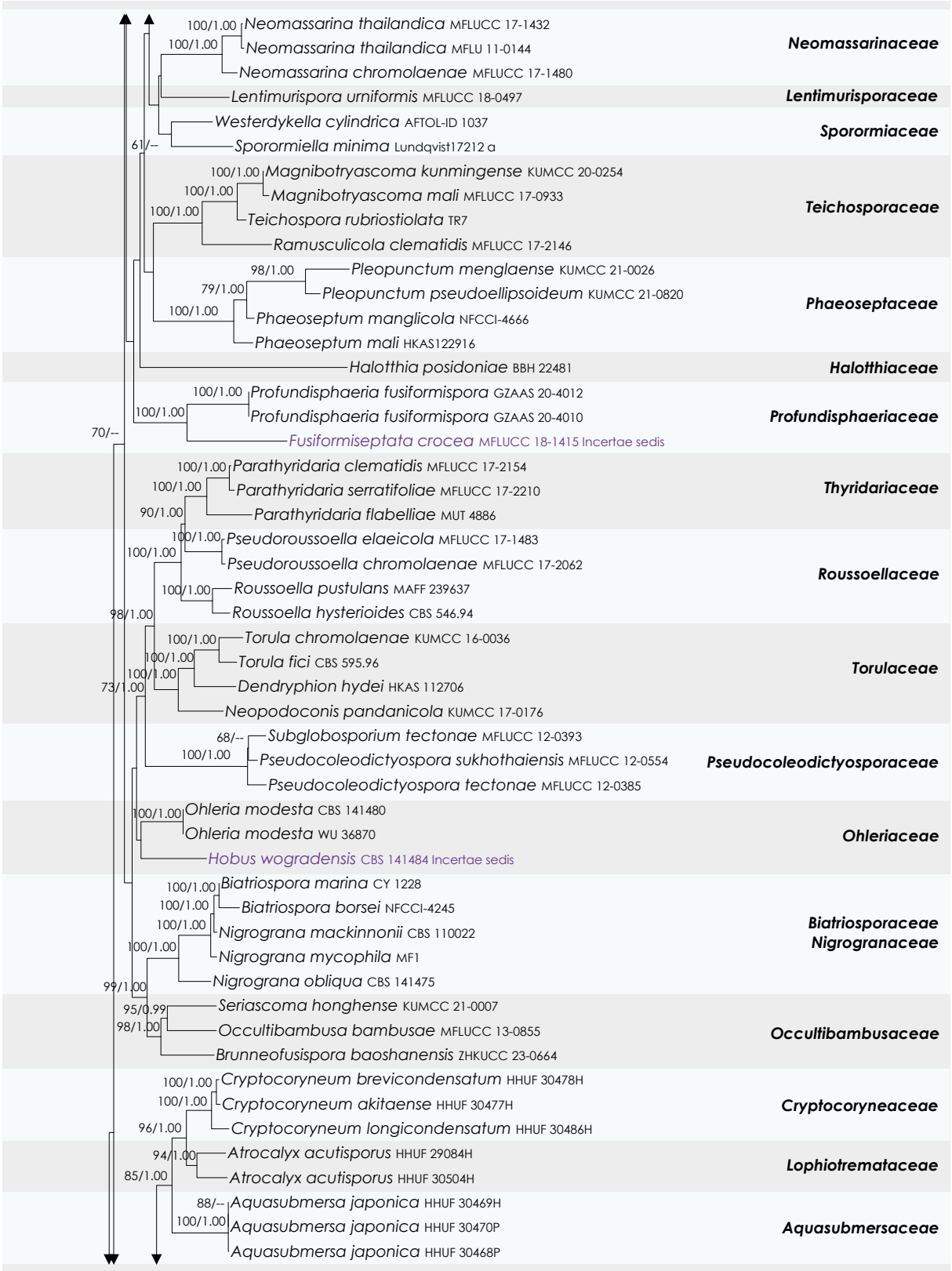

Fig. 29 (to be continued)

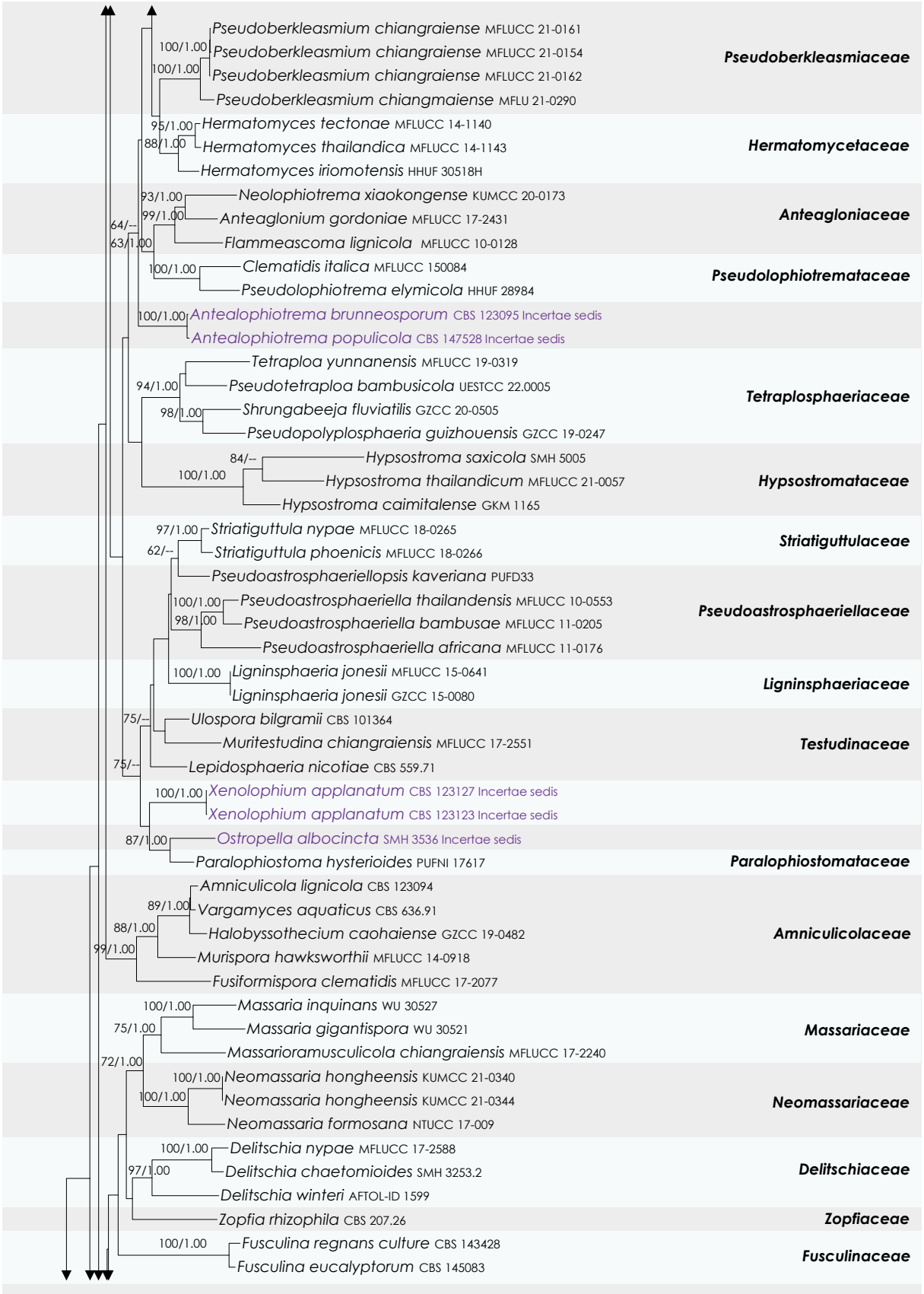

Fig. 29 (to be continued)

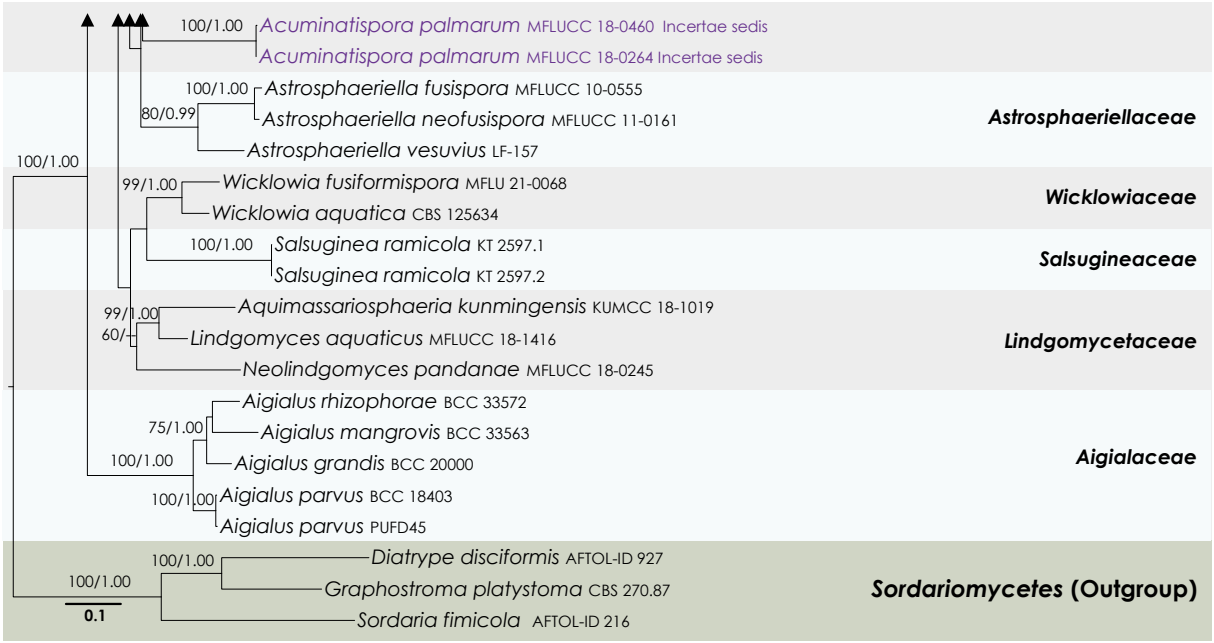

Fig. 29 Maximum Likelihood tree inferred from the concatenated dataset of partial SSU, LSU, 5.8s, *tef*1-α and *rpb*2 sequences. The phylogeny is rooted with *Diatrype disciformis* (AFTOL-ID 927), *Graphostroma platystoma* (CBS 270.87) and *Sordaria fimicola* (AFTOL-ID 216). The final likelihood value is −150,266.016088. The final alignment included 2,812 unique site patterns, with approximately 19.07% of the positions comprising gaps or ambiguous characters. The estimated nucleotide frequencies were as follows: A = 0.250162, C = 0.244801, G = 0.270528, T = 0.234509. The substitution model yielded the following relative rates: AC = 1.409236, AG = 4.442359, AT = 1.464844, CG = 1.164667, CT = 9.104968, GT = 1.000000. The proportion of invariable sites (I) was estimated at 0.409621 and the gamma distribution shape parameter (α) was 0.569317. Bayesian inference reached convergence after 5M generations, when the average standard deviation of split frequencies dropped below 0.01. A total of 50,001 trees were sampled, and 37,501 of these were retained for the final analysis after discarding the initial 25% as burn-in. The alignment also revealed 2,814 distinct informative sites. In the resulting phylograms, newly generated sequences are shown in blue and *Pleosporales* genera *incertae sedis* are in purple. The new family shown in red.

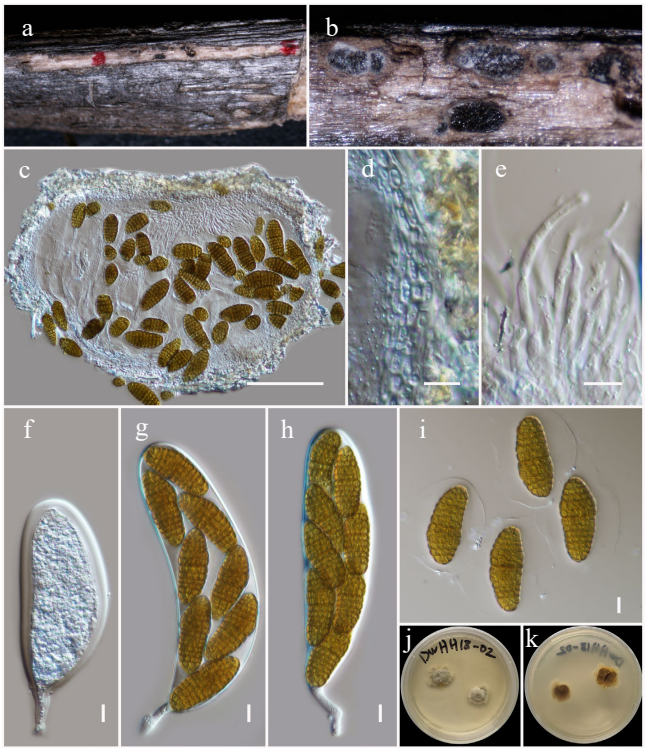

Fig. 30 *Mangifericomes yunnanensis* (HKAS146058, holotype). (a) Ascomata on the dead woody twigs. (b), (c) Cross-section of ascomata. (d) Peridium. (e) Pseudoparaphyses. (f)–(h) Asci. (i) Ascospores. (j), (k) Colony on MEA (k from the bottom). Scale bars: (c) = 100 μm, (d)–(i) = 10 μm.

accepted under *Helminthosporium* (out of 521 species epithets), although most lack sequence data[168]. In the present study, a new species of *Helminthosporium* is introduced.

Helminthosporium hongheense Wanas., Phookamsak, L.S. Dissan. & J.C. Xu, **sp. nov.** (Figs 31 and 32).

MycoBank No: 859363

Etymology: The specific epithet 'hongheense' refers to Honghe, Yunnan Province, where the holotype was collected.

Holotype: HKAS146049

Saprobic on a dead wood of a *Fagaceae* hosts. Sexual morph: Undetermined. Asexual morph: Hyphomycetous. *Colonies* on the host, black, effuse, velvety, appear as clusters. *Mycelium* is composed of branched, septate, smooth, and thick-walled hyphae. *Conidiophores* 220–330 × 8–14 μm ($\bar{x}$ = 283.3 × 12 μm, n = 20), erect, dark brown, mononematous, macronematous, unbranched, multiseptate, flexuous, rounded to obtuse apex, bulbous base, smooth to rough, arise from the host as clusters. *Conidiogenous cells* terminal, polytretic, cylindrical, integrated. *Conidia* 80–140 × 15–20 μm ($\bar{x}$ = 101.8 × 17.9 μm, n = 20), simple, dry, obclavate, acropleurogenous, 10–14-distoseptate, brown, straight to curved, truncate base, rounded apex, slightly paler towards apex. *Hilum* observed as a comparatively dark flat ring. *Conidial secession* schizolytic.

Materials examined: China, Yunnan, Honghe Hani and Yi Autonomous Prefecture, Jianshui County, Chenguan, 23.500871° N, 102.883429° E, 2,062 m, on dead twigs of *Fagaceae* sp., 15 March 2019, D.N. Wanasinghe, DW0527-15 (holotype, HKAS146049); *ibid*., Puxiongxiang 23.521432° N, 103.039049° E, 1,917 m, on dead twigs of *Quercus* sp., DW0528-07 (HKAS146050).

GenBank numbers: HKAS146049: ITS = PV742920, LSU = PV742976, SSU = PV743029, *tef*1-α = PV700655; HKAS146050: ITS = PV742921, LSU = PV742977, SSU = PV743030, *tef*1-α = PV700655.

Notes: In multigene phylogenetic analyses based on a combined SSU, LSU, ITS, *tef*1-*α,* and *rpb*2 dataset, two newly collected strains (HKAS 146049 and HKAS 146050) formed a monophyletic clade (100% MLBS and 1.00 BYPP; Fig. 31) sister to the type strain of *Helminthosporium syzygii* (CPC 35312). Morphologically, *Helminthosporium syzygii* and our new collections are similar in colony characteristics, conidiophore structure, conidiogenous cells and conidial shape, with overlapping measurements[169]. The study initially aimed to clarify whether these strains could be considered conspecific with *H. syzygii*. However, multiple lines of evidence argue against this. The comparison of the ITS region revealed a 5% nucleotide difference between our strains and *H. syzygii* (29/572 bp, including three gaps). *Helminthosporium syzygii* was isolated from bark cankers on *Syzygium* sp. (*Myrtaceae*) in the Eastern Cape Province of South Africa, while our collections were obtained as saprobes on *Quercus* sp. (*Fagaceae*) hosts in Yunnan, China. These differences in host association, lifestyle, geographic origin, and molecular divergence suggest that our collections represent a distinct species. Pending additional morphological evidence (particularly from sexual morphs), our two collections are designated as *Helminthosporium hongheense* sp. nov.

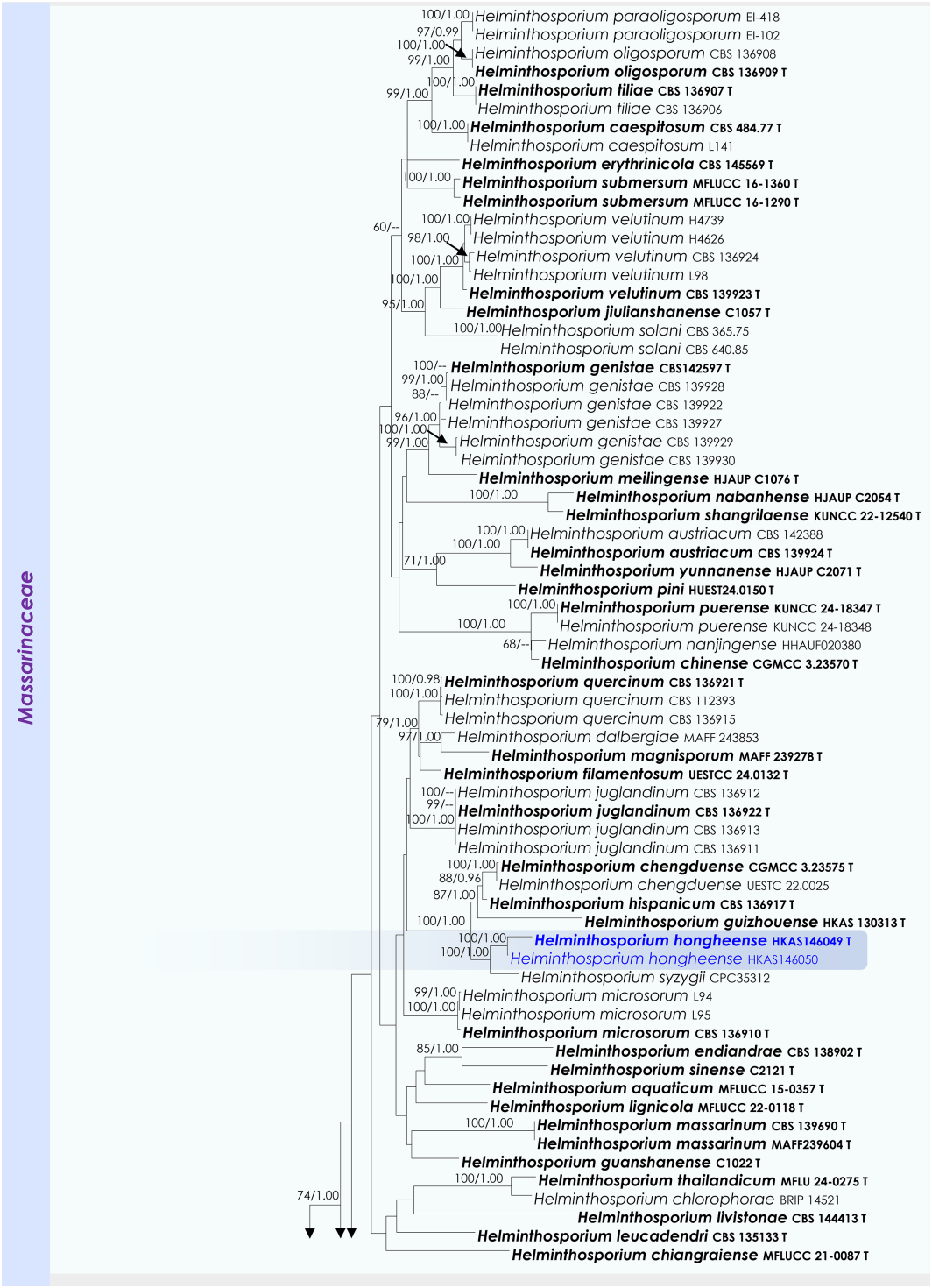

Fig. 31 (to be continued)

Fig. 31 Maximum Likelihood tree inferred from the concatenated dataset of partial SSU, LSU, ITS, *tef*1-α and *rpb*2 sequence analyses. The tree is rooted to *Cyclothyriella rubronotata* (CBS 121892, CBS 141486). The final likelihood value is −35,556.858868. The final alignment included 2,182 unique site patterns, with approximately 38.1% of the positions comprising gaps or ambiguous characters. The estimated nucleotide frequencies were as follows: A = 0.237453, C = 0.256825, G = 0.269094, T = 0.236628. The substitution model yielded the following relative rates: AC = 1.452161, AG = 3.722496, AT = 1.468538, CG = 0.961651, CT = 7.489299 and GT = 1.000000. The proportion of invariable sites (I) was estimated at 0.518695 and the gamma distribution shape parameter (α) was 0.562000. Bayesian inference reached convergence after 1,923,000 generations, when the average standard deviation of split frequencies dropped below 0.01 (observed value: 0.009981). A total of 19,231 trees were sampled, and 14,424 of these were retained for the final analysis after discarding the initial 25% as burn-in. The alignment also revealed 2,183 distinct informative sites. In the resulting phylograms, sequences generated in this study are highlighted in blue, while ex-type or type strains are indicated in boldface.

Fig. 32 *Helminthosporium hongheense* (HKAS146049, holotype). (a)–(d) Dark brown or black colonies on natural substrate. (e)–(g) Conidiophores. (h)–(k) Conidia. Scale bars: (f) = 100 μm, (e), (g)–(k) = 10 μm.

Parabambusicolaceae Kaz. Tanaka & K. Hiray., Studies in Mycology 82: 115.

Neomultiseptospora N. Xie, Phookamsak & Hongsanan, Journal of Fungi 8 (2, no. 109): 8.

Notes: Xie et al.[25] introduced *Neomultiseptospora* to accommodate a single species, *N. yunnanensis*, collected from dead branches of bamboo in Yunnan Province, China. Multigene phylogenetic analyses demonstrated that *Neomultiseptospora* clustered with the genera *Multiseptospora* and *Scolecohyalosporium*. Morphologically, *Neomultiseptospora* resembles *Multiseptospora* in possessing phragmosporous, hyaline, multi-septate ascospores but differs in forming raised, hemispherical to subconical ascomata, whereas *Multiseptospora* develops globose to subglobose ascomata covered with dark, hair-like hyphae and embedded within the host tissue[170]. Although *Neomultiseptospora* is phylogenetically close to *Scolecohyalosporium*, it can be distinguished by having phragmosporous ascospores, compared to the scolecosporous ascospores of *Scolecohyalosporium*[25,67,171]. Morphologically, *Neomultiseptospora* also closely resembles *Parabambusicola*, sharing features such as hemispherical to subconical ascomata and hyaline, fusiform, 5-septate ascospores, and occurrence on bamboo[25,172,173]. However, phylogenetically, the two genera are distinct. In the present study, *Neomultiseptospora hongheensis* is introduced as the second species of the genus, along with an additional collection representing *N. yunnanensis*.

Neomultiseptospora hongheensis Wanas., Phookamsak, L.S. Dissan. & J.C. Xu, **sp. nov.** (Figs 33 and 34).

MycoBank No: 859364

Etymology: The specific epithet 'hongheensis' refers to Honghe, Yunnan Province, where the holotype was collected.

Holotype: HKAS146053

Saprobic on dead sheath of a *Poacea* host. Sexual morph: *Ascomata* 190–250 μm high × 250–320 μm diam. μm ($\bar{x}$ = 233.7 × 283.4 μm, n = 5), scattered to aggregated, semi-immersed to erumpent through host cortex, brown to dark brown, subglobose in surface view, conical and with a flattened base in cross-section, uni-loculate, coriaceous, ostiolate. *Peridium* 10–20 μm wide, comprising thick-walled pigmented cells of *textura angularis*, intermixed with host tissue. *Pseudoparaphyses* 1.5–2 μm wide, filamentous, septate, embedded in a hyaline gelatinous matrix. *Asci* 90–120 × 18–23 μm ($\bar{x}$ = 108 × 21.2 μm, n = 10), 8-spored, bitunicate, fissitunicate, cylindrical to cylindrical-clavate, sessile to short-pedicellate, apically rounded, with a well-developed ocular chamber. *Ascospores* 40–52 × 7.5–10 μm ($\bar{x}$ = 45.3 × 8.4 μm, n = 20), overlapping 2–3-seriate, hyaline, fusiform, straight to slightly curved, 10–11-septate, fifth cell from the apex slightly enlarged, noticeably constricted at the fifth septum, less constricted at the other septa, smooth-walled, guttulate at immaturity, surrounded by a conspicuous, thick mucilaginous sheath. Asexual morph: undetermined.

Materials examined: China, Yunnan, Honghe Hani and Yi Autonomous Prefecture, Honghe County, 23.421068° N, 102.229128° E, 735 m, on dead sheath of a *Poacea* sp., 13 March 2023, D.N. Wanasinghe, DWHH23-80 (holotype, HKAS146053); *ibid*., DWHH23-58-03 (isotype, HKAS146054); *ibid*., 23.421013° N, 102.227243° E, 517 m, 03 December 2020, DWHH17-02 (HKAS146056); *ibid*., DWHH17-02-1 (HKAS146055).

GenBank numbers: HKAS146053: ITS = PV742922, LSU = PV742978, SSU = PV743031, *tef*1-α = PV700657; HKAS146054: ITS = PV742923, LSU = PV742979, SSU = PV743032, *tef*1-α = PV700658; HKAS146056: ITS = PV742924, LSU = PV742980, SSU = PV743033, *tef*1-α = PV700659; HKAS146055: ITS = PV742925, LSU = PV742981, SSU = PV743034, *tef*1-α = PV700660.

Notes: Four strains of *Neomultiseptospora hongheensis* formed a monophyletic clade (100% MLBS; Fig. 33), sister to *N. yunnanensis*. Morphologically, *Neomultiseptospora hongheensis* fits well within the generic circumscription of *Neomultiseptospora*, sharing similar characteristics of the ascomata, peridium, asci, and ascospores. However, the two species can be distinguished based on ascospore size and septation. *Neomultiseptospora hongheensis* possesses comparatively larger ascospores (40–52 × 7.5–10 μm) with 10–11 septa, whereas *N. yunnanensis* has smaller ascospores (22–27 × 5–8.5 μm) with (4–)5 septa[25].

Neomultiseptospora yunnanensis Phookamsak, Hongsanan & N. Xie, Journal of Fungi 8 (2, no. 109): 8 (Figs 33 and 35).

MycoBank No: 559390

Saprobic on dead culms of a *Poaceae* sp. Sexual morph: *Ascomata* 100–150 μm high × 260–320 μm diam. ($\bar{x}$ = 130.7 × 287.4 μm, n = 5), scattered, solitary to aggregated, immersed, visible as raised, black, dome-shaped on host surface, hemispherical to subconical, wedge-shaped at the sides, uni-loculate, glabrous. *Ostioles* inconspicuous.

Peridium unequally thickened, 15–25 μm wide at the apex, 30–50 μm wide at the sides, poorly developed at the base, comprising several layers of brown, thick-walled cells of *textura angularis* to *textura prismatica*, outer layer intermixed with host cortex. *Pseudoparaphyses* 1.5–3 μm wide, numerous, filamentous, septate, slightly constricted at the septa, branched, cellular, anastomosing above the asci. *Asci* 50–90 × 14–20 μm ($\bar{x}$ = 74.9 × 17.3 μm, n = 15), 8-spored, bitunicate, fissitunicate, clavate, short-pedicellate, apically rounded, with a well-developed ocular chamber. *Ascospores* 25–32 × 6.5–8.5 μm ($\bar{x}$ = 28.6 × 7.7 μm, n = 25), overlapping 1–2-seriate, hyaline, fusiform to ellipsoidal or oblong, straight to slightly curved, 5-septate, constricted at the septa, with rounded ends, third cell from apex slightly swollen, guttulate, smooth-walled, surrounded by a distinct, thick (4–7 μm), mucilaginous sheath. Asexual morph: Undetermined.

Material examined: China, Yunnan, Honghe Hani and Yi Autonomous Prefecture, Honghe County, 23.421068° N, 102.229128° E, 735 m, on dead culms of a *Poaceae* sp., 13 March 2023, D.N.

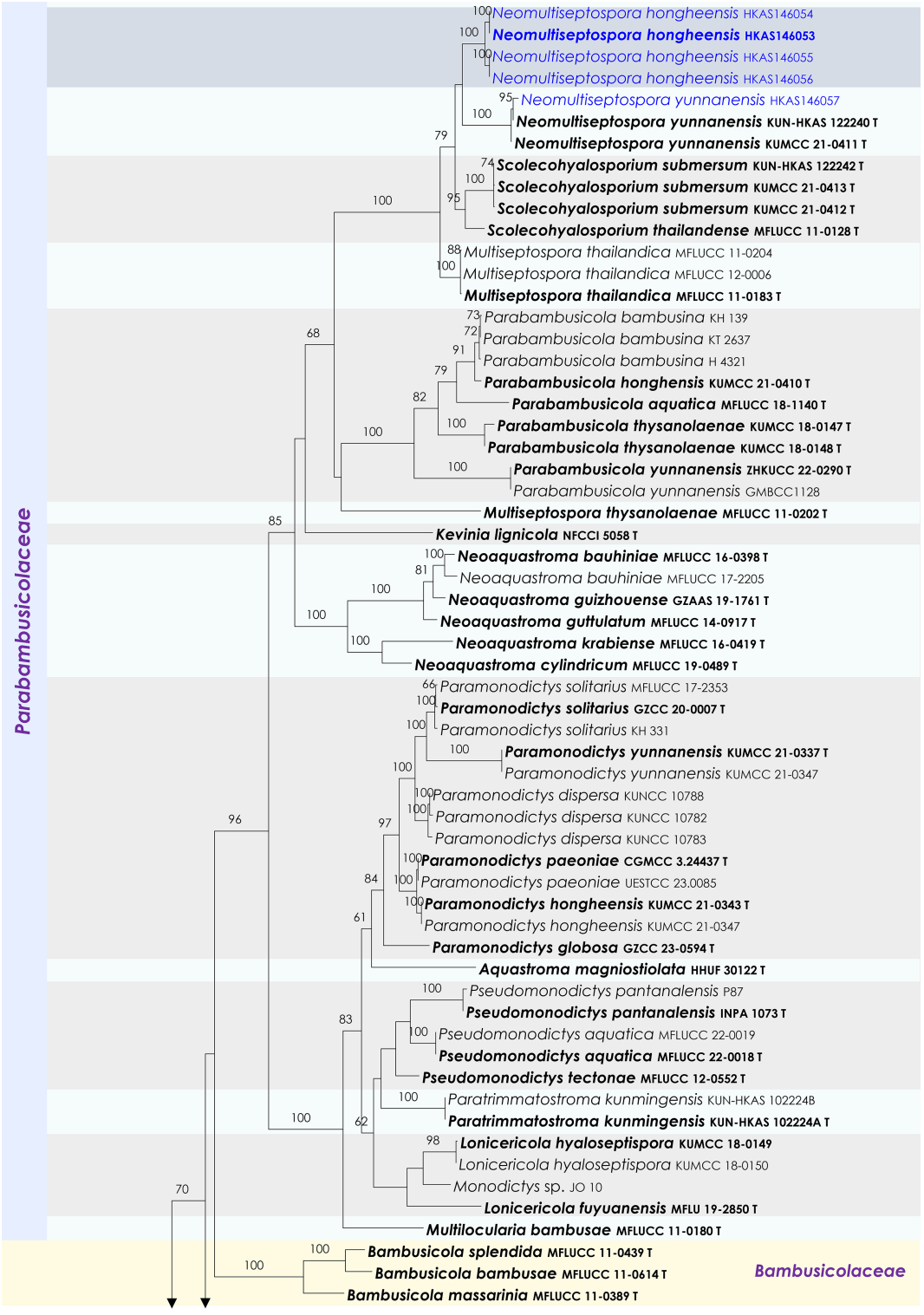

Fig. 33 (to be continued)

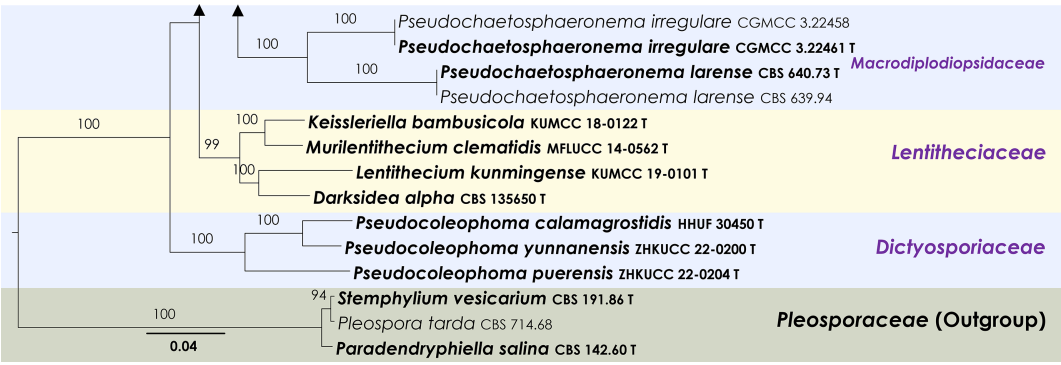

Fig. 33 Maximum Likelihood tree inferred from the concatenated dataset of partial SSU, LSU, ITS, *tef*1-α and *rpb*2 sequences. The phylogeny is rooted with *Paradendryphiella salina* (CBS 142.60), *Pleospora tarda* (CBS 714.68) and *Stemphylium vesicarium* (CBS 191.86). The final likelihood value is –25,430.003747. The final alignment included 1,492 unique site patterns, with approximately 18.07% of the positions comprising gaps or ambiguous characters. The estimated nucleotide frequencies were as follows: A = 0.234317, C = 0.258507, G = 0.272066, T = 0.235111. The substitution model yielded the following relative rates: AC = 1.103972, AG = 2.858045, AT = 1.446677, CG = 1.147080, CT = 5.894779, GT = 1.000000. The proportion of invariable sites (I) was estimated at 0.7274, and the gamma distribution shape parameter (α) was 0.569941. Bayesian inference reached convergence after 761,000 generations, when the average standard deviation of split frequencies dropped below 0.01 (observed value: 0.009992). A total of 7,611 trees were sampled, and 5,709 of these were retained for the final analysis after discarding the initial 25% as burn-in. The alignment also revealed 1,493 distinct informative sites. In the resulting phylograms, sequences generated in this study are highlighted in blue, while ex-type or type strains are indicated in boldface.

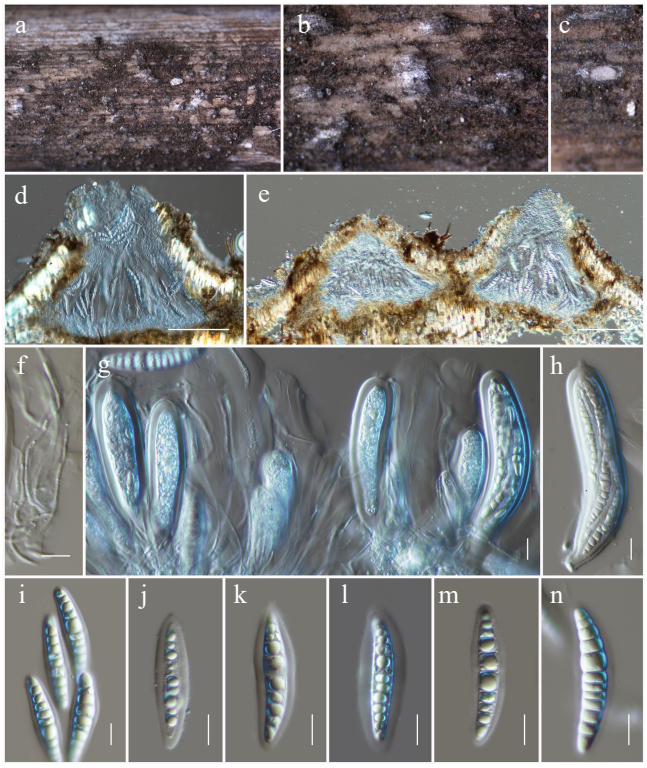

Fig. 34 *Neomultiseptospora hongheensis* (HKAS146053, holotype). (a), (b) Ascomata on the dead woody twigs. (c)–(e) Cross-section of ascomata. (f) Pseudoparaphyses. (g), (h) Asci. (i)–(n) Ascospores. Scale bars: (d), (e) = 100 μm, (f)–(n) = 10 μm.

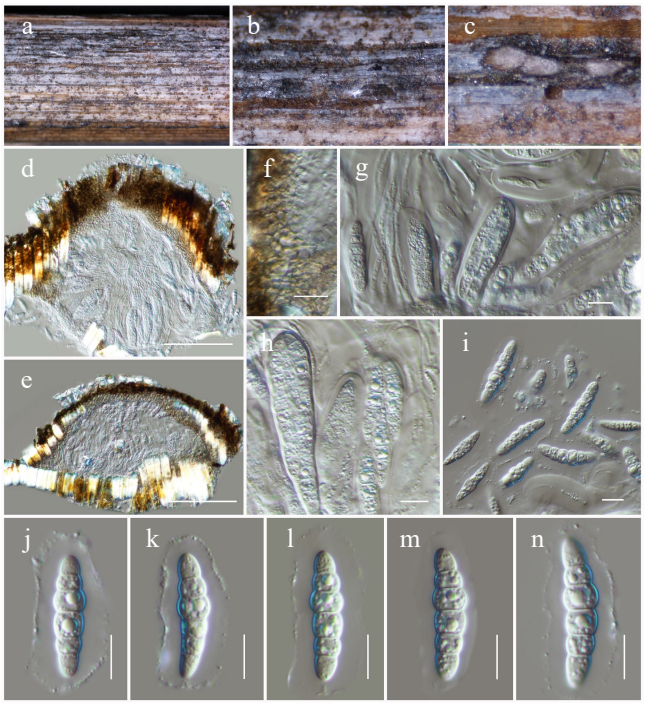

Fig. 35 *Neomultiseptospora yunnanensis* (HKAS146057). (a), (b) Ascomata on the dead woody twigs. (c)–(e) Cross-section of ascomata. (f) Peridium. (g), (h) Asci and pseudoparaphyses. (i)–(n) Ascospores. Scale bars: (d), (e) = 100 μm, (f)–(n) = 10 μm.

Wanasinghe, DWHH23-67 (HKAS146057).

GenBank numbers: HKAS146057: ITS = PV742926, LSU = PV742982, SSU = PV743035, *tef*1-α = PV700661.

Known hosts and distribution: Saprobic on a dead stem of bamboo from a terrestrial environment in Yunnan, China[25]; on dead culms of a *Poaceae* sp. in Yunnan, China (this study).

Notes: Phylogenetic analyses supported our isolate (HKAS146057) as forming a monophyletic clade with the type strain of *Neomultiseptospora yunnanensis*. Given the overlapping morphological characteristics[25] and strong phylogenetic affinity (100% MLBS; Fig. 33), our collection is recognized as another collection of *Neomultiseptospora yunnanensis* from Honghe, Yunnan.

Phaeosphaeriaceae M.E. Barr, Mycologia 71: 948.

Leptospora Rabenh., Hedwigia 1 (18): 116.

Notes: *Leptospora* is characterized by large, flask-shaped ascomata with long, cylindrical asci and phragmosporous to scolecosporous, fusiform, cylindric-clavate to filiform ascospores. Members of this genus have also been reported to produce a reddish-purple pigment that stains the host tissue around the ostiole[131,174,175]. Hyde et al.[131] designated a reference specimen for

the type, *L. rubella*, and confirmed the placement of *Leptospora* in *Phaeosphaeriaceae* based on phylogenetic analyses of ITS, LSU, and SSU sequence data. Species of this genus have been increasingly reported in recent years, mostly from terrestrial habitats[69,123,167,176,177]. Currently, 18 species are accepted in Index Fungorum[89], but sequence data are available in GenBank for only nine species.

Leptospora phraeana Mapook & K.D. Hyde, Fungal Diversity 101: 65 (Figs 36 and 37).

MycoBank No: 557291

Saprobic on dead pods of a *Fabaceae* sp. Sexual morph: *Ascomata* immersed, causing raised regions on the host surface, scattered to gregarious, globose to subglobose, non-ostiolate. *Peridium* 3–4-layered, comprising thick-walled, hyaline cells of *textura angularis* to *textura globosa*. *Pseudoparaphyses* 1.5–2.5 μm wide, hyaline, septate, branched, cellular. *Asci* 80–95 × 9–12 μm ($\bar{x}$ = 86.5 × 10.2 μm, n = 20), 8-spored, bitunicate, fissitunicate, cylindrical-clavate, with long or short pedicel, rounded at the apex, with a small ocular chamber. *Ascospores* 60–80 × 2.8–3.3 μm ($\bar{x}$ = 70.1 × 2.9 μm, n = 30), fasciculate, in parallel, scolecosporous, pale brown to yellowish brown, cylindrical to broadly filiform, 12–17-septate with minute guttule in each cell, straight or slightly curved, with polar appendages. Asexual morph: Undetermined.

Material examined: China, Yunnan, Honghe Hani and Yi Autonomous Prefecture, Honghe County, 23.421013° N, 102.227243° E, 517 m, on dead pods of a *Fabaceae* sp., 14 August 2022, D.N. Wanasinghe, DWHH22-05 (HKAS146060).

GenBank numbers: HKAS146060: ITS = PV742927, LSU = PV742983, SSU = PV743036, *tef*1-α = PV700662.

Known hosts and distribution: Saprobic on dead stems of *Chromolaena odorata* in Phrae Province, Thailand[69]; on dead pods of a *Fabaceae* sp. in Yunnan, China (this study).

Notes: *Leptospora phraeana* was introduced by Mapook et al.[69] based on a collection from Phrae Province, Thailand, on dead stems of *Chromolaena odorata* (*Asteraceae*). This species is characterized by semi-immersed, globose to obpyriform ascomata; hyaline periphysis-like cells near the ostiolar neck; a peridium composed of textura angularis cells; cylindrical, septate, and branched pseudoparaphyses; cylindric-clavate asci with a short pedicel and a prominent ocular chamber; and fasciculate, scolecosporous, pale brown to yellowish-brown, cylindrical to broadly filiform, multi-septate ascospores with polar appendages. During our survey in the Honghe region of Yunnan, China, a fungus exhibiting morphological features consistent with *Leptospora phraeana* was collected. Phylogenetic analyses further supported our isolate as monophyletic with the type strain of *Leptospora phraeana*. Given the overlapping morphological characteristics and strong phylogenetic affinity (100% MLBS and 1.00 BYPP; Fig. 36), our collection is recognized as a new record of *Leptospora phraeana*. Notably, our specimen was isolated from dead pods of a *Fabaceae* species, thereby expanding the known host range and geographic distribution of this species.

Murichromolaenicola Mapook & K.D. Hyde, Fungal Diversity 101: 71.

Notes: *Murichromolaenicola* was introduced by Mapook et al.[69] with two species, *M. chiangraiensis* and *M. chromolaenae*, isolated from dead stems of *Chromolaena odorata* in Thailand. These taxa are characterized by semi-immersed to superficial, solitary or scattered ascomata; fissitunicate, cylindric-clavate asci and overlapping, 1–2-seriate, initially hyaline to golden-yellow, uniseptate ascospores[69]. The asexual morphs are defined by pycnidial, uniloculate, globose conidiomata; phialidic, ampulliform to cylindrical, hyaline, unbranched conidiogenous cells and ellipsoid to broadly fusiform, muriform conidia that are 5–7-transversely septate with 1–2 vertical septa, brown in color, and bearing polar appendages[69]. Subsequently, Htet et al.[178] described *Murichromolaenicola thailandensis* from the same host in Thailand, while Sun et al.[167] reported *M. dendrobii* on twigs of *Dendrobium nobile*, also from Thailand. In the present study, *Murichromolaenicola thailandensis* is reported from Yunnan, China, representing a new geographical record for both the genus and species.

Murichromolaenicola thailandensis Htet, Mapook & K.D. Hyde, Phytotaxa 618 (2): 126 (2023) (Figs 36 and 38).

MycoBank No: 849500

Saprobic on dead twigs of an unidentified host. Asexual morph: *Conidiomata* 100–120 μm high × 150–190 μm diam. ($\bar{x}$ = 111.3 × 173.6 μm, n = 5), immersed, solitary, uni-loculate, globose to subglobose, yellowish-brown to brown. *Conidioma wall* 10–20 μm wide, comprising 4–5 layers of thick-walled cells of *textura angularis*, outer cells yellowish-brown to brown, inner cells brown to subhyaline or hyaline and bearing conidiogenous cells. *Conidiophores* reduced to conidiogenous cells. *Conidiogenous cells* 3–4 × 5–7 μm ($\bar{x}$ = 3.7 × 5.9 μm, n = 10), arising from the innermost layer of the pycnidial wall, discrete, ampulliform to cylindrical, hyaline, holoblastic, phialidic. *Conidia* 15–20 × 7–9 μm ($\bar{x}$ = 17.5 × 7.7 μm, n = 50), ellipsoid to broadly fusiform, hyaline when immature, golden brown to dark brown at maturity, 3–4-transversely septate, not constricted at the septa, 1–3-vertically septate, guttulate, apex rounded, base obtuse to conical, with polar appendages at both ends. Sexual morph: Undetermined.

Culture characteristics: Colonies on PDA at room temperature (25 °C) under normal light, reaching 18–20 mm diam. after two weeks. Colonies dense, circular, slightly raised to low convex, surface smooth to slightly rough, with edge entire, floccose, do not produce pigmentation in PDA. Colonies from above yellow-grey to yellow-pale green, with brown, hyphae at edge; colonies from below black at the margin, brown to dark brown towards the center, with brown, sparse mycelia at the margin.

Material examined: China, Yunnan, Honghe Hani and Yi Autonomous Prefecture, Honghe County, 23.421013° N, 102.227243° E, 517 m, on dead twigs of an unknown deciduous host, 03 December 2020, D.N. Wanasinghe, DWHH14-02 (HKAS146061), living culture KUNCC23-16770.

GenBank numbers: KUNCC23-16770: ITS = PV742928, LSU = PV742984, SSU = PV743037, *tef*1-α = PV700663.

Known hosts and distribution: Saprobic on dead stems of *Chromolaena odorata* in Chiang Rai Province, Thailand[178]; on dead twigs of an unknown deciduous host in Yunnan, China (this study).

Notes: Based on morphological comparisons, *Murichromolaenicola thailandensis* closely resembles *M. chromolaenae* in having immersed conidiomata, yellowish brown to brown cells of textura angularis, and yellowish brown to brown ascospores with both transverse and longitudinal septa[178]. However, *Murichromolaenicola thailandensis* differs from *M. chromolaenae* in comparatively smaller conidiomata (130–150 × 140–160 μm vs 200–235 × 195–230 μm) and smaller conidia with a gelatinous cap (10–20 × 5–10 μm vs 14–25 × 6.5–11 μm). The conidia of *Murichromolaenicola chromolaenae* are ellipsoid to broadly fusiform, with 5–7 transverse septa and polar appendages at both ends, whereas *M. thailandensis* produces oblong to oval or obovoid conidia, rounded at both ends, with 3–5 transverse septa and a gelatinous cap at one end. The morphology of the conidiomata, conidiogenous cells, and conidia in our new collection (HKAS146061) corresponds well with the original description of *Murichromolaenicola thailandensis*, further supported by its placement in a monophyletic clade (99% MLBS and 1.00 BYPP;

Fig. 36) alongside other reported strains of the species. Therefore, our isolate is recognized as a new record of *Murichromolaenicola thailandensis*, extending its known geographical distribution to Yunnan, China.

Pseudostaurosphaeria Mapook & K.D. Hyde, Fungal Diversity 101: 81.

Notes: *Pseudostaurosphaeria* was established by Mapook et al.[69] to accommodate *P. chromolaenae* and *P. chromolaenicola*. The genus is characterized by solitary, immersed to semi-immersed or superficial, uniloculate conidiomata; holoblastic, ampulliform to cylindrical or oblong, hyaline conidiogenous cells, and globose, oblong to obovoid conidia with 1–2 transverse septa[69]. The asexual morph of *Pseudostaurosphaeria* resembles that of *Staurosphaeria*, particularly in producing brown conidia with a transverse septum and vertical septa that eventually divide the conidium into four sections. However, the two genera are not closely related phylogenetically[44]. *Pseudostaurosphaeria* is closely related to *Yunnanensis* in our phylogenetic analysis (Fig. 36), though the latter differs by producing muriform, ellipsoidal to obovoid conidia with three transverse septa and a single vertical septum. In contrast,

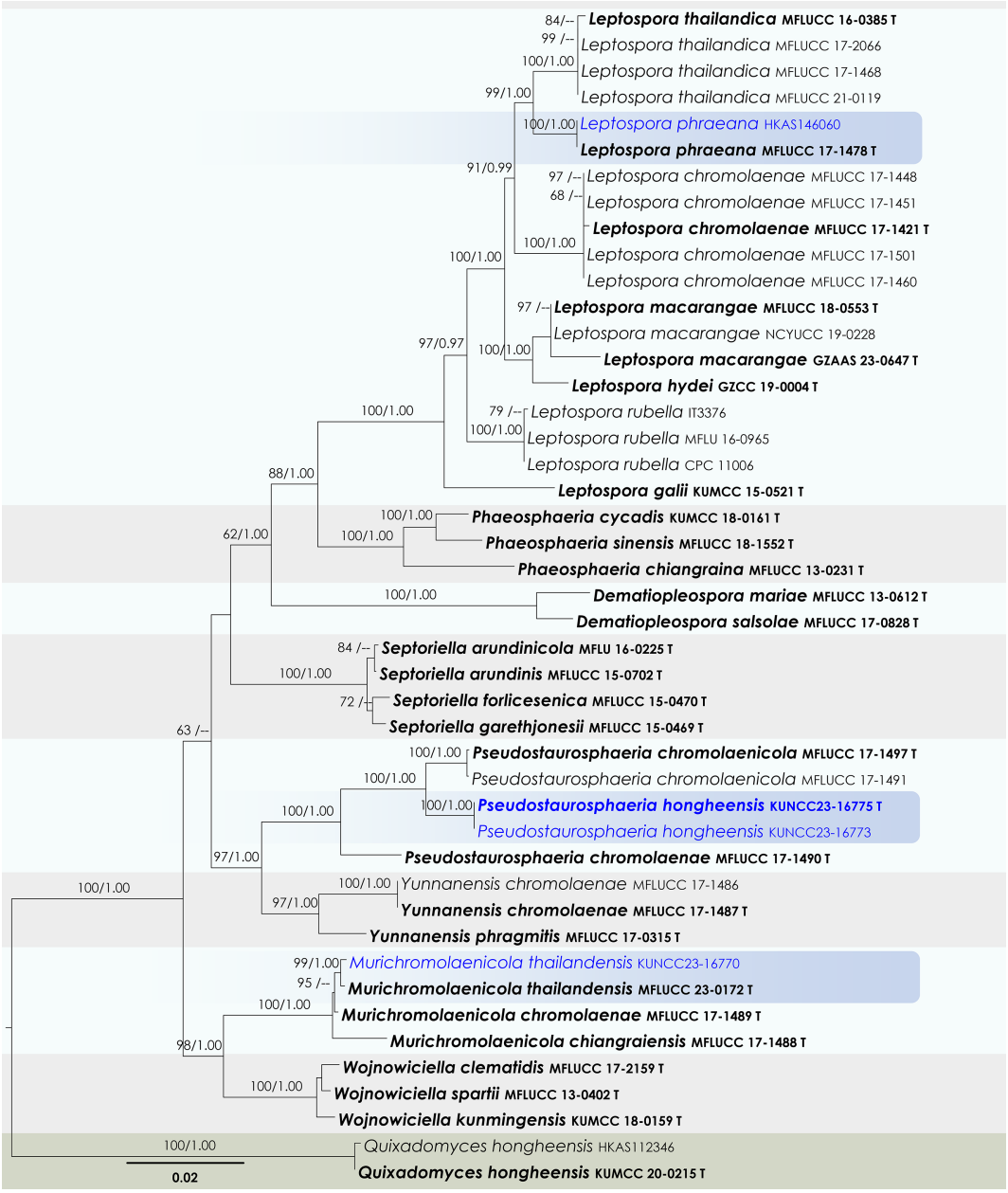

Fig. 36 Maximum Likelihood tree inferred from the concatenated dataset of partial SSU, LSU, ITS, *tef*1-α, and *rpb*2 sequences. The phylogeny is rooted with *Quixadomyces hongheensis* (HKAS112346, KUMCC 20-0215). The final likelihood value is –11,594.436322. The final alignment included 658 unique site patterns, with approximately 9.44% of the positions comprising gaps or ambiguous characters. The estimated nucleotide frequencies were as follows: A = 0.243939, C = 0.239658, G = 0.264036, T = 0.252368. The substitution model yielded the following relative rates: AC = 0.848781, AG = 2.550385, AT = 2.306846, CG = 0.490775, CT = 5.900303 and GT = 1.000000. The proportion of invariable sites (I) was estimated at 0.719615, and the gamma distribution shape parameter (α) was 0.686992. Bayesian inference reached convergence after 221,000 generations, when the average standard deviation of split frequencies dropped below 0.01 (observed value: 0.009792). A total of 2,211 trees were sampled, and 1,659 of these were retained for the final analysis after discarding the initial 25% as burn-in. The alignment also revealed 659 distinct informative sites. In the resulting phylograms, sequences generated in this study are highlighted in blue, while ex-type or type strains are indicated in boldface.

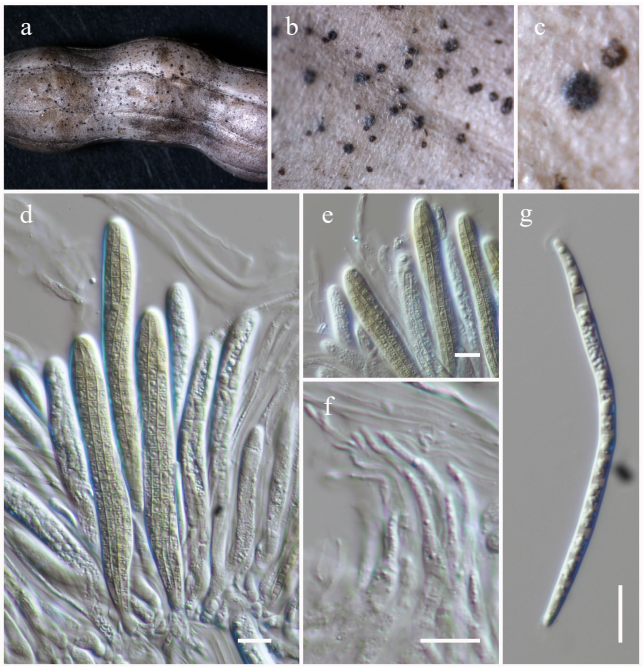

Fig. 37 *Leptospora phraeana* (HKAS146060). (a)–(c) Ascomata on the dead woody twigs. (d), (e) Asci. (f) Pseudoparaphyses. (i) Ascospore. Scale bars: (d)–(g) = 10 μm.

Pseudostaurosphaeria conidia are globose to obovoid with only 1–2 transverse septa[69,179]. Both previously known species in the genus were reported from dead stems of *Chromolaena odorata* in Chiang Rai, Thailand. In this study, a third species is introduced: *Pseudostaurosphaeria hongheensis*, collected from Yunnan, China, thereby extending the known diversity and distribution of the genus.

Pseudostaurosphaeria hongheensis Wanas., Phookamsak & J.C. Xu, **sp. nov.** (Figs 36 and 39).

MycoBank No: 859365

Etymology: The specific epithet 'hongheensis' refers to Honghe, Yunnan Province, where the holotype was collected.

Holotype: HKAS146062

Saprobic on dead twigs of an unidentified host. Asexual morph: *Conidiomata* 90–110 μm high × 100–130 μm diam. ($\bar{x}$ = 103.1 × 116.6 μm, n = 5), immersed to erumpent, solitary, scattered to aggregated, pycnidial, uni-loculate, globose to subglobose, yellowish-brown to brown, ostiolate. *Ostioles* central, protuding through the host surface. *Pycnidial wall* 5–12 μm wide, comprising 3–4 layers of thick-walled cells of *textura angularis*, yellowish-brown to brown on the outer side, inner side becoming hyaline and bearing conidiophores and conidiogenous cells. *Conidiophores* arising from the innermost layer of the pycnidial wall are hyaline, cylindrical, or reduced to conidiogenous cells. *Conidiogenous cells* 6–8 × 3.5–6 μm ($\bar{x}$ = 7.2 × 4.3 μm, n = 10), hyaline, cylindrical, smooth- and thin-walled, holoblastic, phialidic, discrete. *Conidia* 10–13 × 7–9 μm ($\bar{x}$ = 11.1 × 7.8 μm, n = 30), oblong to obovoid or ellipsoidal, yellowish-brown to brown, 3-transverse septate, 1–2-vertical septate, not constricted at the septa, apex broadly rounded, base rounded to conical, smooth-walled, with few small guttules. Sexual morph: Undetermined.

Culture characteristics: Colonies on PDA at room temperature (25 °C) under normal light, reaching 20–25 mm diam. after two weeks. Colonies circular, dense, and floccose with a cottony to velvety texture, whitish to creamy coloration across the surface, with a slightly raised central zone and a lighter, slightly wrinkled area in the middle. The colony margin is regular and well-defined; colonies

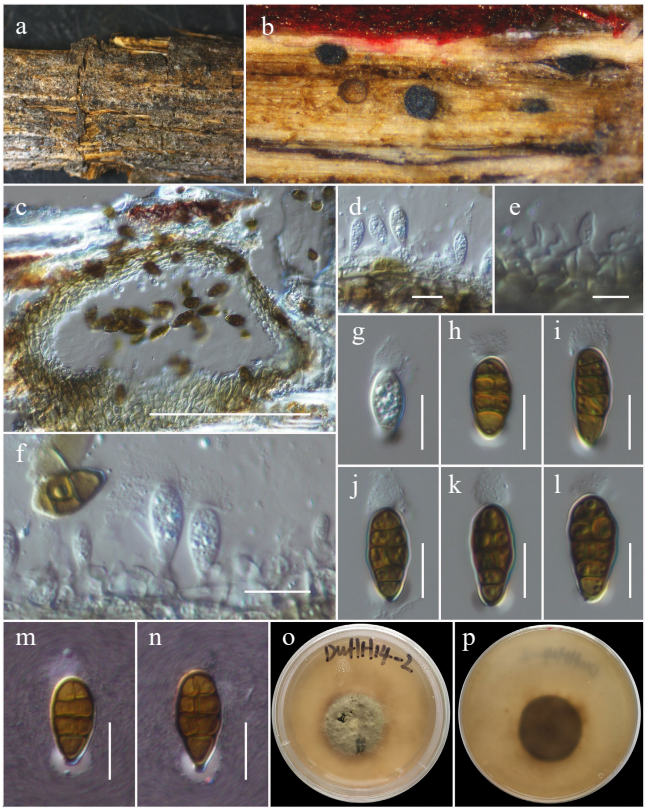

Fig. 38 *Murichromolaenicola thailandensis* (HKAS146061). (a), (b) Conidiomata on host. (c) Section of a conidioma. (d)–(f) Conidiogenous cells. (g)–(n) Conidia (m and n with the Indian Ink). (o), (p) Colony on MEA (p from the bottom). Scale bars: (c) = 50 μm, (d)–(f) = 10 μm, (g)–(n) = 5 μm.

from below are pigmented, showing a dark brown center that diffuses outward into lighter brown zones toward the margin. The pigment production is intense and localized at the colony center.

Materials examined: China, Yunnan, Honghe Hani and Yi Autonomous Prefecture, Honghe County, 23.421013° N, 102.227243° E, 517 m, on dead twigs of an unknown deciduous host, 03 December 2020, D.N. Wanasinghe, DWHH17-01 (holotype, HKAS146062), extype, KUNCC23-16775; *ibid*., DWHH16-03 (HKAS146063), living culture KUNCC23-16773.

GenBank numbers: KUNCC23-16775: ITS = PV742929, LSU = PV742985, SSU = PV743038, *tef*1-α = PV700664; KUNCC23-16773: ITS = PV742930, LSU = PV742986, SSU = PV743039, *tef*1-α = PV700665.

Notes: Morphologically, *Pseudostaurosphaeria hongheensis* conforms well to the generic circumscription of *Pseudostaurosphaeria* in terms of its conidiomata, conidiogenous cells and conidial features. In our multigene phylogenetic analysis, *Pseudostaurosphaeria hongheensis* forms a sister relationship with *P. chromolaenicola* within the genus (100% MLBS and 1.00 BYPP; Fig. 36). While both species exhibit similar conidiomatal structure and conidiogenous cell morphology, their conidia differ in septation and size. *Pseudostaurosphaeria chromolaenicola* produces conidia with a single transverse septum and one vertical septum at maturity, whereas *P. hongheensis* has conidia with three transverse septa and 1–2 vertical septa. The conidia of *Pseudostaurosphaeria hongheensis* (10–13 × 7–9 μm) are notably longer and wider than those of *P. chromolaenicola* (6.5–9 × 5–6.5 μm).

Roussoellaceae J.K. Liu, Phookamsak, D.Q. Dai & K.D. Hyde, Phytotaxa 181 (1): 7 (2014)

Neoroussoella Jian K. Liu, Phookamsak & K.D. Hyde, Phytotaxa 181

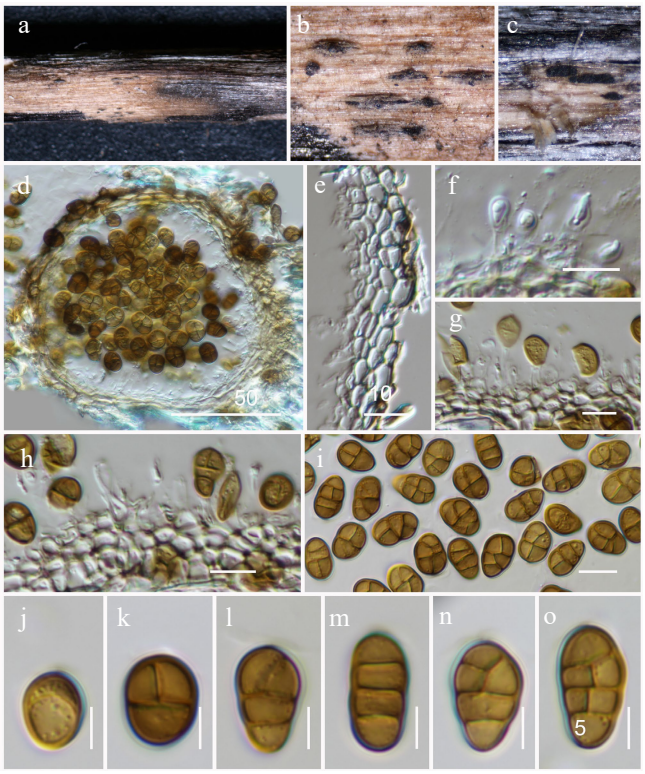

Fig. 39 *Pseudostaurosphaeria hongheensis* (HKAS146062, holotype). (a)–(c) Conidiomata on host. (d) Section of a conidioma. (e) Pycnidial wall. (f)–(h) Conidiogenous cells. (i)–(o) Conidia. Scale bars: (d) = 50 μm, (e)–(h) = 10 μm, (i)–(o) = 5 μm.

(1): 21 (2014)

Notes: *Neoroussoella* was introduced by Liu et al.[180] to accommodate *N. bambusae*, which was collected from dead branches of *Bambusa* species in Thailand. Species of *Neoroussoella* are morphologically distinct from those of *Roussoella* by possessing unilocular ascomata and a coelomycetous asexual morph that produces hyaline to pale brown, smooth-walled conidia[180]. Currently, there are 18 accepted species accommodated in this genus[93,108,123,180–186].

Neoroussoella bambusae Phookamsak, J.K. Liu & K.D. Hyde, Phytotaxa 181 (1): 23 (2014) (Figs 40 and 41).

MycoBank No: 550669

Saprobic on dead branches of *Bougainvillea* sp. Sexual morph: Undetermined. Asexual morph: *Conidiomata* 170–220 μm high × 200–300 μm diam. ($\bar{x}$ = 195.4 × 269.4 μm, n = 5), pycnidial, immersed under a clypeus or epidermis, raised, appearing as hemispherical on the host, dark brown to black, scattered to aggregated, subgloblose or irregular in shape, uni-loculate, glabrous, with an inconspicuous ostiole. *Pycnidial wall* 10–25 μm wide, comprising 2–3 layers of thick-walled, yellowish-brown to brown cells of *textura angularis*, innermost side bearing conidiogenous cells. *Conidiophores* hyaline, unbranched, cylindrical to ampulliform or lageniform, aseptate, arising from the innermost layer of the pycnidial wall. *Conidiogenous cells* 2.5–4 × 1.2–2 μm ($\bar{x}$ = 3.2 × 1.7 μm, n = 10), hyaline, cylindrical to ampulliform or lageniform, smooth-walled, blastic, phialidic. *Conidia* 4–5 × 1.8–2.3 μm ($\bar{x}$ = 4.3 × 2.1 μm, n = 20), oblong to ellipsoidal, sub-hyaline to pale brown, aseptate, with two or more guttules, ends rounded, smooth-walled.

Material examined: China, Yunnan, Honghe Hani and Yi Autonomous Prefecture, Honghe County, 23.421068° N, 102.229128° E, 735 m, on dead branches of *Bougainvillea* sp., 23 April 2020, D.N. Wanasinghe, DWHH23-50 (HKAS146064), living culture, KUNCC23-16816.

GenBank numbers: KUNCC23-16816: ITS = PV742931, LSU = PV742987, SSU = PV743040, *tef*1-α = PV700666, *rpb*2 = PV700694.

Known hosts and distribution: Saprobic on dead bamboo culms in a terrestrial habitat in Thailand[180]; on submerged wood in a stream in Yunnan, China[138]; on dead bamboo culms in Yunnan, China[187]; on dead branches of *Bougainvillea* sp. in Yunnan, China (this study).

Notes: *Neoroussoella bambusae* was originally described from dead bamboo culms in a terrestrial habitat in Thailand[180]. It is characterized by semi-immersed to immersed, solitary ascostromata, cylindrical asci, and relatively small, brown, longitudinally ribbed, two-celled ascospores. It is an asexual morph, produced in culture, forms small, hyaline, smooth-walled conidia[180]. Subsequent records include reports from Yunnan, China, on submerged wood in a stream[138] and on dead bamboo culms in a bamboo garden[187]. In our phylogenetic analysis of *Roussoellaceae*, the new strain (KUNCC23-16816) isolated from *Bougainvillea* sp. formed a monophyletic clade with previously identified strains of *Neoroussoella bambusae* (98% MLBS and 1.00 BYPP; Fig. 40). Morphologically, our collection is consistent with the original description of the holotype[180]. Based on both phylogenetic and morphological evidence, *Neoroussoella bambusae* from *Bougainvillea* sp. is reported as a new host association for this species.

Xenoroussoella Mapook & K.D. Hyde, Fungal Diversity 101: 93.

Notes: *Xenoroussoella* was introduced by Mapook et al.[69] as a monotypic genus to accommodate the roussoella-like taxa and is typified by *Xenoroussoella triseptata*. The genus is initially known only its sexual morph, characterizing by immersed, solitary or scattered, globose to subglobose, brown to dark brown, coriaceous ascomata with protruding ostiolar neck, 8-spored, bitunicate, cylindric-clavate to clavate asci, embeded in oblong to cylindrical, septate, branched pseudoparaphyses, and hyaline to pale brown, or dark brown at maturity, ellipsoid to obovoid, 1–3-septate ascospores, with irregular longitudinal striations[69]. *Xenoroussoella* is morphologically similar to *Roussoella* and *Pseudoroussoella* but phylogenetically distant[69]. Subsequently, de Silva et al.[93], Ryu et al.[188], Tian et al.[189], and Guo et al.[186] reported the coelomycetous asexual morph of *Xenoroussoella triseptata* that is characterized by pycnidial, solitary to gregarious, immersed to erumpent, uni- to multi-loculate, dark brown to black conidiomata, with an inconspicuous ostiolar, phialidic, ampulliform to cylindrical, hyaline, smooth-walled conidiogenous cells and hyaline to pale brown, oblong to ovoid, aseptate, smooth-walled conidia. Presently, only a single species, *X. triseptata*, is accommodated in this genus.

Xenoroussoella triseptata Mapook & K.D. Hyde, Fungal Diversity 101: 95 (Figs 40 and 42).

MycoBank No: 557368

Saprobic on *Bougainvillea* sp. Asexual morph: *Conidiomata* 140–180 μm high × 160–220 μm diam. ($\bar{x}$ = 161.4 × 182.7 μm, n = 5), pycnidial, semi-immersed to erumpent, appearing as dark spots on host surface, scattered to gregarious, uni-loculate, yellowish brown to brown, globose to subglobose. *Pycnidial wall* 10–20 μm wide, comprising 2–3 layers of thick-walled, yellowish-brown to brown cells of *textura angularis*, the innermost layer bearing conidiogenous cells. *Conidiophores* reduced to conidiogenous cells. *Conidiogenous cells* 4.5–5.5 × 3–3.5 μm ($\bar{x}$ = 5.1 × 3.3 μm, n = 15), hyaline, cylindrical or ampulliform, blastic, phialidic, arising from innermost layer of pycnidial wall, distinct to inconspicuous. *Conidia* 3.5–4.5 × 2.5–3.5 μm ($\bar{x}$ = 4 × 3.1 μm, n = 40), globose to subglobose or oblong to teardrop-shaped, unicellular, aseptate, hyaline to sub-hyaline or yellowish-brown, containing one or more small guttules, smooth-walled, lacking appendages or sheath. Sexual morph:

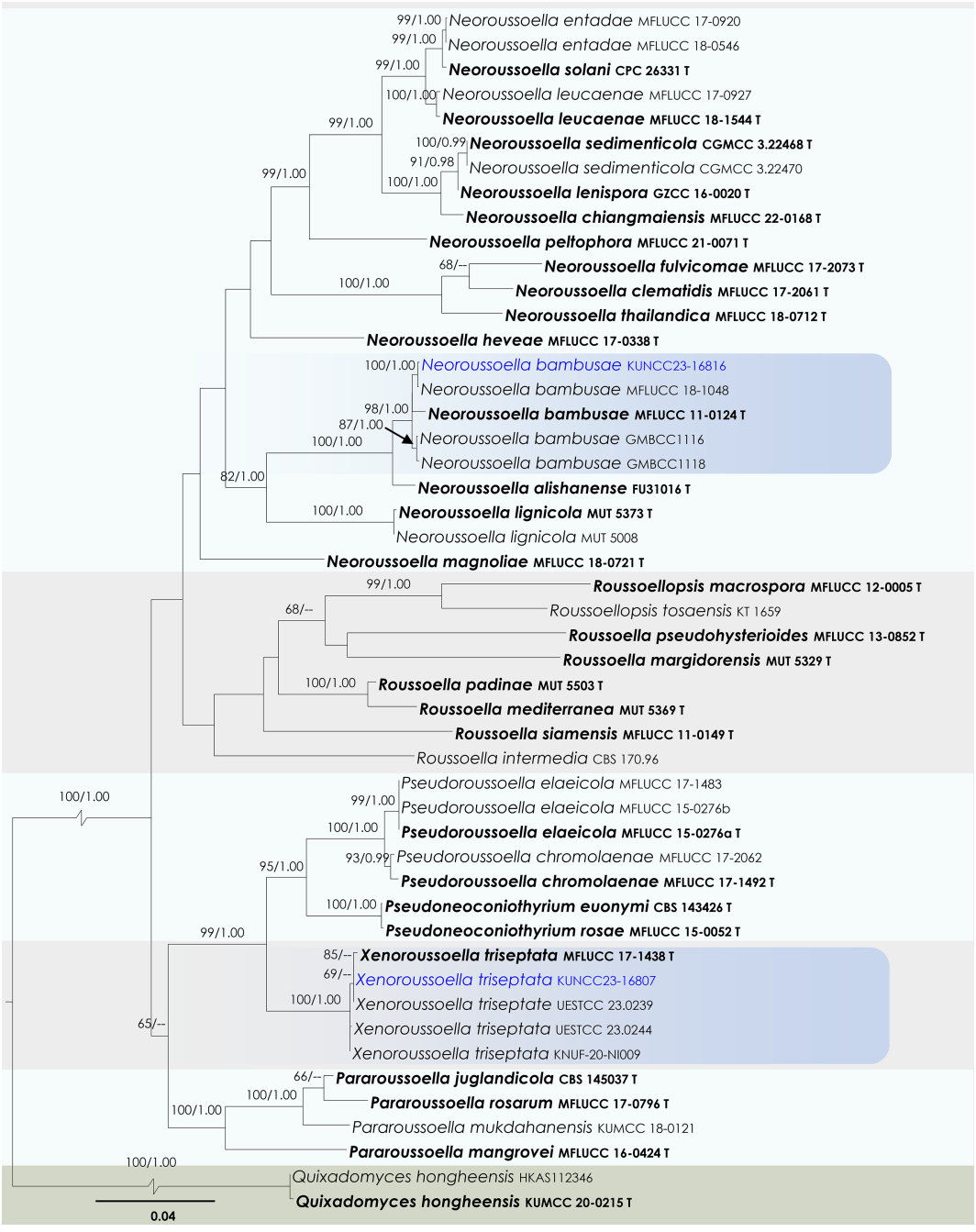

Fig. 40 Maximum Likelihood tree inferred from the concatenated dataset of partial SSU, LSU, ITS, *tef*1-α, and *rpb*2 sequences. The phylogeny is rooted with *Quixadomyces hongheensis* (HKAS112346, KUMCC 20-0215). The final likelihood value is –24,601.887530. The final alignment included 1,510 unique site patterns, with approximately 21.76% of the positions comprising gaps or ambiguous characters. The estimated nucleotide frequencies were as follows: A = 0.246109, C = 0.256427, G = 0.266572, T = 0.230892. The substitution model yielded the following relative rates: AC = 1.941609, AG = 5.780010, AT = 2.469287, CG = 1.378238, CT = 11.805823, GT = 1.000000. The proportion of invariable sites (I) was estimated at 0.570250, and the gamma distribution shape parameter (α) was 0.468549. Bayesian inference reached convergence after 1,104,000 generations, when the average standard deviation of split frequencies dropped below 0.01 (observed value: 0.009906). A total of 11,041 trees were sampled, and 8,281 of these were retained for the final analysis after discarding the initial 25% as burn-in. The alignment also revealed 1,511 distinct informative sites. In the resulting phylograms, sequences generated in this study are highlighted in blue, while ex-type or type strains are indicated in boldface.

Undetermined.

Material examined: China, Yunnan, Honghe Hani and Yi Autonomous Prefecture, Honghe County, 23.421068° N, 102.229128° E, 735 m, on dead branches of *Bougainvillea* sp., 23 April 2020, D.N. Wanasinghe, DWHH23-29 (HKAS146065), living culture, KUNCC23-16807.

GenBank numbers: KUNCC23-16807: ITS = PV742932, LSU = PV742988, SSU = PV743041, *tef*1-α = PV700667, *rpb*2 = PV700695.

Known hosts and distribution: Saprobic on dead stems of *Chromolaena odorata* in Thailand[69]; on dead twigs of *Anomianthus dulcis* and *Desmos chinensis* in Thailand[93]; on dead stems of *Cycas revoluta* in China[189]; on dead wood culms in Guizhou Province, China[186]; on dead branches of *Bougainvillea* sp. in Yunnan, China (this study).

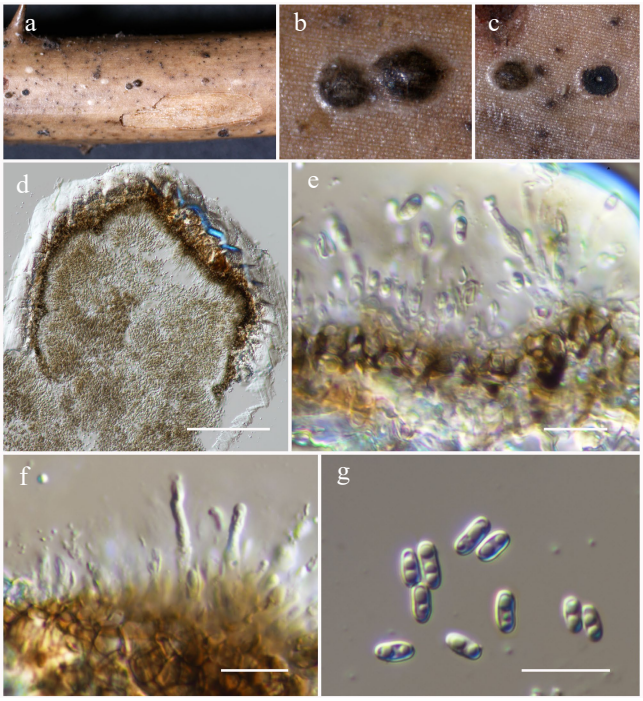

Fig. 41 *Neoroussoella bambusae* (HKAS146064). (a)–(c) Conidiomata on host. (d) Section of a conidioma. (e), (f) Conidiogenous cells. (g) Conidia. Scale bars: (d) = 100 μm, (e)–(g) = 10 μm.

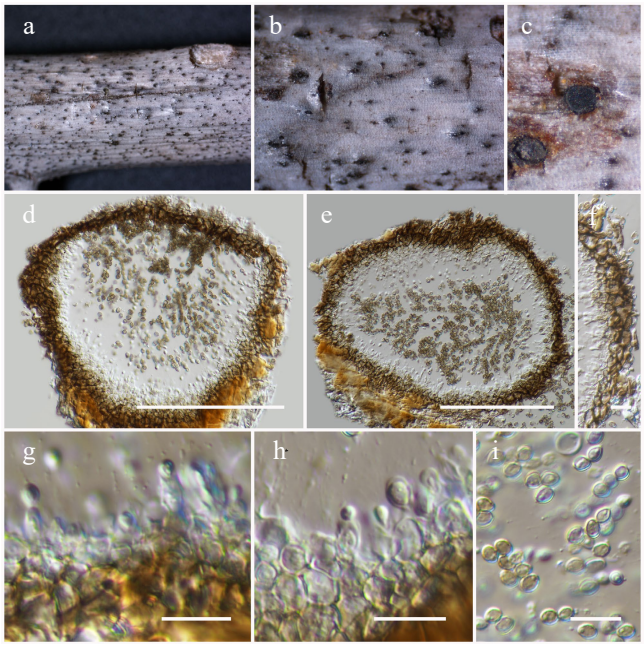

Fig. 42 *Xenoroussoella triseptata* (HKAS146065). (a)–(c) Conidiomata on host. (d), (e) Section of a conidioma. (f) Pycnidial wall. (g), (h) Conidiogenous cells. (i) Conidia. Scale bars: (d), (e) = 100 μm, (f)–(i) = 10 μm.

Notes: In our study, phylogenetic analysis based on a combined dataset of SSU, LSU, ITS, *tef*1-*α,* and *rpb*2 gene regions placed one of our new isolates, KUNCC23-16807, within the same clade as the type and previously reported strains of *Xenoroussoella triseptata* (100% MLBS and 1.00 BYPP; Fig. 40). The morphological characteristics observed in our collection are consistent with those described in earlier studies[93,186,189]. Therefore, this isolate is reported as a new host and geographical record of *Xenoroussoella triseptata* from *Bougainvillea* in Yunnan Province, China.

Sulcatisporaceae Kaz. Tanaka & K. Hiray., Studies in Mycology 82: 119.

Anthosulcatispora Phukhams. & K.D. Hyde, Fungal Diversity 102: 117.

Notes: *Anthosulcatispora* was introduced by Phukhamsakda et al.[123] to accommodate *A. brunnea* (= *Neobambusicola brunnea*) and *A. subglobosa*. The sexual morph was originally described from *Neobambusicola brunnea*[182]. Within *Sulcatisporaceae*, *Anthosulcatispora* is distinct in producing brown ascospores, in contrast to the hyaline, broadly fusiform ascospores with entire sheaths found in *Parasulcatispora*, *Kazuakitanaka* and *Sulcatispora*[24,123,172]. The asexual morph of *Anthosulcatispora* resembles that of *Neobambusicola* and *Pseudobambusicola*, sharing solitary, unilocular pycnidia, phialidic conidiogenesis, and hyaline conidia. However, it differs by having subglobose conidiomata, elongate, cylindrical to truncate conidiogenous cells, and oblong, aseptate conidia[179]. Phylogenetically, *Anthosulcatispora* forms a distinct lineage within *Sulcatisporaceae* (Fig. 43).

Anthosulcatispora hongheensis Wanas., Phookamsak, L.S. Dissan. & J.C. Xu, **sp. nov.** (Figs 43 and 44).

MycoBank No: 859366

Etymology: The specific epithet 'hongheensis' refers to Honghe, Yunnan Province, where the holotype was collected.

Holotype: HKAS146066

Saprobic on dead branches of an unknown host. Sexual morph: *Ascomata* 220–300 μm high × 180–250 μm diam. ($\bar{x}$ = 268.8 × 230.7 μm, n = 5), immersed, appearing as black dots, scattered to grouped, perithecial, globose or subglobose to pyriform, brown to dark brown, ostiolate. *Ostiolar necks* protruding through the host surface, central, short papillate. *Peridium* 15–25 μm wide at the sides, 30–50 μm wide near the ostiolar neck, 15–20 μm wide at the base, comprising thick-walled brown cells of *textura angularis* on surface view, consisting of several layers of thick-walled, dark brown cells of *textura angularis* to *textura intricata* in longitudinal section. *Hamathecium* 1.5–3 μm wide, cylindrical, branched, septate, anastomosed pseudoparaphyses, embedded in a gelatinous matrix. *Asci* 80–100 × 9–12 μm ($\bar{x}$ = 88.3 × 10.4 μm, n = 10), 8-spored, bitunicate, fissitunicate, cylindrical to cylindric-clavate, straight or curved, apically rounded, with an ocular chamber, short-pedicellate. *Ascospores* 17–20 × 4.5–6.5 μm ($\bar{x}$ = 18.8 × 5.2 μm, n = 30), overlapping uni- to bi-seriate, hyaline, fusiform with rounded to obtuse ends, 1-septate, not constricted at the septum, symmetrical or upper cell slightly longer than lower cell, straight to slightly curved, smooth-walled, guttulate at immaturity, surrounded by a thick or spreading mucilaginous sheath. Asexual morph: Undetermined.

Materials examined: China, Yunnan, Honghe Hani and Yi Autonomous Prefecture, Honghe County, 23.421068° N, 102.229128° E, 735 m, on dead branches of an unknown host, 23 April 2020, D.N. Wanasinghe, DWHH23-54 (holotype, HKAS146066); *ibid*., DWHH23-54-2 (HKAS146067).

GenBank numbers: HKAS146066: ITS = PV742933, LSU = PV742989, SSU = PV743042, *tef*1-*α* = PV700668; HKAS146067: ITS = PV742934, LSU = PV742990, SSU = PV743043, *tef*1-*α* = PV700669.

Notes: In this study, *Anthosulcatispora hongheensis* is introduced as the third species within the genus *Anthosulcatispora*. The new species is currently known only from its sexual morph and resembles members of *Sulcatisporaceae* in having hyaline, broadly fusiform ascospores with an entire sheath[24,123,172,179]. However, it is different from the sexual morph of *Anthosulcatispora,* which is distinct in producing brown, oblong to ellipsoidal ascospores with rounded ends[182]. Despite these morphological differences, our

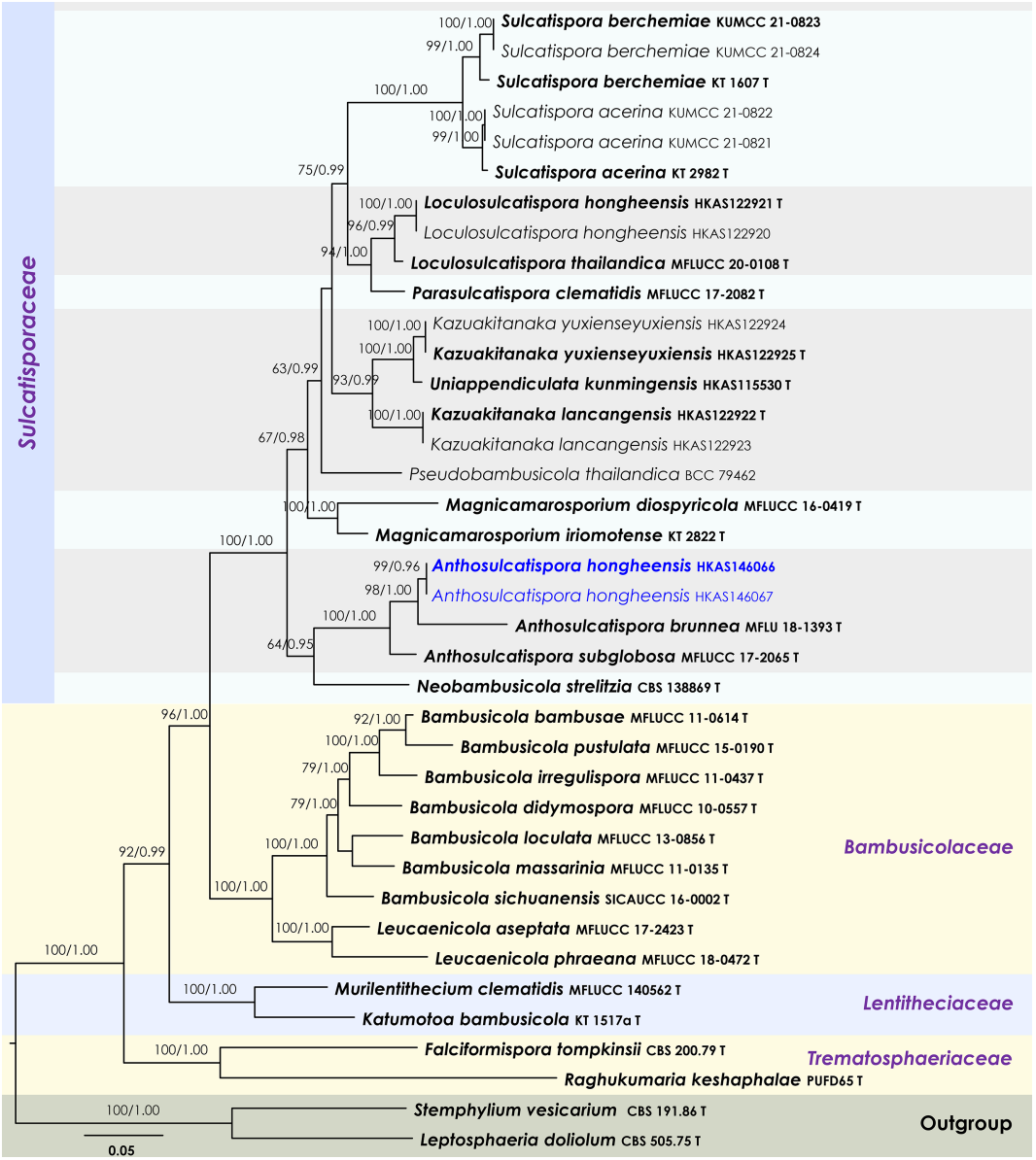

Fig. 43 Maximum Likelihood tree inferred from the concatenated dataset of partial SSU, LSU, ITS, *tef*1-*α*, and *rpb*2 sequences. The phylogeny is rooted with *Leptosphaeria doliolum* (CBS 505.75) and *Stemphylium vesicarium* (CBS 191.86). The final likelihood value is −29,929.948064. The final alignment included 1,836 unique site patterns, with approximately 21.67% of the positions comprising gaps or ambiguous characters. The estimated nucleotide frequencies were as follows: A = 0.239264, C = 0.259016, G = 0.269652, T = 0.232068. The substitution model yielded the following relative rates: AC = 1.148753, AG = 2.643315, AT = 1.114998, CG = 0.875753, CT = 6.054602, GT = 1.000000. The proportion of invariable sites (I) was estimated at 0.469606, and the gamma distribution shape parameter (α) was 0.537534. Bayesian inference reached convergence after 11,000 generations, when the average standard deviation of split frequencies dropped below 0.01 (observed value: 0.007950). A total of 111 trees were sampled, and 84 of these were retained for the final analysis after discarding the initial 25% as burn-in. The alignment also revealed 1,838 distinct informative sites. In the resulting phylograms, sequences generated in this study are highlighted in blue, while ex-type or type strains are indicated in boldface.

phylogenetic analysis based on combined SSU, LSU, ITS, *tef*1-*α*, and *rpb*2 sequence data places *A. hongheensis* in a monophyletic clade within *Anthosulcatispora*, with 100% MLBS and 1.00 BYPP support values, showing a close relationship to *A. brunnea* (Fig. 43). Unfortunately, the asexual morph of *Anthosulcatispora hongheensis* was not observed, and thus comparisons with asexual characteristics across the genus could not be made. Nevertheless, given its phylogenetic placement and morphological affinities within *Sulcatisporaceae*, the study proposes the inclusion of this species within *Anthosulcatispora*. Future studies with additional sexual morphs are warranted to further resolve the phylogenetic framework and clarify morphological variation within the genus.

Teichosporaceae M.E. Barr, Mycotaxon 82: 374 (2002)

Magnibotryascoma Thambug. & K.D. Hyde, Fungal Diversity 74: 249 (2015)

Notes: Thambugala et al.[136] introduced *Magnibotryascoma* to accommodate *M. uniseriatum* (= *Misturatosphaeria uniseriata*) within *Floricolaceae*. The genus is characterized by solitary or aggregated ascomata, fissitunicate, cylindrical to cylindrical-clavate asci, and partially overlapping, brown to dark brown, fusiform to elliptical, usually 1–3-septate ascospores[136,190]. Jaklitsch et al.[191] synonymized *Magnibotryascoma* with *Teichospora*, yet morphological differences are notable: *Magnibotryascoma* species (*M. melanommoides*, *M. rubriostiolatum,* and *M. uniseriatum*) possess fusiform,

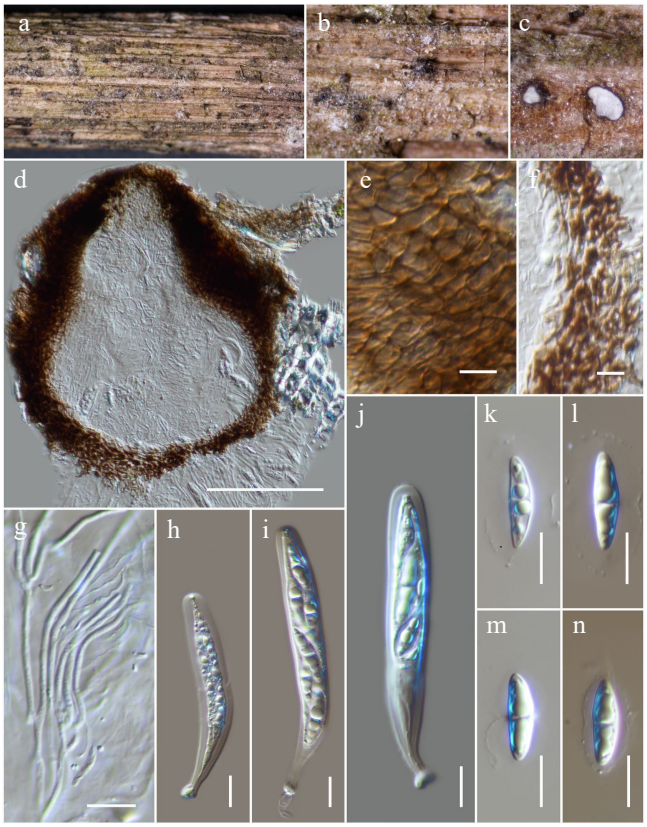

Fig. 44 *Anthosulcatispora hongheensis* (HKAS146066, holotype). (a)–(c) Ascomata on the dead woody twigs. (d) Cross-section of an ascoma. (e), (f) Peridium. (g) Pseudoparaphyses. (h)–(j) Asci. (k)–(n) Ascospores. Scale bars: (d) = 100 μm, (e)–(n) = 10 μm.

elliptical, 1–3-septate ascospores, whereas *Teichospora* (i.e., *T. pusilla* and *T. trabicola*) produces ellipsoid to oblong, muriform ascospores[191]. Furthermore, phylogenetic analyses by Hongsanan et al.[110] positioned *Magnibotryascoma* as a distinct lineage separate from *Teichospora* within *Teichosporaceae*, thereby supporting its recognition as a distinct genus.

The asexual morph of *Magnibotryascoma rubriostiolata* was described by Phukhamsakda et al.[123] from dead stems of *Clematis vitalba* in the UK, characterized by pycnidial, uniloculate, scattered, semi-erumpent to superficial, subglobose to globose, dark brown to black conidiomata, multi-layered conidiomatal walls, enteroblastic, phialidic, integrated, truncate to cylindrical, hyaline conidiogenous cells, and hyaline (young) to reddish-brown (mature), aseptate conidia. Subsequently, Mortimer et al.[23] introduced another asexual species, *M. kunmingense*, isolated from dead twigs of *Machilus yunnanensis*, exhibiting morphological similarities to previously described *Magnibotryascoma* species. Tennakoon et al.[192] transferred *Curreya acaciae*[193] as *Magnibotryascoma acaciae* to *Magnibotryascoma* based on molecular phylogenetic evidence. The current study introduces an additional species closely resembling other known asexual morphs within *Magnibotryascoma*[23,123,192,194].

Magnibotryascoma hongheense Wanas., Phookamsak, L.S. Dissan. & J.C. Xu, **sp. nov.** (Figs 45 and 46).

MycoBank No: 859367

Etymology: The specific epithet 'hongheense' refers to Honghe, Yunnan Province, where the holotype was collected.

Holotype: HKAS146068

Saprobic on dead twigs of *Fagaceae* hosts. Sexual morph: Undetermined. Asexual morph: *Conidiomata* 100–150 μm high, 250–350 μm diam. ($\bar{x}$ = 132.5 × 294.8 μm, n = 5), pycnidial, immersed to semi-immersed or erumpent, scattered to aggregated, uni-loculate, globose to subglobose or sometimes collabent, light brown to brown, uni-loculate, centrally ostiolate, papillate. *Pycnidial wall* 10–20 μm wide, comprising two strata; outer region made up 2–3 layers of brown to light brown cells of *textura angularis*, inner layer comprising 3–4 layers of hyaline cells of *textura angularis*, bearing conidiogenous cells. *Conidiophores* reduced to conidiogenous cells. *Conidiogenous cells* 3.5–4.5 × 3.5–4 μm ($\bar{x}$ = 4.1 × 3.7 μm, n = 15), arising from the innermost layer of the pycnidial wall, hyaline, ampulliform to subcylindrical, blastic, annelledic, smooth-walled, discrete to inconspicuous. *Conidia* 3.2–4 × 2.5–3 μm ($\bar{x}$ = 3.7 × 2.8 μm, n = 30), subglobose to oval, hyaline when immature, pale brown to golden brown when mature, aseptate, smooth-walled.

Materials examined: China, Yunnan, Honghe Hani and Yi Autonomous Prefecture, Honghe County, 23.421013° N, 102.227243° E, 517 m, on dead twigs of *Fagaceae* sp., 14 August 2022, D.N. Wanasinghe, DWHH22-12 (holotype, HKAS146068), ex-type KUNCC23-16800; *ibid*., DWHH22-12-02 (isotype, HKAS146069).

GenBank numbers: KUNCC23-16800: ITS = PV742935, LSU = PV742991, SSU = PV743044, *tef*1-α = PV700670, *rpb*2 = PV700696; HKAS146069: ITS = PV742936, LSU = PV742992, SSU = PV743045, *tef*1-α = PV700671, *rpb*2 = PV700697.

Notes: The new species introduced in this study formed a distinct lineage, closely related to *Macrodiplodiopsis desmazieri*, within the genus *Magnibotryascoma* (99% MLBS and 1.00 BYPP; Fig. 45). Morphologically, the new species differs notably from *Macrodiplodiopsis desmazieri* by having unicellular conidia, whereas *M. desmazieri* produces 3-distoseptate conidia[195]. The asexual morphology of *Macrodiplodiopsis desmazieri* differs from the generic description of *Magnibotryascoma*. *Macrodiplodiopsis desmazieri* is characterized by immersed conidiomata, annellidic conidiogenous cells, and 3-distoseptate conidia[195], whereas *Magnibotryascoma* exhibits superficial conidiomata, enteroblastic phialidic conidiogenous cells, and unicellular, brown conidia[23,123,192,194]. Therefore, studying the sexual morphology of *Macrodiplodiopsis desmazieri* is necessary to clarify its taxonomic placement within the genus.

Paulkirkia Wijayaw., Wanas., Tangthir., Camporesi & K.D. Hyde, Fungal Diversity 77: 198 (2016)

Notes: Wijayawardene et al.[196] introduced the genus *Paulkirkia* to accommodate *P. arundinis*, isolated as a saprobe on dead stems of *Arundo plinii* (*Poaceae*) in Italy. Morphologically, *Paulkirkia* is characterized by globose to subglobose, unilocular, dark brown to black conidiomata, holoblastic conidiogenous cells, and ellipsoidal or oblong to irregular, 1-septate conidia[196]. This genus shares similarities with *Microdiplodia* and *Verrucoconiothyrium*. However, the validity of *Microdiplodia* remains questionable due to the absence of sequence data from its type species. In recent phylogenetic analyses, *Paulkirkia arundinis* (MFLU 13-0315) grouped closely with *Teichospora kingiae* (CPC 29104), both nested within *Teichosporaceae* (*Floricolaceae*)[192]. *Teichospora kingiae* was described by Crous et al.[197] from leaf substrates of *Kingia australis* in Western Australia. Morphologically, *Teichospora kingiae* can be distinguished from *Paulkirkia arundinis* by its verruculose, subcylindrical, 1–3-septate conidia, whereas *P. arundinis* has ellipsoidal to oblong, 1-septate conidia[196,197]. The sexual-asexual morphological connections between these two species remain unproven. Phylogenetic resolution of these taxa remains ambiguous due to limited sequence availability (LSU and ITS data for *T. kingiae* and only LSU data for *P. arundinis*). The present study conducted a robust phylogenetic analysis using combined SSU, LSU, ITS, *tef*1-α, and *rpb*2 gene regions across *Teichosporaceae*. Our results confirm a close phylogenetic relationship between *Teichospora kingiae* and *Paulkirkia arundinis*. Additionally, two new isolates obtained in our study clustered

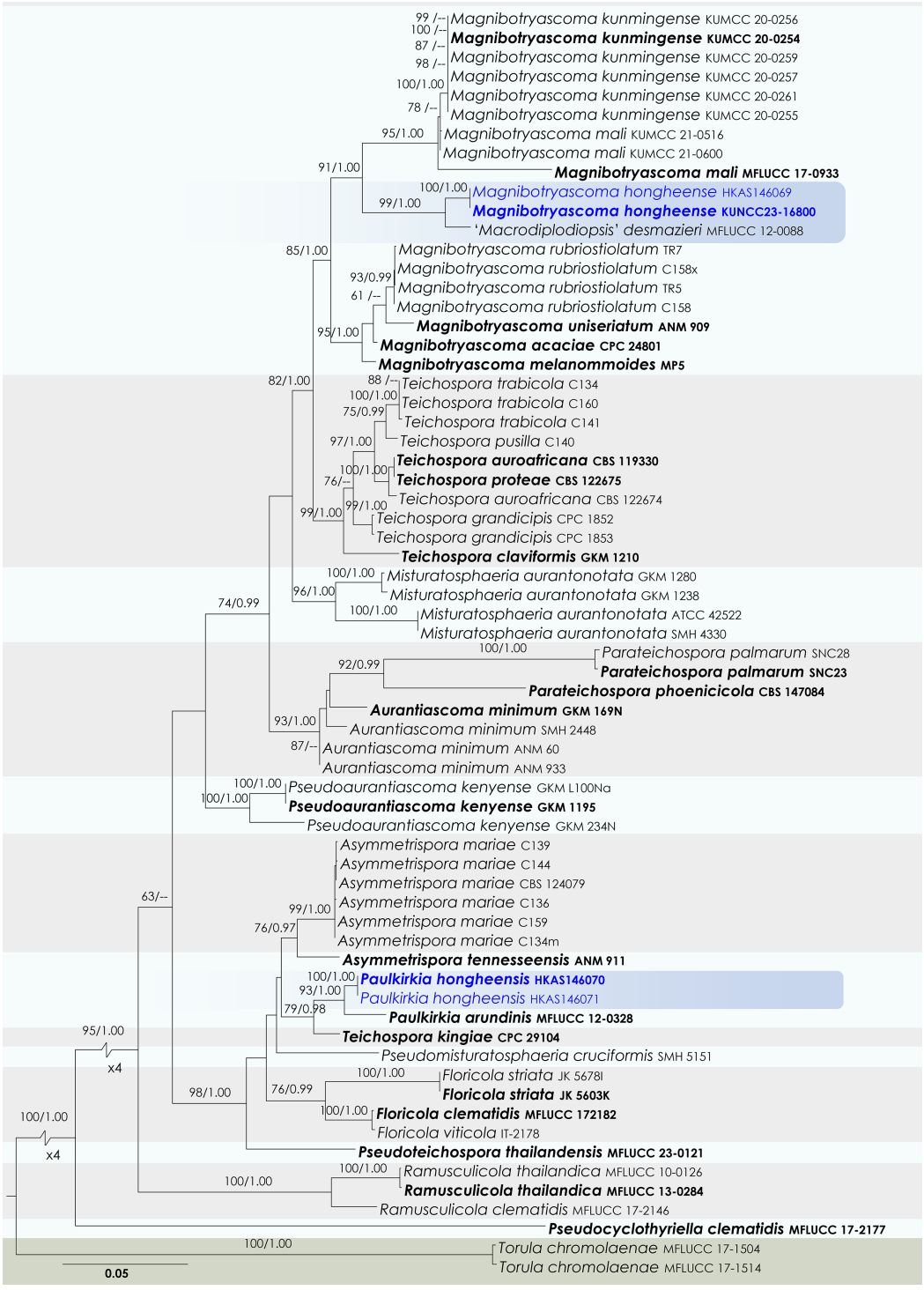

Fig. 45 Maximum Likelihood tree inferred from the concatenated dataset of partial SSU, LSU, ITS, *tef*1-*α*, and *rpb*2 sequences. The phylogeny is rooted with *Torula chromolaenae* (MFLUCC 17-1504, MFLUCC 17-1514). The final likelihood value is –21,213.763713. The final alignment included 1,467 unique site patterns, with approximately 43.11% of the positions comprising gaps or ambiguous characters. The estimated nucleotide frequencies were as follows: A = 0.243744, C = 0.254910, G = 0.276839, T = 0.224507. The substitution model yielded the following relative rates: AC = 1.338566, AG = 3.975920, AT = 1.726619, CG = 1.303434, CT = 9.924008, GT = 1.000000. The proportion of invariable sites (I) was estimated at 0.496561, and the gamma distribution shape parameter (α) was 0.466889. Bayesian inference reached convergence after 755,000 generations, when the average standard deviation of split frequencies dropped below 0.01 (observed value: 0.009983). A total of 7,551 trees were sampled, and 5,664 of these were retained for the final analysis after discarding the initial 25% as burn-in. The alignment also revealed 1,468 distinct informative sites. In the resulting phylograms, sequences generated in this study are highlighted in blue, while ex-type or type strains are indicated in boldface.

with *Paulkirkia arundinis* with statistical support values of 93% MLBS and 1.00 BYPP (Fig. 45). Morphologically, our isolates fit well within the circumscription of *Paulkirkia*. However, pending further studies with additional strains and sequence data, it is important to refrain from transferring *Teichospora kingiae* into *Paulkirkia* at this time.

Paulkirkia hongheensis Wanas., Phookamsak, L.S. Dissan. & J.C. Xu, **sp. nov.** (Figs 45 and 47).

MycoBank No: 859368

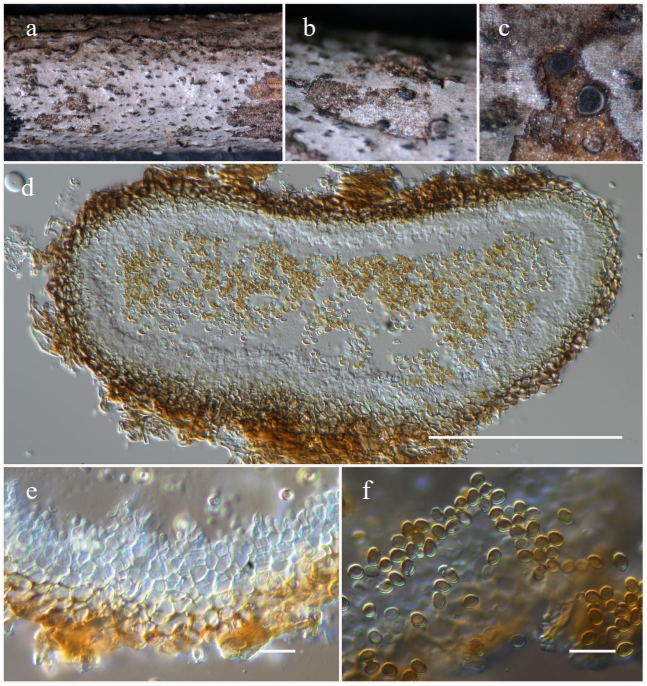

Fig. 46 *Magnibotryascoma hongheense* (HKAS146068, holotype). (a)–(c) Conidiomata on host. (d) Section of a conidioma. (e) Conidiogenous cells. (f) Conidia. Scale bars: (d) = 100 μm, (e), (f) = 10 μm.

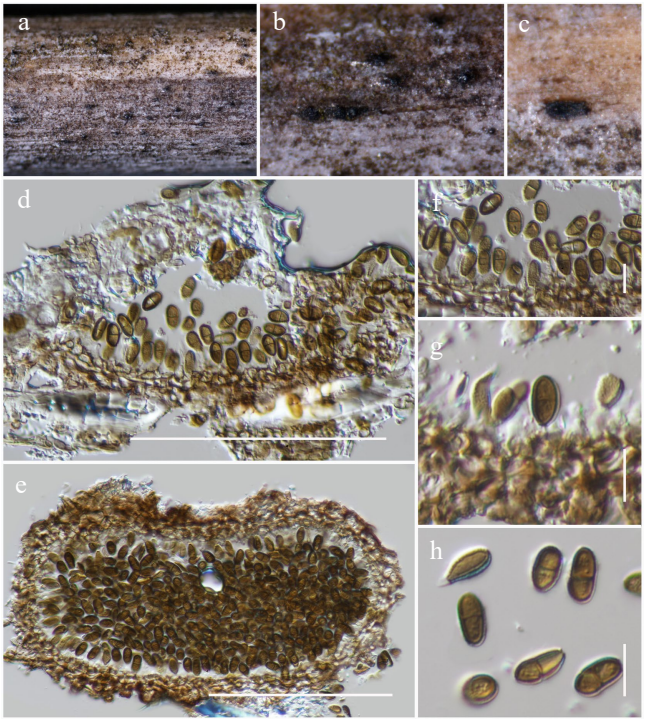

Fig. 47 *Paulkirkia hongheensis* (HKAS146070, holotype). (a)–(c) Conidiomata on host. (d) Vertical section of a conidioma. (e) Horizontal section of a conidioma. (f), (g) Conidiogenous cells. (h) Conidia. Scale bars: (d), (e) = 100 μm, (f)–(h) = 10 μm.

Etymology: The specific epithet 'hongheensis' refers to Honghe, Yunnan Province, where the holotype was collected.

Holotype: HKAS146070

Saprobic on dead stems of a *Poaceae* host. Sexual morph: Undetermined. Asexual morph: *Conidiomata* 190–230 μm high, 100–150 μm diam. ($\bar{x}$ = 209.1 × 124.5 μm, n = 5), pycnidial, immersed to erumpent, scattered to grouped, uni-loculate, subglobose, brown to dark brown. *Pycnidial wall* 10–15 μm wide, comprising 3–4 layers of brown cells of *textura angularis*, innermost layer bearing conidiogenous cells. *Conidiophores* reduced to conidiogenous cells. *Conidiogenous cells* 3.2–4.1 × 3.1–3.6 μm ($\bar{x}$ = 3.6 × 3.4 μm, n = 10), arising from the innermost layer of the pycnidial wall, hyaline, ampulliform to subcylindrical, blastic, annellidic, discrete to inconspicuous. *Conidia* 9–12 × 4.5–6 μm ($\bar{x}$ = 10.3 × 5.1 μm, n = 30), subcylindrical or ellipsoidal, golden brown to brown, 1-septate, not constricted at the septum, apex rounded, base rounded to obtuse, comprising small guttules, verruculose, thick-walled.

Materials examined: China, Yunnan, Honghe Hani and Yi Autonomous Prefecture, Honghe County, 23.421068° N, 102.229128° E, 735 m, on dead stems of a *Poaceae* sp., 23 April 2020, D.N. Wanasinghe, DWHH23-56 (holotype, HKAS146070); *ibid*., DWHH23-56-2 (isotype, HKAS146071).

GenBank numbers: HKAS146070: ITS = PV742937, LSU = PV742993, SSU = PV743046, *tef*1-α = PV700672, *rpb*2 = PV700698; HKAS146071: ITS = PV742938, LSU = PV742994, SSU = PV743047, *tef*1-α = PV700673, *rpb*2 = PV700699.

Notes: Our newly isolated strains (HKAS146070 and HKAS146071) were collected from dead stems of a *Poaceae* sp. Morphological examination reveals features consistent with the genus *Paulkirkia*, including dark, globose to subglobose conidiomata, blastic conidiogenous cells, and ellipsoidal, 1-septate conidia. Phylogenetic analyses using combined sequence data (SSU, LSU, ITS, *tef*1-α, and *rpb*2) robustly place our isolates in close relationship with the type species, *Paulkirkia arundinis* (Fig. 45). Despite morphological variations from the type species, particularly in conidial dimensions (7–10 × 4–6 μm vs 9–12 × 4.5–6 μm), our strains resemble the generic boundaries of *Paulkirkia*.

Torulaceae Corda, Deutschlands Flora, Abt. III. Die Pilze Deutschlands 2: 71 (1829)

Dendryphion Wallr., Flora Cryptogamica Germaniae 2: 300 (1833)

Notes: *Dendryphion* was established by Wallroth[198] with *D. comosum* as the type species to accommodate a group of hyphomycetous fungi. These fungi are typically saprobic, occurring on decaying wood and dead stems of herbaceous plants. The genus is morphologically defined by erect, solitary conidiophores that are branched in the upper region and polytretic. Conidiophores typically possess septate, pigmented, thick-walled stipes with finely roughened surfaces and a well-developed conidiogenous apparatus characterized by prominent scars. The conidia are brown, septate, and produced in simple or branched chains, often displaying didymo- or cheiro-type forms[199]. Species within *Dendryphion* are reported from both terrestrial and freshwater environments. Currently there are 29 species accepted in the genus Species Fungorum[168], although only eight have been confirmed through DNA-based evidence.

Dendryphion hydei J.F. Li, Phookamsak & Jeewon, PLoS ONE 15 (2): e0228067, 6 (Figs 48 and 49).

MycoBank No: 556746

Saprobic on dead twigs of an unknown host. Asexual morph: *Colonies* on substratum superficial, effuse, gregarious, hairy, brown to dark brown. *Mycelium* composed of branched, septate, brown to dark brown hyphae. *Conidiophores* 260–330 μm long × 6–14 μm diam. ($\bar{x}$ = 305.6 × 10.2 μm, n = 10) macronematous, mononematous, straight to flexuous, brown, septate, verrucose, thick-walled, branching simple or penicillate at the tip of primary branches. *Conidiogenous cells* 7–12 μm long × 4–7 μm diam. ($\bar{x}$ = 10.3 × 5.1 μm, n = 20) terminal, integrated, pale brown, polytretic. *Conidia* 25–35 μm × 5.5–8 μm ($\bar{x}$ = 30.4 × 6.8 μm, n = 20) single, monilioid, subhya-

line to pale olivaceous brown, end cells slightly paler, verrucose, 2–4(–5)-septate, constricted at the septa. *Conidial secession* schizolytic. Sexual morph: Undetermined.

Material examined: China, Yunnan, Honghe Hani and Yi Autonomous Prefecture, Honghe County, 23.421068° N, 102.229128° E, 735 m, on dead twigs of an unknown host, 23 April 2020, D.N. Wanasinghe, DWHH23-45B (HKAS146072), living culture, KUNCC23-16813.

GenBank numbers: KUNCC23-16813: ITS = PV742939, LSU = PV742995, SSU = PV743048, *tef*1-α = PV700674, *rpb*2 = PV700700.

Known hosts and distribution: Saprobic on branch litter of *Bidens pilosa* in Chiang Mai Province, Thailand[200]; submerged wood in freshwater habitats in Yunnan, China[148,201]; dead twigs of an unknown host in Yunnan, China (this study).

Notes: *Dendryphion hydei* was originally described from the branch litter of *Bidens pilosa* in Chiang Mai Province, Thailand[200]. Subsequently, Boonmee et al.[148] and Wang et al.[201] reported this species from submerged wood in freshwater habitats in Yunnan Province, China. In our phylogenetic analysis, the newly obtained isolate (KUNCC23-16813) formed a monophyletic clade with the ex-type strain (HKAS 97479) with 70% MLBS and 0.98 BYPP support values (Fig. 48) and the aforementioned Chinese collections. Morphologically, our specimen fits well with the holotype; however, the other collections exhibit longer conidia and conidiophores in comparison[148,200,201].

Discussion

Dothideomycetes from a savanna-like ecosystem

This study presents a comprehensive investigation of microfungal diversity associated with terrestrial plant debris in a subtropical savanna-like ecosystem of Honghe, Yunnan Province, China. Field collections were conducted across both dry (March, April, December) and rainy (June, August) seasons, capturing a broad temporal representation of fungal diversity. The majority of samples were collected from an approximately 5 ha area at the Centre for Mountain Futures (CMF), which is situated in a subtropical plateau humid monsoon climate zone at low latitude. The sampling environment is marked by steep valleys and highly eroded, nutrient-poor soils. Vegetation is sparse, composed mainly of perennial grasses interspersed with scattered deciduous trees and shrubs, including xerophytic and thorny species adapted to periodic drought and soil instability. More than 100 isolates were obtained during this investigation, of which only those assignable to *Dothideomycetes* are treated herein. These taxa were isolated from aerially exposed substrates, including senescent foliar material, decorticated twigs, lignified culms, and woody litter. The preferential colonization of such recalcitrant substrates reflects the saprotrophic ecological guild that typifies *Dothideomycetes*, particularly in seasonally dry, disturbance-prone environments[21,75,110,179]. Members of this class are documented as primary decomposers capable of enzymatic degradation of lignocellulosic plant components[75,110,202] and are characterized by stress-tolerant reproductive traits[203–205]. Taxonomic classification of the isolates, using both morphological features and multigene phylogenetic analyses, revealed a high diversity. The fungi were placed within six orders of *Dothideomycetes viz*. *Botryosphaeriales*, *Dyfrolomycetales*, *Hysteriales*, *Mycosphaerellales*, *Patellariales,* and *Pleosporales*. Within these orders, taxa distributed across 18 families and 26 genera were identified. Among the collected samples, 34.9% of isolates represented new species described herein. This high novelty rate (> 1/3 of all *Dothideomycetes* isolates) emphasizes the neglected fungal diversity harbored in this subtropical savanna-like ecosystem. Totally, 34 microfungal taxa, including two new families, two new genera, 15 new species, and 15 new records, were documented.

Phylogenetic resolution of *Pleosporales* taxa

Our phylogenetic analyses highlight several unresolved taxonomic placements within *Pleosporales*, emphasizing areas that require further taxonomic clarification (Fig. 29). Notably, strains of *Lizonia sexangularis* (M179 and M222), are grouped closely with members of *Didymellaceae*. This placement highlights the need for comprehensive future studies involving morphological reassessment and additional molecular data to clarify the familial status of *Lizoniaceae*. To further resolve taxonomic uncertainties, *Pleosporales* genera *incertae sedis* taxa with available DNA sequence data were included in the family-level phylogeny in *Pleosporales*. Our findings revealed that several genera previously treated as *incertae sedis* require reassignment to families where they exhibit strong phylogenetic relationships, contingent upon detailed morphological validation. Among our newly generated sequences, only *Mangifericomes* displayed clear phylogenetic relationships with them. Consequently, establishing a new family, *Mangifericomitaceae*, is proposed to accommodate *Mangifericomes*. Other novel sequences that were generated did not show a clear phylogenetic relationship with existing *incertae sedis* taxa, highlighting the necessity for further in-depth morphological and molecular studies on these taxa.

Our analyses also supported specific taxonomic transfers and placements. *Setophaeosphaeria citricola* (CBS 143179) clustered within *Neopyrenochaetaceae* (97% MLBS and 1.00 BYPP; Fig. 29), indicating that *Setophaeosphaeria* likely belongs in this family. Similarly, *Phialophorophoma litoralis* (CBS 129112) was strongly affiliated with *Cucurbitariaceae* (98% MLBS and 1.00 BYPP; Fig. 29), affirming its probable relationship within this family. Additionally, *Pyrenochaeta nobilis* (CBS 407.76) formed a distinct lineage, emerging as a sister group to *Cucurbitariaceae*, suggesting a potential novel familial lineage or the expansion of existing family circumscriptions. Likewise, *Parastenospora pini* (CPC 40385) showed a strong phylogenetic relationship with *Pseudopyrenochaetaceae* (91% MLBS and 1.00 BYPP; Fig. 29), indicating its likely close affinity to this family. *Inflatispora caryotae* (MFLUCC 13-0825) and *I. pseudostromatica* (IFRD 2013) grouped within *Pleomonodictydaceae* (99% MLBS and 1.00 BYPP; Fig. 29), warranting their transfer from *Pleosporales* genera *incertae sedis* to *Pleomonodictydaceae*. The phylogenetic results of our study support previous suggestions regarding the placement of *Inflatispora*, initially considered within the *Massarineae* genera *incertae sedis* by Tibpromma et al.[206]. However, later *Inflatispora* was treated as *Pleosporales incertae sedis* in subsequent studies[59,75,110,207–210].

Further taxonomic uncertainties were observed with taxa like *Hobus wogradensis* (CBS 141484), which emerged as sister to *Ohleriaceae* without strong statistical support, indicating the necessity for additional sequence data and thorough morphological studies to resolve its precise familial affinity. *Antealophiotrema brunneosporum* (CBS 123095) and *A. populicola* (CBS 147528), *Xenolophium applanatum* (CBS 123127, CBS 123123), and *Acuminatispora palmarum* (MFLUCC 18-0460, MFLUCC 18-0264) each formed well-supported independent monophyletic clades with 100% MLBS and 1.00 BYPP statistical values (Fig. 29). These results suggest that each clade potentially represents separate familial lineages, meriting recognition as distinct families pending further morphological and molecular investigation. *Ostropella albocincta* (SMH 3536) was affiliated as a sister lineage to *Paralophiostoma hysterioides* (PUFNI 17617) within *Paralophiostomataceae*, with 87% MLBS and 1.00 BYPP support (Fig. 29). This grouping indicates that

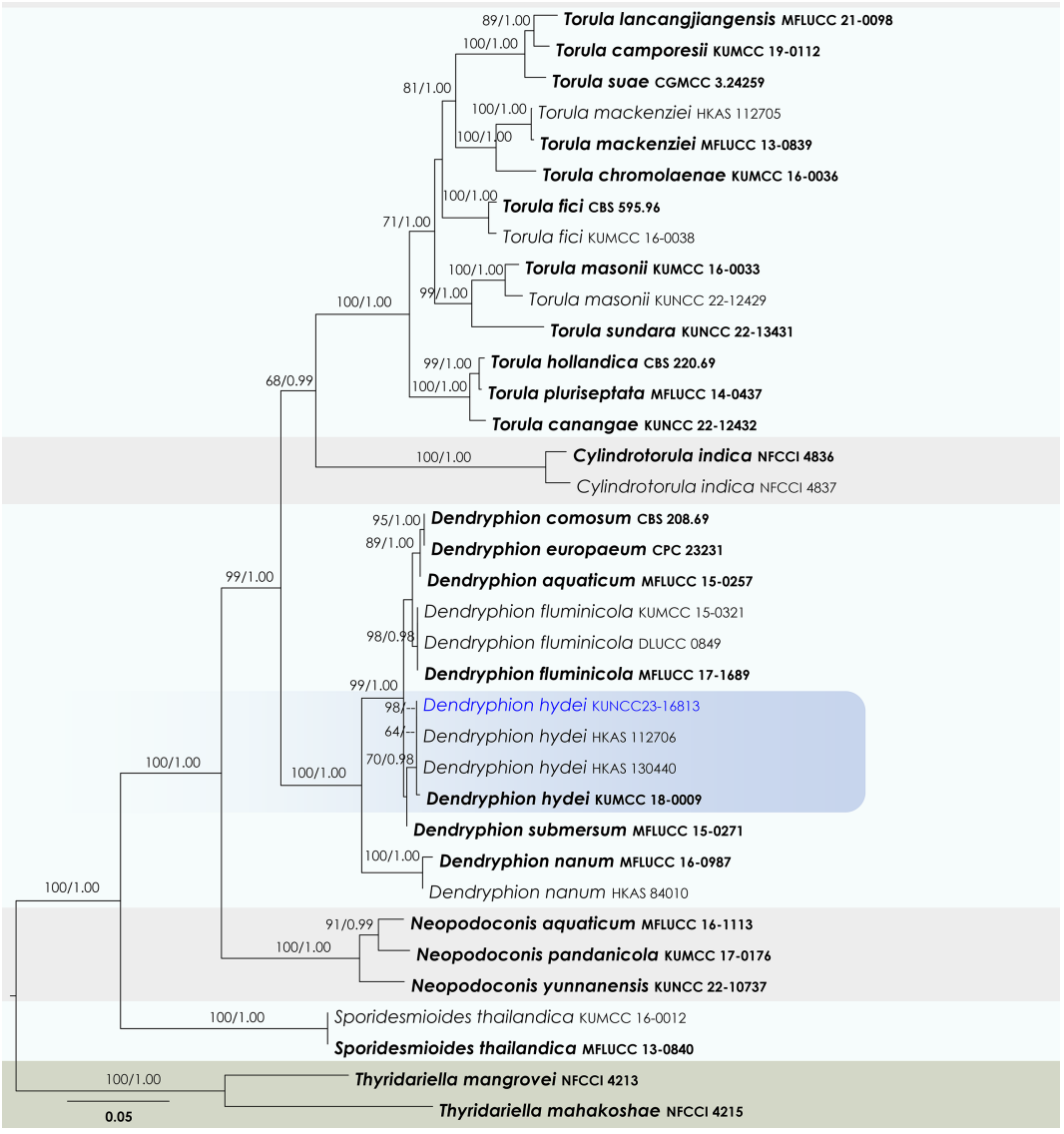

Fig. 48 Maximum Likelihood tree inferred from the concatenated dataset of partial SSU, LSU, ITS, *tef*1-α, and *rpb*2 sequences. The phylogeny is rooted with *Thyridariella mangrovei* (NFCCI 4213), and *T. mahakoshae* (NFCCI 4215). The final likelihood value is –20,543.293701. The final alignment included 1,363 unique site patterns, with approximately 22.3% of the positions comprising gaps or ambiguous characters. The estimated nucleotide frequencies were as follows: A = 0.245801, C = 0.261172, G = 0.268740, T = 0.224288. The substitution model yielded the following relative rates: AC = 1.969233, AG = 4.496613, AT = 1.690807, CG = 1.174737, CT = 9.891350 and GT = 1.000000. The proportion of invariable sites (I) was estimated at 0.574647, and the gamma distribution shape parameter (α) was 0.522487. Bayesian inference reached convergence after 183,000 generations, when the average standard deviation of split frequencies dropped below 0.01 (observed value: 0.009703). A total of 1,831 trees were sampled, and 1,374 of these were retained for the final analysis after discarding the initial 25% as burn-in. The alignment also revealed 1,364 distinct informative sites. In the resulting phylograms, sequences generated in this study are highlighted in blue, while ex-type or type strains are indicated in boldface.

the precise familial placement of these taxa requires additional molecular evidence from broader sampling.

Morphological adaptations to dry-hot environments

The diverse assemblage of microfungal taxa documented in this study likely reflects a suite of ecological and morphological adaptations to the extreme environmental conditions prevalent in dry-hot valleys. Among the most conspicuous adaptive traits observed was the fully or semi-immersed development of conidiomata and ascomata, with the majority of species forming fruiting bodies beneath the host epidermis. This subepidermal development likely serves as a protective mechanism against desiccation, facilitating successful sporulation under dry conditions. Only three taxa *viz. Anteaglonium hongheense*, *Patellaria microspora* and *Rhytidhysteron neorufulum* were found to produce superficial fruiting bodies (Figs 8, 12 and 14). These species possessed distinctly carbonaceous outer peridial layers, which may function as a mechanical barrier against environmental stressors, particularly heat and desiccation. Such carbonized structures are associated with drought-tolerant fungi and may indicate convergent adaptations to extreme terrestrial habitats. Hyphomycetous taxa were notably rare in our collections. Only *Dendryphion hydei* and *Helminthosporium hongheense* exhibited hyphomycetous morphologies. This suggests a limited representation of this asexual reproductive strategy in the sampled habitat. Instead, a balanced representation of sexual and asexual morphs was observed, highlighting the reproductive versatility of the assemblage. Sexual morphs frequently produced ascospores with terminal appendages or encased in hyaline gelatinous sheaths. They may facilitate hydration retention or delayed germination under harsh conditions. Interestingly, such spore ornamentation was

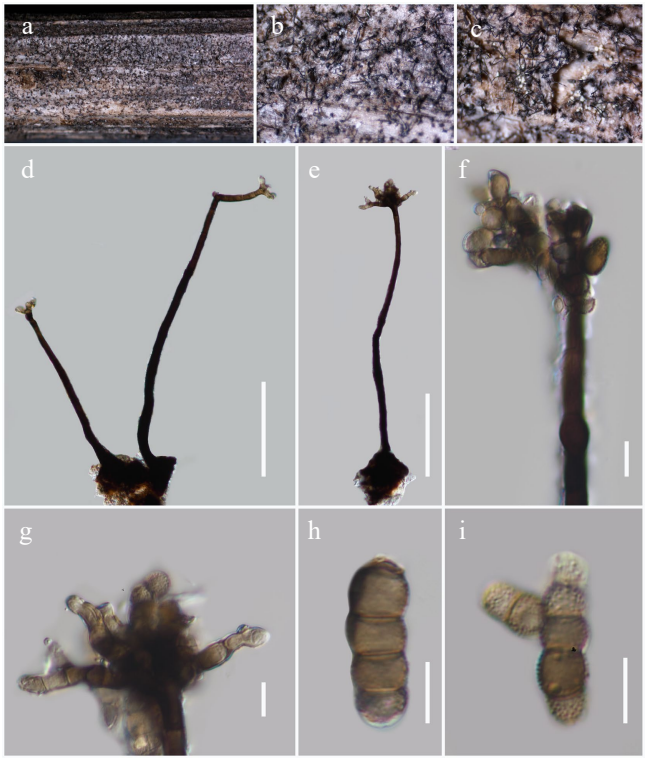

Fig. 49 *Dendryphion hydei* (HKAS146072). (a)–(c) Colonies on host. (d), (e) Conidiophores. (f), (g) Apex of conidiophores with conidial structures. (h), (i) Conidia. Scale bars: (d), (e) = 100 μm, (f)–(i) = 10 μm.

absent in species possessing carbonaceous peridia, suggesting potential functional redundancy or divergence in survival strategies. No other consistent spore traits indicative of specific environmental specialization was observed across taxa. Variation in ascospore, morphology including shape, pigmentation, and septation, was evident but not taxonomically or ecologically uniform. These findings suggest that while certain morphological traits (i.e., immersion of fruiting structures, ascospore sheaths) may confer adaptive advantages under drought conditions, many of the observed taxa rely on a combination of generalized and lineage-specific features to persist in these challenging environments.

Conservation and future perspectives

Biodiversity conservation emerges as a critical theme within the context of this study. The rich and novel microfungal diversity documented emphasizes the ecological significance and uniqueness of the subtropical savanna-like ecosystems in Honghe. Given the high novelty rate observed, these ecosystems clearly harbor substantial undocumented fungal biodiversity. However, the dry-hot valleys face threats from climate change, habitat degradation, and anthropogenic disturbances[13,211–214], emphasizing the urgency of conservation efforts. Preserving this fungal diversity contributes to maintaining ecosystem integrity, function, and safeguards ecological resilience against environmental stressors. Effective conservation strategies must therefore incorporate comprehensive biodiversity assessments, habitat protection measures, and continuous ecological monitoring to ensure the long-term preservation of these distinctive microbial communities and their associated ecological processes. Future comparative analyses of fungal diversity observed here with similar extreme or arid ecosystems worldwide may yield valuable insights into global patterns of fungal distribution and adaptation. Such comparative analyses could help explain biogeographic patterns and evolutionary processes shaping fungal diversity. While our methodological approach, integrating morphological and molecular analyses, provided robust taxonomic resolution, there are potential biases from selective sampling and culture-dependent methods. Future research could benefit from incorporating complementary methods such as environmental DNA sequencing[215–217]. Detailed ecological studies, investigations into host-fungus interactions, and long-term monitoring of microfungal community dynamics across seasons represent important avenues for further research. Multidisciplinary collaborations integrating taxonomy, ecology, molecular biology, and environmental sciences will be essential for comprehensively understanding and conserving the fungal biodiversity in these ecologically distinctive regions.

Author contributions

The authors confirm their contributions to the paper as follows: conceptualization, formal analysis, writing – original draft: Wanasinghe DN; data curation: Wanasinghe DN, Dissanayake LS; methodology: Wanasinghe DN, Phookamsak R, Dissanayake LS; resources, project administration: Wanasinghe DN, Xu J; supervision: Xu J; writing – review and editing: Phookamsak R, Dissanayake LS. All authors reviewed the results and approved the final version of the manuscript.

Data availability

The datasets generated for this study can be found in the NCBI, GenBank and MycoBank.

Acknowledgments

Dhanushka N. Wanasinghe is funded by the Distinguished Scientist Fellowship Program (DSFP), King Saud University, Kingdom of Saudi Arabia. Rungtiwa Phookamsak sincerely acknowledges the Talent Introduction Plan of Kunming Institute of Botany, Chinese Academy of Sciences, Yunnan Revitalization Talent Support Program 'Young Talent' Project (Grant No. YNWR-QNBJ-2020-120), Yunnan Revitalization Talent Support Program: High-end Foreign Expert Project (Grant No. XDYC-GDWZ-2024-0016), Independent Research of Department of Economic Plants and Biotechnology, Yunnan Key Laboratory for Wild Plant Resources, Kunming Institute of Botany, Chinese Academy of Sciences (Grant No. Y537731261), Yunnan Provincial Department of Human Resources and Social Security, Yunnan Province Foreign Expert Project (Grant No. 202505AO120002) and Yunnan Intelligence Union Program for Young Scientists, Yunnan, China (Grant No. 202503AM140005). Lakmali Dissanayake is supported by the State Administration of Foreign Expert Affairs (Grant No. Y20240197). Jianchu Xu thanks the Yunnan Department of Sciences and Technology of China (Grant Nos 202302AE090023, 202303AP140001).

Conflict of interest

The authors declare that they have no conflict of interest. Wanasinghe DN, Phookamsak R, and Xu J are the Editorial Board members of *Studies in Fungi* who were blinded from reviewing or making decisions on the manuscript. The article was subject to the journal's standard procedures, with peer-review handled independently of these Editorial Board members and the research groups.

Dates

Received 30 May 2025; Revised 2 July 2025; Accepted 7 July 2025;

Published online 27 August 2025

References

1. Dighton J. 2016. Fungi in ecosystem processes. Boca Raton: CRC press. doi: 10.1201/9781315371528
2. Frey SD. 2019. Mycorrhizal fungi as mediators of soil organic matter dynamics. *Annual Review of Ecology, Evolution, and Systematics* 50(1):237–59
3. Bahram M, Netherway T. 2022. Fungi as mediators linking organisms and ecosystems. *FEMS Microbiology Reviews* 46(2):fuab058
4. Powell JR, Rillig MC. 2018. Biodiversity of arbuscular mycorrhizal fungi and ecosystem function. *New Phytologist* 220(4):1059–75
5. Adnan M, Islam W, Gang L, Chen HYH. 2022. Advanced research tools for fungal diversity and its impact on forest ecosystem. *Environmental Science and Pollution Research* 29(30):45044–62
6. Runnel K, Tedersoo L, Krah FS, Piepenbring M, Scheepens JF, et al. 2025. Toward harnessing biodiversity–ecosystem function relationships in fungi. *Trends in Ecology & Evolution* 40(2):180–90
7. Magan N. 2007. Fungi in extreme environments. *Mycota* 4:85–103
8. Coleine C, Stajich JE, de Los Ríos A, Selbmann L. 2021. Beyond the extremes: Rocks as ultimate refuge for fungi in drylands. *Mycologia* 113(1):108–33
9. Coleine C, Stajich JE, Selbmann L. 2022. Fungi are key players in extreme ecosystems. *Trends in Ecology & Evolution* 37(6):517–28
10. Maharachchikumbura SSN, Wanasinghe DN, Cheewangkoon R, Al-Sadi AM. 2021. Uncovering the hidden taxonomic diversity of fungi in Oman. *Fungal Diversity* 106:229–68
11. Rundel P, Villagra PE. 2007. Arid and semi-arid ecosystems. In *The Physical Geography of South America*. Oxford. UK: Oxford University Press. pp. 158–83. doi: 10.1093/oso/9780195313413.003.0018
12. Zhou Y, Yi YJ, Liu HX, Tang CH, Zhu YL, et al. 2022. Effect of geomorphologic features and climate change on vegetation distribution in the arid hot valleys of Jinsha River, Southwest China. *Journal of Mountain Science* 19(10):2874–85
13. He G, Shi Z, Fang H, Shi L, Wang Y, et al. 2024. Climate and soil stressed elevation patterns of plant species to determine the aboveground biomass distributions in a valley-type Savanna. *Frontiers in Plant Science* 15:1324841
14. Hyde KD, Norphanphoun C, Chen J, Dissanayake AJ, Doilom M, et al. 2018. Thailand's amazing diversity: up to 96% of fungi in northern Thailand may be novel. *Fungal Diversity* 93:215–39
15. Hyde KD, Saleh A, Aumentado HDR, Boekhout T, Bera I, et al. 2024. Fungal numbers: global needs for a realistic assessment. *Fungal Diversity* 128:191–225
16. Wanasinghe DN, Mortimer PE, Bezerra JDP. 2022. Editorial: Fungal Systematics and Biogeography. *Frontiers in Microbiology* 12:827725
17. Naranjo-Ortiz MA, Gabaldón T. 2019. Fungal evolution: major ecological adaptations and evolutionary transitions. *Biological Reviews* 94(4):1443–76
18. Hyde KD, Jeewon R, Chen YJ, Bhunjun CS, Calabon MS, et al. 2020. The numbers of fungi: is the descriptive curve flattening? *Fungal Diversity* 103:219–71
19. Zhu H, Tan Y, Yan L, Liu F. 2020. Flora of the savanna-like vegetation in hot dry valleys, southwestern China with implications to their origin and evolution. *The Botanical Review* 86:281–97
20. Hawksworth DL. 1991. The fungal dimension of biodiversity: magnitude, significance, and conservation. *Mycological research* 95:641–655
21. Wanasinghe DN, Mortimer PE, Xu J. 2021. Insight into the systematics of microfungi colonizing dead woody twigs of *Dodonaea viscosa* in Honghe (China). *Journal of Fungi* 7(3):180
22. Jiang HB, Zhang SJ, Phookamsak R, Promputtha I, Kakumyan P, et al. 2021. *Amphibambusa hongheensis* sp. nov., a novel bambusicolous ascomycete from Yunnan, China. *Phytotaxa* 505(2):201–12
23. Mortimer PE, Jeewon R, Xu JC, Lumyong S, Wanasinghe DN. 2021. Morpho-phylo taxonomy of novel Dothideomycetous fungi associated with dead woody twigs in Yunnan Province, China. *Frontiers in Microbiology* 12:654683
24. Wanasinghe DN, Ren GC, Xu JC, Cheewangkoon R, Mortimer PE. 2022. Insight into the taxonomic resolution of the pleosporalean species associated with dead woody litter in natural forests from Yunnan, China. *Journal of Fungi* 8:375
25. Xie N, Phookamsak R, Jiang HB, Zeng YJ, Zhang H, et al. 2022. Morpho-molecular characterization of five novel taxa in *Parabambusicolaceae* (*Massarineae, Pleosporales*) from Yunnan, China. *Journal of Fungi* 8:108
26. Yang EF, Karunarathna SC, Dai DQ, Stephenson SL, Elgorban AM, et al. 2022. Taxonomy and phylogeny of fungi associated with *Mangifera indica* from Yunnan, China. *Journal of Fungi* 8:1249
27. Yang EF, Dai DQ, Bhat JD, Dawoud TM, Promputtha I, et al. 2023. Taxonomic and phylogenetic studies of saprobic fungi associated with *Mangifera indica* in Yunnan, China. *Journal of Fungi* 9:680
28. Yang EF, Karunarathna SC, Elgorban AM, Soytong K, Promputtha I, et al. 2024. Taxonomy and phylogeny of endophytic *Chaetomium* (*Chaetomiaceae*) associated with mango (*Mangifera indica*) in Yunnan, China. *New Zealand Journal of Botany* 62:481–500
29. Dissanayake LS, Samarakoon MC, Maharachchikumbura SSN, Hyde KD, Tang X, et al. 2024. Exploring the taxonomy and phylogeny of *Sordariomycetes* taxa emphasizing *Xylariomycetidae* in Southwestern China. *Mycosphere* 15:1675–793
30. Dissanayake LS, Phookamsak R, Xu JC, Wanasinghe DN. 2024. *Oxydothis ailaoshanensis* sp. nov. (*Oxydothidaceae, Xylariales*) from dead bamboo culms in Yunnan Province, China. *Studies in Fungi* 9:e016
31. Liu RM, Wang HH, Zhang GQ, Dai DQ, Elgorban AM, et al. 2024. *Amphisphaeria hongheensis* sp. nov. (*Amphisphaeriaceae, Amphisphaeriales*) from Yunnan Province, China. *Phytotaxa* 670(4):273–84
32. Phookamsak R, Hongsanan S, Bhat DJ, Wanasinghe DN, Promputtha I, et al. 2024. Exploring ascomycete diversity in Yunnan II: Introducing three novel species in the suborder *Massarineae* (*Dothideomycetes, Pleosporales*) from fern and grasses. *MycoKeys* 104:9–50
33. Shen HW, Luo ZL, Bao DF, Luan S, Bhat DJ, et al. 2024. Lignicolous freshwater fungi from China IV: morphology and phylogeny reveal new species of *Pleosporales* from plateau lakes in Yunnan Province, China. *Mycosphere* 15(1):6439–24
34. Gao Y, Zhong T, Wanasinghe DN, Eungwanichayapant PD, Jayawardena RS, et al. 2024. *Phlyctema yunnanensis* (*Dermateaceae, Helotiales*), a novel species from herbaceous plants in grassland ecosystems of Yunnan, China. *Studies in Fungi* 9:e019
35. Xu RJ, Boonmee S, Dong W, Guo YY, Yang QY, et al. 2024. *Savoryella claviformis* (*Savoryellaceae*), a new freshwater hyphomycetous species from the Tibetan Plateau, China. *Studies in Fungi* 9:e009
36. Li JF, Jiang HB, Jeewon R, Hongsanan S, Bhat DJ, et al. 2023. *Alternaria*: update on species limits, evolution, multi-locus phylogeny, and classification. *Studies in Fungi* 8:1
37. Li XH, Phookamsak R, Sun FQ, Jiang HB, Xu JC, et al. 2024. *Torula aquilariae* sp. nov. (*Torulaceae, Pleosporales*), a new species associated with *Aquilaria sinensis* from Yunnan, China. *Studies in Fungi* 9:e020
38. Mapook A, Hyde KD, Huanraluek N, Boonmee S. 2023. Addition to *Microascales* (*Sordariomycetes*, *Ascomycota*): *Synnematotriadelphiaceae* fam. nov. , *Triadelphia mukdahanensis* sp. nov. (*Triadelphiaceae*) and the validation of *Graphiaceae*. *Studies in Fungi* 8:10
39. Chaiwan N, Gomdola D, Wang S, Monkai J, Tibpromma S, et al. 2021. https://gmsmicrofungi.org: an online database providing updated information of microfungi in the Greater Mekong Subregion. *Mycosphere* 12(1):1513–26
40. MycoBank. 2025. *Deposit new basionym, combination or nomen novum*. www.mycobank.org/Registration%20home (Accessed on February 2025)
41. Rayner. 1970. A mycological colour chart. Commonwealth Mycological Institute, Kew, p 34
42. Jeewon R, Hyde KD. 2016. Establishing species boundaries and new taxa among fungi: recommendations to resolve taxonomic ambiguities. *Mycosphere* 7:1669–77
43. Maharachchikumbura SSN, Chen Y, Ariyawansa HA, Hyde KD, Haelewaters D. et al. 2021. Integrative approaches for species delimitation in *Ascomycota*. *Fungal Diversity* 109:155–79
44. Wanasinghe DN, Hyde KD, Jeewon R, Crous PW, Wijayawardene NN. et al. 2017. Phylogenetic revision of *Camarosporium* (*Pleosporineae, Dothideomycetes*) and allied genera. *Studies in Mycology* 87:207–56
45. Wijesinghe SN, Calabon MS, Xiao Y, Jones EBG, Hyde KD. 2023. A novel

coniothyrium-like genus in *Coniothyriaceae* (*Pleosporales*) from salt marsh ecosystems in Thailand. *Studies in Fungi* 8:6
46. Htet ZH, Mapook A, Chethana KWT. 2024. Molecular taxonomy reveals new records of *Chromolaenicola* (*Didymosphaeriaceae, Pleosporales*) and potential antibacterial properties. *Studies in Fungi* 9:e006
47. Kuraku S, Zmasek CM, Nishimura O, Katoh K. 2013. aLeaves facilitates on-demand exploration of metazoan gene family trees on MAFFT sequence alignment server with enhanced interactivity. *Nucleic acids research* 41:22–28
48. Katoh K, Rozewicki J, Yamada KD. 2019. MAFFT online service: multiple sequence alignment, interactive sequence choice and visualization. *Briefings in Bioinformatics* 20:1160–66
49. Hall TA. 1999. BioEdit: a user-friendly biological sequence alignment editor and analysis program for Windows 95/98/NT. *Nucleic acids Symposium Series* 41:95–98
50. Nylander JAA. 2004. *MrModeltest v2. Program distributed by the author*. Evolutionary Biology Centre, Uppsala University.
51. Swofford DL. 2002. *PAUP: phylogenetic analysis using parsimony, version 4.0b10*. Sinauer Associates, Sunderland.
52. Miller MA, Pfeiffer W, Schwartz T. 2010. Creating the CIPRES Science Gateway for inference of large phylogenetic trees. *2010 Gateway Computing Environments Workshop (GCE). New Orleans, LA, USA, 14 November 2010*. USA: IEEE. pp. 1–8. doi: 10.1109/GCE.2010.5676129
53. Stamatakis A. 2014. RAxML version 8: a tool for phylogenetic analysis and post-analysis of large phylogenies. *Bioinformatics* 30:1312–13
54. Ronquist F, Teslenko M, Van Der Mark P, Ayres DL, Darling A, et al. 2012. MrBayes 3.2: efficient Bayesian phylogenetic inference and model choice across a large model space. *Systematic Biology* 61(3):539–42
55. Rambaut A, Drummond AJ. 2012. *FigTree: Tree Figure Drawing Tool*. Edinburgh, Scotland: Institute of Evolutionary Biology, University of Edinburgh. http://tree.bio.ed.ac.uk/software/figtree/
56. Damm U, Fourie PH, Crous PW. 2007. *Aplosporella prunicola*, a novel species of anamorphic Botryosphaeriaceae. *Fungal Diversity* 27:35–43
57. Fan X, Yang Q, Cao B, Liang Y, Tian C. 2015. New record of *Aplosporella javeedii* on five hosts in China based on multi-gene analysis and morphology. *Mycotaxon* 130:749–56
58. Ekanayaka AH, Dissanayake AJ, Jayasiri SC, To-anun C, Jones EBG, et al. 2016. *Aplosporella thailandica*; a novel species revealing the sexual-asexual connection in *Aplosporellaceae* (*Botryosphaeriales*). *Mycosphere* 7:440–47
59. Hyde KD, Noorabadi MT, Thiyagaraja V, Mq H, Johnston PR, et al. 2024. The 2024 outline of fungi and fungus-like taxa. *Mycosphere* 15(1):5146–6239
60. Jia H, Liu Z, O S, Yao C, Chen J, et al. 2019. First report of *Aplosporella javeedii* causing branch blight disease of Mulberry (*Morus alba*) in China. *Journal of Plant Diseases and Protection* 126:475–77
61. Wan X, Zhao Y, Zhang Y, Wei C, Du H, et al. 2021. Molecular characterization of a novel partitivirus isolated from the phytopathogenic fungus *Aplosporella javeedii*. *Archives of Virology* 166(4):1237–40
62. Lin L, Pan M, Gao H, Tian C, Fan X. 2023. The potential fungal pathogens of *Euonymus japonicus* in Beijing, China. *Journal of Fungi* 9(2):271
63. Yao C, Liu X, Diao G. 2023. First report of branch blight disease caused by *Aplosporella longipes* on *Physocarpus amurensis* in China. *Forest Pathology* 53:e12788
64. Phillips AJL, Hyde KD, Alves A, Liu JK. 2019. Families in *Botryosphaeriales*: a phylogenetic, morphological and evolutionary perspective. *Fungal Diversity* 94:1–22
65. Trakunyingcharoen T, Lombard L, Groenewald JZ, Cheewangkoon R, To-anun C, et al. 2015. Caulicolous *Botryosphaeriales* from Thailand. *Persoonia* 34:87–99
66. Jayawardena RS, Hyde KD, Wang S, Sun YR, Suwannarach N, et al. 2022. Fungal diversity notes 1512–1610: taxonomic and phylogenetic contributions on genera and species of fungal taxa. *Fungal Diversity* 117:1–272
67. Ren GC, Jayasiri SC, Tibpromma S, De Farias ARG, Chethana KWT, et al. 2024. Saprobic ascomycetes associated with woody litter from the Greater Mekong Subregion (Southwestern China and Northern Thailand). *Mycosphere* 15(1):954–1082
68. Sahoo S, Subban K, Chelliah J. 2021. Diversity of marine macro-algicolous endophytic fungi and cytotoxic potential of *Biscogniauxia petrensis* metabolites against cancer cell lines. *Frontiers in Microbiology* 12:650177
69. Mapook A, Hyde KD, McKenzie EHC, Jones EBG, Bhat DJ, et al. 2020. Taxonomic and phylogenetic contributions to fungi associated with the invasive weed *Chromolaena odorata* (Siam weed). *Fungal Diversity* 101:1–175
70. Yang T, Groenewald JZ, Cheewangkoon R, Jami F, Abdollahzadeh J, et al. 2017. Families, genera, and species of *Botryosphaeriales*. *Fungal Biology* 121(4):322–46
71. Vu D, Groenewald M, de Vries M, Gehrmann T, Stielow B, et al. 2019. Large-scale generation and analysis of filamentous fungal DNA barcodes boosts coverage for kingdom fungi and reveals thresholds for fungal species and higher taxon delimitation. *Studies in Mycology* 92:1–20
72. Deepika YS, Mahadevakumar S, Amruthesh KN, Lakshmidevi N. 2020. A new collar rot disease of cowpea (*Vigna unguiculata*) caused by *Aplosporella hesperidica* in India. *Letters in applied microbiology* 71(2):154–63
73. Dissanayake AJ, Chen YY, Cheewangkoon R, Liu JK. 2021. Occurrence and Morpho-molecular identification of *Botryosphaeriales* species from Guizhou Province, China. *Journal of Fungi* 7:893
74. Spegazzini CL. 1882. Fungi Argentini. Pugillus Quartus [cont.]. *Anales de la Sociedad Científica Argentina* 13(1):11–35
75. Hongsanan S, Hyde KD, Phookamsak R, Wanasinghe DN, McKenzie EHC, et al. 2020. Refined families of *Dothideomycetes*: orders and families *incertae sedis* in *Dothideomycetes*. *Fungal Diversity* 105:17–318
76. Li WL, Maharachchikumbura SSN, Cheewangkoon R, Liu JK. 2022. Reassessment of *Dyfrolomyces* and four new species of *Melomastia* from olive (*Olea europaea*) in Sichuan Province, China. *Journal of Fungi* 8(1):76
77. Kularathnage ND, Tennakoon DS, Zhu X, Zhou J, Su B, et al. 2023. Reinstating *Dyfrolomyces* and introducing *Melomastia pyriformis* sp. nov. (*Pleurotremataceae, Dyfrolomycetales*) from Guangdong Province, China. *Current Research in Environmental & Applied Mycology* 13(1):426–38
78. Kumar V, Cheewangkoon R, Thambugala KM, Jones GEB, Brahmanage RS, et al. 2019. *Rhytidhysteron mangrovei* (*Hysteriaceae*), a new species from mangroves in Phetchaburi Province, Thailand. *Phytotaxa* 401:166–78
79. Dayarathne MC, Jones EBG, Maharachchikumbura SSN, Devadatha B, Sarma VV, et al. 2020. Morpho-molecular characterization of microfungi associated with marine based habitats. *Mycosphere* 11:1–188
80. Du TY, Dai DQ, Mapook A, Lu L, Stephenson SL, et al. 2023. Additions to *Rhytidhysteron* (*Hysteriales, Dothideomycetes*) in China. *Journal of Fungi* 9:148
81. Senwanna C, Suwannarach N, Phookamsak R, Kumla J, Hongsanan S. 2023. New host and geographical records of *Rhytidhysteron* in northern Thailand, and species synonymization. *Phytotaxa* 601:157–173
82. Mahajan VK, Sharma V, Prabha N, Thakur K, Sharma NL, et al. 2014. A rare case of subcutaneous phaeohyphomycosis caused by a *Rhytidhysteron* species: a clinico-therapeutic experience. *International Journal of Dermatology* 53:1485–1489
83. Thambugala KM, Hyde KD, Eungwanichayapant PD, Romero AI, Liu ZY. 2016. Additions to the genus *Rhytidhysteron* in *Hysteriaceae*. *Cryptogamie, Mycologie* 37:99–116
84. Chander J, Singla N, Kundu R, Handa U, Chowdhary A. 2017. *Phaeohyphomycosis* caused by *Rhytidhysteron rufulum* and review of literature. *Mycopathologia* 182:403–407
85. Rashmi M, Kushveer JS, Sarma VV. 2019. A worldwide list of endophytic fungi with notes on ecology and diversity. *Mycosphere* 10:798–1079
86. Dingle TC, Jansen B, Walker C, Sam M, Verity B. 2022. Implantation subcutaneous phaeohyphomycosis caused by *Rhytidhysteron rufulum*: A case report. *Medical Mycology Case Reports* 36:16–18
87. Spegazzini CL. 1881. Fungi argentini additis nonnullis brasiliensibus montevideensibusque. *Pugillus quartus* (Continuacion). *Sociedad*

Científica Argentina 12:97–117
88. Clements FE, Shear CL. 1931. *The Genera of Fungi*. New York, NY, USA: Hafner Publishing Co. 632 pp.
89. Index Fungorum. 2025. www.indexfungorum.org/names/Names.asp
90. Huanraluek N, Jayawardena RS, Thambugala KM, Tian Q. 2020. New host records for three saprobic *Dothideomycetes* in Thailand. *Asian Journal of Mycology* 3:345–61
91. Senwanna C, Mapook A, Samarakoon MC, Karunarathna A, Wang Y. 2021. Ascomycetes on Para rubber (*Hevea brasiliensis*). *Mycosphere* 12:1230–408
92. Ren GC, Wanasinghe DN, Jeewon R, Monkai J, Mortimer PE, et al. 2022. Taxonomy and phylogeny of the novel rhytidhysteron-like collections in the Greater Mekong Subregion. *MycoKeys* 86:65–85
93. de Silva NI, Hyde KD, Lumyong S, Phillips AJL, Bhat DJ, et al. 2022. Morphology, phylogeny, host association and geography of fungi associated with plants of *Annonaceae, Apocynaceae* and *Magnoliaceae*. *Mycosphere* 13:955–1076
94. de Almeida DAC, Gusmão LFP, Miller AN. 2014. A new genus and three new species of hysteriaceous ascomycetes from the semiarid region of Brazil. *Phytotaxa* 176:298–308
95. Boehm EWA, Mugambi GK, Miller AN, Huhndorf SM, Marincowitz S, et al. 2009. A molecular phylogenetic reappraisal of the *Hysteriaceae, Mytilinidiaceae* and *Gloniaceae* (*Pleosporomycetidae, Dothideomycetes*) with keys to world species. *Studies in Mycology* 64:49–83
96. Cobos-Villagrán A, Hernández-Rodríguez C, Valenzuela R, Villa-Tanaca L, Calvillo-Medina RP, et al. 2020. El género *Rhytidhysteron* (*Dothideomycetes, Ascomycota*) en México. *Acta Botanica Mexicana* 127:e1675 (in Spanish)
97. Quaedvlieg W, Binder M, Groenewald JZ, Summerell BA, Carnegie AJ, et al. 2014. Introducing the consolidated species concept to resolve species in the *Teratosphaeriaceae*. *Persoonia-Molecular Phylogeny and Evolution of Fungi* 33:1–40
98. Verkley GJM, Crous PW, Groenewald JZ, Braun U, Aptroot A. 2004. *Mycosphaerella punctiformis* revisited: morphology, phylogeny, and epitypification of the type species of the genus *Mycosphaerella* (*Dothideales, Ascomycota*). *Mycological Research* 108:1271–82
99. Crous PW, Braun U, Schubert K, Groenewald JZ. 2007. Delimiting *Cladosporium* from morphologically similar genera. *Studies in Mycology* 58:33–56
100. Crous PW, Schoch CL, Hyde KD, Wood AR, Gueidan C, et al. 2009. Phylogenetic lineages in the *Capnodiales*. *Studies in Mycology* 64:17–47
101. Trovão J, Tiago I, Soares F, Paiva DS, Mesquita N, et al. 2019. Description of *Aeminiaceae* fam. nov., *Aeminium* gen. nov. and *Aeminium ludgeri* sp. nov. (*Capnodiales*), isolated from a biodeteriorated art-piece in the Old Cathedral of Coimbra, Portugal. *MycoKeys* 45:57–73
102. Lücking R, Hodkinson BP, Leavitt SD. 2017. The 2016 classification of lichenized fungi in the *Ascomycota* and *Basidiomycota* – Approaching one thousand genera. *The Bryologist* 119(4):361–416
103. Kohlmeyer J, Volkmann-Kohlmeyer B, Eriksson OE. 1999. Fungi on *Juncus roemerianus* 12. Two new species of *Mycosphaerella* and *Paraphaeosphaeria* (*Ascomycotina*). *Botanica Marina* 42(6):505–11
104. García-Jacobo I, Raymundo T, Martínez-González CR, Martínez-Pineda M, Valenzuela R. 2025. Phylogenetic and morphological analyses reveal twelve new species of the genus *Patellaria* (*Dothideomycetes, Ascomycota*) from Mexico. *Journal of Fungi* 11:44
105. Fries EM. 1822. Systema Mycologicum. Gryphiswaldiae: Sumtibus Ernesti Mauritti. volume 2. pp. 275
106. Yacharoen S, Tian Q, Chomnunti P, Boonmee S, Chukeatirote E, et al. 2015. *Patellariaceae* revisited. *Mycosphere* 6(3):290–326
107. Jayasiri SC, Jones EBG, Kang JC, Promputtha I, Bahkali AH, et al. 2016. A new species of genus *Anteaglonium* (*Anteagloniaceae, Pleosporales*) with its asexual morph. *Phytotaxa* 263:233–44
108. Jayasiri SC, Hyde KD, Jones EBG, McKenzie EHC, Jeewon R, et al. 2019. Diversity, morphology and molecular phylogeny of *Dothideomycetes* on decaying wild seed pods and fruits. *Mycosphere* 10:1–186
109. Jaklitsch WM, Fournier J, Voglmayr H. 2018. Two unusual new species of *Pleosporales: Anteaglonium rubescens* and *Atrocalyx asturiensis*. *Sydowia* 70:129
110. Hongsanan S, Hyde KD, Phookamsak R, Wanasinghe DN, McKenzie EHC, et al. 2020. Refined families of *Dothideomycetes: Dothideomycetidae* and *Pleosporomycetidae*. *Mycosphere* 11:1553–2107
111. Tan YP, Bishop-Hurley SL, Shivas RG, Cowan DA, Maggs-Kölling G, et al. 2022. Fungal Planet description sheets: 1436–1477. *Persoonia-Molecular Phylogeny and Evolution of Fungi* 49(1):261–350
112. Suwannarach N, Kumla J, Khuna S, Thitla T, Senwanna C, et al. 2023. *Anteaglonium saxicola* (*Anteagloniaceae, Pleosporales*), a new species isolated from rocks in northern Thailand. *Phytotaxa* 629(1):75–84
113. Mugambi GK, Huhndorf SM. 2009. Parallel evolution of hysterothecial ascomata in ascolocularous fungi (*Ascomycota, Fungi*). *Systematics and Biodiversity* 7(4):453–64
114. Chen Q, Jiang JR, Zhang GZ, Cai L, Crous PW. 2015. Resolving the *Phoma enigma*. *Studies in Mycology* 82:137–217
115. Chen Q, Hou LW, Duan WJ, Crous PW, Cai L. 2017. *Didymellaceae* revisited. *Studies in Mycology* 87(1):105–59
116. Valenzuela-Lopez N, Cano-Lira JF, Guarro J, Sutton DA, Wiederhold N, et al. 2018. Coelomycetous *Dothideomycetes* with emphasis on the families *Cucurbitariaceae* and *Didymellaceae*. *Studies in Mycology* 90(1):1–69
117. Wanasinghe DN, Phukhamsakda C, Hyde KD, Jeewon R, Lee HB, et al. 2018. Fungal diversity notes 709–839: taxonomic and phylogenetic contributions to fungal taxa with an emphasis on fungi on *Rosaceae*. *Fungal Diversity* 89:1–236
118. Hou LW, Groenewald JZ, Pfenning LH, Yarden O, Crous PW, et al. 2020. The phoma-like dilemma. *Studies in Mycology* 96:309–396
119. Hou L, Hernández-Restrepo M, Groenewald JZ, Cai L, Crous PW. 2020. Citizen science project reveals high diversity in *Didymellaceae* (*Pleosporales, Dothideomycetes*). *MycoKeys* 65:49–99
120. Aveskamp MM, de Gruyter J, Woudenberg JH, Verkley GJ, Crous PW. 2010. Highlights of the *Didymellaceae*: a polyphasic approach to characterise *Phoma* and related pleosporalean genera. *Studies in Mycology* 65(1):1–60
121. de Gruyter J, Woudenberg JH, Aveskamp MM, Verkley GJ, Groenewald JZ, et al. 2013. Redisposition of *Phoma*-like anamorphs in *Pleosporales*. *Studies in Mycology* 75(1):1–36
122. de Gruyter J, Aveskamp MM, Woudenberg JHC, Verkley GJM, Groenewald JZ, et al. 2009. Molecular phylogeny of *Phoma* and allied anamorph genera: towards a reclassification of the *Phoma* complex. *Mycological Research* 113(4):508–519
123. Phukhamsakda C, McKenzie EHC, Phillips AJL, Jones EBG, Bhat DJ, et al. 2020. Microfungi associated with *Clematis* (*Ranunculaceae*) with an integrated approach to delimiting species boundaries. *Fungal Diversity* 102:1–203
124. Tian XG, Bao DF, Karunarathna SC, Jayawardena RS, Hyde KD, et al. 2024. Taxonomy and phylogeny of ascomycetes associated with selected economically important monocotyledons in China and Thailand. *Mycosphere* 15(1):1–274
125. Ren G, Wanasinghe DN, de Farias ARG, Hyde KD, Yasanthika E, et al. 2022. Taxonomic novelties of woody litter fungi (*Didymosphaeriaceae, Pleosporales*) from the Greater Mekong Subregion. *Biology* 11(11):1660
126. Eriksson OE. 1967. On graminicolous pyrenomycetes from Fennoscandia II. Phragmosporous and scolecosporous species. *Arkiv för Botanik Series 2* 6(4–5):381–440
127. Ariyawansa HA, Tanaka K, Thambugala KM, Phookamsak R, Tian Q, et al. 2014. A molecular phylogenetic reappraisal of the *Didymosphaeriaceae* (= *Montagnulaceae*). *Fungal Diversity* 68:69–104
128. Verkley GJM, Dukik K, Renfurm R, Göker M, Stielow JB. 2014. Novel genera and species of coniothyrium-like fungi in *Montagnulaceae* (*Ascomycota*). *Persoonia – Molecular Phylogeny and Evolution of Fungi* 32(1):25–51
129. Tan YP, Shivas RG. 2023. Novel microfungi from Australia. *Index of Australian Fungi* 19:5
130. Kohlmeyer J, Volkmann-Kohlmeyer B, Eriksson OE. 1995. Fungi on *Juncus roemerianus* 2. New dictyosporous ascomycetes. *Botanica Marina* 38:165–74
131. Hyde KD, Hongsanan S, Jeewon R, Bhat DJ, McKenzie EHC, et al. 2016. Fungal diversity notes 367–490: taxonomic and phylogenetic contributions to fungal taxa. *Fungal Diversity* 80:1–270

132. Hyde KD, Dong Y, Phookamsak R, Jeewon R, Bhat DJ, et al. 2020. Fungal diversity notes 1151–1276: taxonomic and phylogenetic contributions on genera and species of fungal taxa. *Fungal Diversity* 100:5–277
133. Feng Y, Zhang SN, Liu ZY. 2019. *Tremateia murispora* sp. nov. (*Didymosphaeriaceae, Pleosporales*) from Guizhou, China. *Phytotaxa* 416(1):79–87
134. Devadatha B, Jones EBG, Wanasinghe DN, Bahkali AH, Hyde KD. 2023. Characterization of novel estuarine *Ascomycota* based on taxonomic and phylogenetic evaluation. *Botanica Marina* 66(4):281–300
135. Hashimoto A, Hirayama K, Takahashi H, Matsumura M, Okada G, et al. 2018. Resolving the *Lophiostoma bipolare* complex: generic delimitations within *Lophiostomataceae*. *Studies in Mycology* 90(1):161–89
136. Thambugala KM, Hyde KD, Tanaka K, Tian Q, Wanasinghe DN, et al. 2015. Towards a natural classification and backbone tree for *Lophiostomataceae, Floricolaceae*, and *Amorosiaceae* fam. nov. *Fungal Diversity* 74:199–266
137. Bao DF, Su HY, Maharachchikumbura SSN, Liu JK, Nalumpang S, et al. 2019. Lignicolous freshwater fungi from China and Thailand: multigene phylogeny reveals new species and new records in *Lophiostomataceae*. *Mycosphere* 10:1080–1099
138. Dong W, Wang B, Hyde KD, McKenzie EHC, Raja HA, et al. 2020. Freshwater *Dothideomycetes*. *Fungal Diversity* 105:319–575
139. Yang CL, Xu XL, Zeng Q, Lv YC, Liu SY, et al. 2021. First report of *Neovaginatispora fuckelii* causing leaf spot on *Phoenix canariensis*. *Plant Disease* 105(1):223
140. Magaña-Dueñas V, Cano-Lira JF, Stchigel AM. 2022. Novel Freshwater Ascomycetes from Spain. *Journal of Fungi* 8(8):849
141. Tennakoon DS, Kuo CH, Jeewon R, Thambugala KM, Hyde KD. 2018. Saprobic *Lophiostomataceae* (*Dothideomycetes*): *Pseudolophiostoma mangiferae* sp. nov. and *Neovaginatispora fuckelii*, a new record from *Mangifera indica*. *Phytotaxa* 364(2):157–71
142. Li WL, Liang RR, Dissanayake AJ, Liu JK. 2023. Mycosphere Notes 413–448: *Dothideomycetes* associated with woody oil plants in China. *Mycosphere* 14(1):1436–529
143. Han Y, Chen J, Tang J, Lv Z, Zheng Y, et al. 2021. First report of *Neovaginatispora fuckelii* causing stem blight on *Rosa chinensis* in China. *Journal of Plant Pathology* 103(4):1351–1352
144. Andreasen M, Skrede I, Jaklitsch WM, Voglmayr H, Nordén B. 2021. Multi-locus phylogenetic analysis of lophiostomatoid fungi motivates a broad concept of *Lophiostoma* and reveals nine new species. *Persoonia – Molecular Phylogeny and Evolution of Fungi* 46:240–71
145. Hyde KD, Suwannarach N, Jayawardena RS, Manawasinghe IS, Liao CF, et al. 2021. Mycosphere notes 325–344: novel species and records of fungal taxa from around the world. *Mycosphere* 12(1):1101–56
146. Punithalingam E. 1979. *Sphaeropsidales* in culture from humans. *Nova Hedwigia* 31(1/3):119–58
147. Ahmed SA, Desbois N, Quist D, Miossec C, Atoche C, et al. 2015. Phaeohyphomycosis caused by a novel species, *Pseudochaetosphaeronema martinelli*. *Journal of Clinical Microbiology* 53(9):2927–2934
148. Boonmee S, Wanasinghe DN, Calabon MS, Huanraluek N, Chandrasiri SKU, et al. 2021. Fungal diversity notes 1387–1511: taxonomic and phylogenetic contributions on genera and species of fungal taxa. *Fungal Diversity* 111:1–335
149. Xu RF, Karunarathna SC, Phukhamsakda C, Dai DQ, Elgorban AM, et al. 2024. Four new species of *Dothideomycetes* (*Ascomycota*) from Pará Rubber (*Hevea brasiliensis*) in Yunnan Province, China. *MycoKeys* 103:71–95
150. Zhang T, Deng X, Yu Y, Zhang M, Zhang Y. 2016. *Pseudochaetosphaeronema ginkgonis* sp. nov., an endophyte isolated from *Ginkgo biloba*. *International Journal of Systematic and Evolutionary Microbiology* 66(11):4377–81
151. Tan YP, Shivas RG. 2022. Nomenclatural novelties of microfungi from Australia. *Index of Australian Fungi* 2:12
152. Li M, Raza M, Song S, Hou L, Zhang ZF, et al. 2023. Application of culturomics in fungal isolation from mangrove sediments. *Microbiome* 11:272
153. Apurillo CC, Phukhamsakda C, Hyde KD, Thiyagaraja V, Jones EG. 2025. New fungal genus, three novel species and one new record from mangroves, with reclassification of *Melanconiella* (*Melanconiellaceae*) species. *MycoKeys* 116:25–52
154. Manawasinghe IS, Hyde KD, Wanasinghe DN, Karunarathna SC, Maharachchikumbura SSN, et al. 2025. Fungal diversity notes 1818–1918: taxonomic and phylogenetic contributions on genera and species of fungi. *Fungal Diversity* 130(1):1–261
155. Tan YP, Shivas RG. 2024. Nomenclatural novelties. *Index of Australian Fungi* 46:13
156. Yang EF, Tibpromma S, Karunarathna SC, Phookamsak R, Xu JC, et al. 2022. Taxonomy and phylogeny of novel and extant taxa in *Pleosporales* associated with *Mangifera indica* from Yunnan, China (Series I). *Journal of Fungi* 8(2):152
157. Du TY, Karunarathna SC, Hyde KD, Nilthong S, Mapook A, et al. 2025. New *Aquilariomyces* and *Mangifericomes* species (Pleosporales, Ascomycota) from *Aquilaria* spp. in China. *MycoKeys* 112:103–25
158. Ariyawansa HA, Hyde KD, Jayasiri SC, Buyck B, Chethana KT, et al. 2015. Fungal diversity notes 111–252—taxonomic and phylogenetic contributions to fungal taxa. *Fungal Diversity* 75:27–274
159. Link JHF. 1809. Observationes in ordines plantarum naturales. Dissertatio 1ma. Magazin. *Gesellschaft Naturforschender Freunde zu Berlin* 3:3–42
160. Zhu D, Luo ZL, Baht DJ, Mckenzie EHC, Bahkali AH, et al. 2016. *Helminthosporium velutinum* and *H. aquaticum* sp. nov. from aquatic habitats in Yunnan Province, China. *Phytotaxa* 253:179–90
161. Voglmayr H, Jaklitsch WM. 2017. *Corynespora, Exosporium* and *Helminthosporium* revisited-new species and generic reclassification. *Studies in Mycology* 87:43–76
162. Konta S, Hyde KD, Karunarathna SC, Mapook A, Senwanna C, et al. 2021. Multi-gene phylogeny and morphology reveal *Haplohelminthosporium* gen. nov. and *Helminthosporiella* gen. nov. associated with palms in Thailand and a checklist for *Helminthosporium* reported worldwide. *Life* 11:454
163. Chen Y, Tian W, Guo Y, Madrid H, Maharachchikumbura SSN. 2022. *Synhelminthosporium* gen. et sp. nov. and two new species of *Helminthosporium* (*Massarinaceae, Pleosporales*) from Sichuan Province, China. *Journal of Fungi* 8:712
164. Liu J, Hu Y, Luo X, Castañeda-Ruíz RF, Ma J. 2022. Three novel species of *Helminthosporium* (*Massarinaceae, Pleosporales*) from China. *MycoKeys* 94:73–89
165. Hu YF, Liu JW, Xu ZH, Castañeda-Ruíz RF, Zhang K, et al. 2023. Morphology and multigene phylogeny revealed three new species of *Helminthosporium* (*Massarinaceae, Pleosporales*) from China. *Journal of Fungi* 9:280
166. Lu L, Karunarathna SC, Rajeshkumar KC, Elgorban AM, Jayawardena RS, et al. 2025. Unveiling fungal diversity associated with coffee trees in China using a polyphasic approach and a global review of coffee saprobic fungi. *IMA Fungus* 16:e144874
167. Sun YR, Hyde KD, Liu NG, Jayawardena RS, Wijayawardene NN, et al. 2025. Micro-fungi in southern China and northern Thailand: emphasis on medicinal plants. *Fungal Diversity* 131:99–299
168. Species Fungorum. 2025. www.speciesfungorum.org/Names/Names.asp (accessed on May 2025)
169. Crous PW, Carnegie AJ, Wingfield MJ, Sharma R, Mughini G, et al. 2019. Fungal Planet description sheets: 868–950. *Persoonia: Molecular Phylogeny and Evolution of Fungi* 42:291–473
170. Liu JK, Hyde KD, Jones EBG, Ariyawansa HA, Bhat DJ, et al. 2015. Fungal diversity notes 1–110: taxonomic and phylogenetic contributions to fungal species. *Fungal diversity* 72:1–97
171. Phookamsak R, Hongsanan S, Bhat DJ, Xu J, Mortimer PE, et al. 2023. *Scolecohyalosporium thailandense* sp. nov. (*Parabambusicolaceae, Pleosporales*) collected on *Imperata* sp. (*Poaceae*) in northern Thailand. *Phytotaxa* 594(4):267–82
172. Tanaka K, Hirayama K, Yonezawa H, Sato G, Toriyabe A, et al. 2015. Revision of the *Massarineae* (*Pleosporales, Dothideomycetes*). *Studies in Mycology* 82:75–136
173. Han LS, Dai DQ, Du TY, Wijayawardene NN, Promputtha I, et al. 2023. Taxonomy and phylogenetic studies revealed *Parabambusicola yunna-*

nensis sp. nov. (*Parabambusicolaceae, Pleosporales*) on bamboo from Yunnan, China. *Phytotaxa* 589(3):245–58
174. Walker JM. 1980. *Gaeumannomyces, Linocarpon, Ophiobolus* and several other genera of scolecospored ascomycetes and *Phialophora* conidial states, with a note on hyphopodia. *Mycotaxon* 11:1–129
175. Phookamsak R, Wanasinghe DN, Hongsanan S, Phukhamsakda C, Huang SK, et al. 2017. Towards a natural classification of *Ophiobolus* and ophiobolus-like taxa; introducing three novel genera *Ophiobolopsis, Paraophiobolus* and *Pseudoophiobolus* in *Phaeosphaeriaceae* (*Pleosporales*). *Fungal Diversity* 87(1):299–339
176. Zhang JF, Liu JK, Jeewon R, Wanasinghe DN, Liu ZY. 2019. Fungi from Asian Karst formations III. Molecular and morphological characterization reveal new taxa in *Phaeosphaeriaceae*. *Mycosphere* 10:202–20
177. Tennakoon DS, Kuo CH, Maharachchikumbura SSN, Thambugala KM, Gentekaki E, et al. 2021. Taxonomic and phylogenetic contributions to *Celtis formosana, Ficus ampelas, F. septica, Macaranga tanarius* and *Morus australis* leaf litter inhabiting microfungi. *Fungal Diversity* 108:1–215
178. Htet ZH, Tibpromma S, Mapook A, Chethana KWT, Hyde KD. 2023. *Murichromolaenicola thailandensis* sp. nov. (*Phaeosphaeriaceae, Dothideomycetes*) from *Chromolaena odorata* (*Asteraceae*) in northern Thailand. *Phytotaxa* 618(2):120–32
179. Pem D, Hyde KD, McKenzie EHC, Hongsanan S, Wanasinghe DN, et al. 2024. A comprehensive overview of genera in *Dothideomycetes*. *Mycosphere* 15(1):2175–4568
180. Liu JK, Phookamsak R, Dai DQ, Tanaka K, Jones EBG, et al. 2014. *Roussoellaceae*, a new pleosporalean family to accommodate the genera *Neoroussoella* gen. nov., *Roussoella* and *Roussoellopsis*. *Phytotaxa* 181(1):1–33
181. Karunarathna A, Phookamsak R, Jayawardena RS, Cheewangkoon R, Hyde KD, et al. 2019. The holomorph of *Neoroussoella alishanense* sp. nov. (*Roussoellaceae, Pleosporales*) on *Pennisetum purpureum* (*Poaceae*). *Phytotaxa* 406(4):218–36
182. Phookamsak R, Hyde KD, Jeewon R, Bhat DJ, Jones EBG, et al. 2019. Fungal diversity notes 929–1035: taxonomic and phylogenetic contributions on genera and species of fungi. *Fungal Diversity* 95:1–273
183. Hyde KD, Norphanphoun C, Ma J, Yang HD, Zhang JY, et al. 2023. Mycosphere notes 387–412-novel species of fungal taxa from around the world. *Mycosphere* 14(1):663–744
184. Htet ZH, Hyde KD, Alotibi FO, Chethana TK, Mapook A. 2024. Multigene phylogeny, taxonomy, and potential biological properties of *Pseudoroussoella* and *Neoroussoella* species (*Roussoellaceae, Dothideomycetes*) from *Asteraceae* weeds in northern Thailand. *MycoKeys* 111:129–46
185. Chang R, Yan Z, Jiang J, Wang Y, Si H, et al. 2025. Four novel endolichenic fungi from *Usnea* spp. (*Lecanorales, Parmeliaceae*) in Yunnan and Guizhou, China: Taxonomic description and preliminary assessment of bioactive potentials. *MycoKeys* 118:55–80
186. Guo SQ, Norphanphoun C, Hyde KD, Fu SM, Sun JE, et al. 2025. Three novel species and a new record of *Pleosporales* (*Didymellaceae, Roussoellaceae*) from China. *MycoKeys* 113:295–320
187. Dai DQ, Wijayawardene NN, Dayarathne MC, Kumla J, Han LS, et al. 2022. Taxonomic and phylogenetic characterizations reveal four new species, two new asexual morph reports, and six new country records of bambusicolous *Roussoella* from China. *Journal of Fungi (Basel)* 8(5):532
188. Ryu JJ, Lee SY, Kang IK, Ten LN, Jung HY. 2022. First report of *Xenoroussoella triseptata* isolated from soil in Korea. *The Korean Journal of Mycology* 50(3):195–204
189. Tian WH, Liu JW, Jin Y, Chen YP, Zhou YF, et al. 2024. Morphological and phylogenetic studies of *Ascomycota* from gymnosperms in Sichuan Province, China. *Mycosphere* 15(1):1794–1900
190. Mugambi GK, Huhndorf SM. 2009. Molecular phylogenetics of *Pleosporales: Melanommataceae* and *Lophiostomataceae* re-circumscribed (*Pleosporomycetidae, Dothideomycetes, Ascomycota*). *Studies in Mycology* 64:103–21
191. Jaklitsch WM, Olariaga I, Voglmayr H. 2016. *Teichospora* and the *Teichosporaceae*. *Mycological Progress* 15:31
192. Tennakoon DS, Jeewon R, Thambugala KM, Gentekaki E, Wanasinghe DN, et al. 2021. Biphasic taxonomic approaches for generic relatedness and phylogenetic relationships of *Teichosporaceae*. *Fungal Diversity* 110:199–241
193. Crous PW, Schumacher RK, Wingfield MJ, Lombard L, Giraldo A, et al. 2015. Fungal Systematics and Evolution: FUSE 1. *Sydowia* 67:81–118
194. Hyde KD, Norphanphoun C, Abreu VP, Bazzicalupo A, Chethana KWT, et al. 2017. Fungal diversity notes 603–708: taxonomic and phylogenetic notes on genera and species. *Fungal Diversity* 87:1–235
195. Wijayawardene NN, Camporesi E, Bhat DJ, Song Y, Chethana KWT, et al. 2014. *Macrodiplodiopsis* in *Lophiostomataceae, Pleosporales*. *Phytotaxa* 176:192–200
196. Wijayawardene NN, Hyde KD, Wanasinghe DN, Papizadeh M, Goonasekara ID, et al. 2016. Taxonomy and phylogeny of dematiaceous coelomycetes. *Fungal Diversity* 77:1–316
197. Crous PW, Wingfield MJ, Burgess TI, Hardy GSJ, Crane C, et al. 2016. Fungal Planet description sheets: 469–557. *Persoonia: Molecular Phylogeny and Evolution of Fungi* 37:218–403
198. Wallroth CFW. 1833. *Flora Cryptogamica Germaniae*. Compendium florae Germaniae. Joseph BM, Norimbergae, Schragius. 923 pp.
199. Su XJ, Luo ZL, Jeewon R, Bhat DJ, Bao DF, et al. 2018. Morphology and multigene phylogeny reveal new genus and species of *Torulaceae* from freshwater habitats in northwestern Yunnan, China. *Mycological Progress* 17(5):531–45
200. Li J, Jeewon R, Mortimer PE, Doilom M, Phookamsak R, et al. 2020. Multigene phylogeny and taxonomy of *Dendryphion hydei* and *Torula hydei* spp. nov. from herbaceous litter in northern Thailand. *PLoS One* 15(2):e0228067
201. Wang WP, Hyde KD, Bao DF, Wanasinghe DN, Lin CG, et al. 2024. Lignicolous freshwater fungi from karst landscapes in Yunnan Province, China. *Mycosphere* 15(1):6525–640
202. Wang W, Zhang Q, Sun X, Chen D, Insam H, et al. 2019. Effects of mixed–species litter on bacterial and fungal lignocellulose degradation functions during litter decomposition. *Soil Biology & Biochemistry* 141:107690
203. Tesei D, Marzban G, Zakharova K, Isola D, Selbmann L, et al. 2012. Alteration of protein patterns in black rock inhabiting fungi as a response to different temperatures. *Fungal Biology* 116:932–40
204. Röhrig L, Dussart F. 2022. Does abiotic host stress favour *Dothideomycete*-induced disease development? *Plants* 11:1615
205. Gomez-Gutierrrez SV, Sic-Hernandez WR, Haridas S, LaButti K, Eichenberger J, et al. 2024. Comparative genomics of the extremophile *Cryomyces antarcticus* and other psychrophilic *Dothideomycetes*. *Frontiers in Fungal Biology* 5:1418145
206. Tibpromma S, Hyde KD, Jeewon R, Maharachchikumbura SSN, Liu JK, et al. 2017. Fungal diversity notes 491–602: taxonomic and phylogenetic contributions to fungal taxa. *Fungal Diversity* 83:1–261
207. Wijayawardene NN, Hyde KD, Lumbsch HT, Liu JK, Maharachchikumbura SSN, et al. 2018. Outline of *Ascomycota*: 2017. *Fungal diversity* 88:167–263
208. Wijayawardene NN, Hyde KD, Al-Ani LK, Tedersoo L, Haelewaters D, et al. 2020. Outline of *Fungi* and fungus-like taxa. *Mycosphere* 11(1):1060–456
209. Wijayawardene NN, Hyde KD, Dai DQ, Sánchez-García M, Goto BT, et al. 2022. Outline of *Fungi* and fungus-like taxa–2021. *Mycosphere* 13(1):53–453
210. Thiyagaraja V, Hyde KD, Piepenbring M, Davydov EA, Dai DQ, et al. 2025. Orders of *Ascomycota*. *Mycosphere* 16:536–1411
211. Li J, Liu Z, He C, Tu W, Sun Z. 2016. Are the drylands in northern China sustainable? A perspective from ecological footprint dynamics from 1990 to 2010. *Science of the Total Environment* 553:223–31
212. Zhou L, Chen H, Hua W, Dai Y, Wei N. 2016. Mechanisms for stronger warming over drier ecoregions observed since 1979. *Climate Dynamics* 47:2955–2974
213. Huang J, Li Y, Fu C, Chen F, Fu Q, et al. 2017. Dryland climate change: Recent progress and challenges. *Reviews of Geophysics* 55:719–78
214. Huo H, Sun C. 2024. Land surface temperature variations in the Yunnan Province of Southwest China. *Environmental Monitoring and Assessment* 197:65
215. Tedersoo L, Bahram M, Põlme S, Kõljalg U, Yorou NS, et al. 2014. Global diversity and geography of soil fungi. *Science* 346(6213):1256688

216. Wu B, Hussain M, Zhang W, Stadler M, Liu X, et al. 2019. Current insights into fungal species diversity and perspective on naming the environmental DNA sequences of fungi. *Mycology* 10(3):127–40
217. Nimalrathna TS, Fan H, Campos-Arceiz A, Nakamura A. 2025. Dung beetle iDNA provides an effective way to detect diverse mycological communities. *Molecular Ecology Resources* 25:e14091